MODAL PARAMETER IDENTIFICATION OF CIVIL ENGINEERING STRUCTURES BY USING AN OUTPUT-ONLY SYSTEM IDENTIFICATION TECHNIQUE

A Thesis Submitted to
the Graduate School of Engineering and Sciences of
İzmir Institute of Technology
in Partial Fulfillment of the Requirements for the Degree of

MASTER OF SCIENCE

in Civil Engineering

by
Hasan CEYLAN

July 2015
İZMİR

We approve the thesis of **Hasan CEYLAN**

Examining Committee Members:

Assist. Prof. Dr. Gürsoy TURAN
Department of Civil Engineering, İzmir Institute of Technology

Assoc. Prof. Dr. Cemalettin DÖNMEZ
Department of Civil Engineering, İzmir Institute of Technology

Prof. Dr. Ahmet TÜRER
Department of Civil Engineering, Middle East Technical University

Prof. Dr. Alemdar BAYRAKTAR
Department of Civil Engineering, Karadeniz Technical University

Assoc. Prof. Dr. Özgür ÖZÇELİK
Department of Civil Engineering, Dokuz Eylül University

8 July 2015

Assist. Prof. Dr. Gürsoy TURAN
Supervisor, Department of Civil Engineering
İzmir Institute of Technology

Prof. Dr. Gökmen TAYFUR
Head of the Department of Civil Engineering

Prof. Dr. Bilge KARAÇALI
Dean of the Graduate School of
Engineering and Sciences

ACKNOWLEDGEMENTS

First of all, I would like to express my appreciation to my supervisor, Assist. Prof. Dr. Gürsoy TURAN, for all of his guidance, friendly attitude, patience, support and excitement in regard to teaching throughout this study and throughout my graduate education.

I would like to thank to my examining committee members; Assoc. Prof. Dr. Cemalettin DÖNMEZ, Prof. Dr. Ahmet TÜRER, Prof. Dr. Alemdar BAYRAKTAR and Assoc. Prof. Dr. Özgür ÖZÇELİK for providing very useful recommendations for my thesis and for my further studies.

I would also like to thank my colleagues at the Civil Engineering Department of Izmir Institute of Technology and all of those who helped me in anyway during the completion of my thesis study.

Finally, I would like to express my deepest appreciation to my beloved parents and my beloved sister for their endless encouragement during my education life and support throughout my life.

ABSTRACT

MODAL PARAMETER IDENTIFICATION OF CIVIL ENGINEERING STRUCTURES BY USING AN OUTPUT-ONLY SYSTEM IDENTIFICATION TECHNIQUE

Civil engineering structures are designed for a limited lifetime. Due to environmental effects and degradation of these structures, engineers need to decide on their structural safety and sustainability from time to time. To this end, structural health monitoring techniques could be employed to determine the current structural state. Current conditions of structures could be investigated by system identification techniques that is based on the modal parameters (modal frequencies, modal damping ratios and mode shapes) of structures.

In this thesis, output-only system identification of civil structures is studied to estimate modal parameters of two different types of structures. For this purpose, a combination of the Natural Excitation Technique (NExT) and the Eigensystem Realization Algorithm (ERA) is coded within Matlab environment. The first study consists of a numerical and an experimental phase. In the numerical phase, the technique is implemented on the mathematical model of a three-story model building. In the experimental phase, it is implemented on the physical model of this three-story model building. 10 different scenarios of structural conditions are simulated by means of changes in story masses of the structure. By using NExT-ERA, the calculated modal frequencies and mode shapes are in good agreement with the results of the eigenvalue analysis. Further, the simulated mass change in each scenario is detected by a least squares approach. Changes in story masses are detected within reasonable errors. In the second study, a methodology is proposed to acquire measurements of large structures by using a few sensors, only. These sensors are used in a segmental way to measure the whole structure. The sensors are grouped and the groups of sensors are shifted on the model to obtain the response measurements from the whole structure. Then the grouped response measurements that are obtained at different time frames are transformed into the equivalent response data as if being acquired at a single time interval. To implement the methodology, a finite element model of a continuous beam bridge is constructed. Modal parameters of the model are estimated by using NExT-ERA and the results show that the first 10 modal frequencies are consistent with those of the eigenvalue analysis of the model, but only the first 6 mode shapes are successfully identified.

ÖZET

İNŞAAT MÜHENDİSLİĞİ YAPILARININ MODAL PARAMETRELERİNİN SADECE-ÇIKTI SİSTEM TANILAMA YÖNTEMLERİNDEN BİRİ KULLANILARAK BELİRLENMESİ

İnşaat mühendisliği yapıları sınırlı bir zaman zarfında hizmet verecek şekilde tasarlanmaktadır. Çevrenin yapılar üzerindeki etkisi nedeniyle yapılar zaman zaman güvenlik kontrolünden geçirilme ihtiyacı duyarlar. Yapıların mevcut durumları, yapı sağlığı izleme yöntemleriyle kontrol edilebilmektedir. Günümüzde modal parametrelerin (mod frekansları, modal sönüm oranları ve mod şekilleri) tayinine dayanan sistem tanılama yöntemleriyle yapıların mevcut durumları hakkında bilgi sahibi olunabilmektedir.

Sunulan bu tez kapsamında, sadece-çıktı sistem tanılama ile iki farklı inşaat yapısının modal parametrelerinin tayini üzerine çalışılmıştır. Bu amaçla, Doğal Uyarım Tekniği (NExT) ve Özsistem Realizasyonu Algoritması (ERA)'nın bir kombinasyonu Matlab ortamında programlanmıştır. İlk çalışma sayısal ve deneysel çalışma olarak iki kısımdan oluşmaktadır. Sayısal çalışmada yöntem üç katlı bir model binanın matematiksel modeli üzerinde uygulanmıştır. Deneysel çalışmada ise yöntem bu üç katlı binanın fiziksel modeli üzerinde uygulanmıştır. Yapısal değişimleri inceleyebilmek adına, kat kütlelerindeki değişimle 10 farklı yapısal durumun davranış benzetimi yapılmıştır. NExT-ERA kullanılarak hesaplanan mod frekanslarının ve mod şekillerinin modelin özdeğer analizi sonuçlarıyla uyumlu olduğu gözlenmiştir. Yapısal durum tespitinde en küçük kareler yöntemi kullanılmıştır. Tespit edilen kütle değişimleri gerçek değişim değerleriyle yakın sonuçlar vermiştir. İkinci çalışmada, büyük inşaat yapılarının sınırlı sayıda algılayıcı kullanılarak ölçümlerinin yapılabilmesi için bir yöntem önerilmiştir. Algılayıcılar gruplar halinde kullanılarak yapının tüm ölçümü alınabilmiştir. Farklı zaman aralıklarında alınan grup ölçümleri yapının eş zamanlı alınan tek bir ölçümüne dönüştürülmüştür. Uygulama için sürekli kiriş bir köprünün sonlu elemanlar modeli oluşturulmuş, NExT-ERA ile modal parametreleri tahmin edilmiştir. Tahmin edilen ilk 10 modun frekansı modelin özdeğer analiz sonuçlarıyla yakın çıkmıştır. Fakat, modelin sadece ilk 6 mod şekli başarılı bir şekilde tahmin edilebilmiştir.

TABLE OF CONTENTS

LIST OF FIGURES

LIST OF TABLES

Table **Page**

CHAPTER 1

INTRODUCTION

1.1. Introduction to Structural Health Monitoring

Structural Health Monitoring (SHM) is the process of evaluating in-service performance of engineering structures (Nagy-Grögy, 2012). In other words, SHM can be defined as frequent or continuous observation of structural conditions of any type of structure. It is intended to control the structures against possible damages which might occur during their life periods. Further, SHM involves the fullest extent of damage detection strategies from the engineering point of view. Chang (1999) also defined SHM as the developments of autonomous systems for the continuous monitoring, inspection, and damage detection of structures with minimum labor involvement.

Structural damage is defined as adverse changes in structural properties of a system, which affect the system's performance. These changes may result in malfunctioning of existing structures and it might be required that in-service structures are being closed to usage. From the civil engineering point of view, consider that a busy running bridge in a metropolis is required to be closed to traffic due to a damage on the bridge. No doubt that all city life will be adversely affected in such a situation. More importantly, adverse changes in structures may cause unexpected and abrupt failure of the structures, threatening human life. It is inevitable for a civil structure to lose the ability to perform its intended function because of environmental effects, such as aging and corrosion. For instance, some cables of a cable-stayed bridge may corrode or some screws of a steel construction may loosen over time resulting in a reduction in the reliability of those structures. In addition, structures might be exposed to overloads due to large scale earthquakes or heavier loads within their lifespan. This means that every existing structure may be subjected to damage sooner or later. Therefore, damage detection comes into prominence from the civil engineering point of view, especially for the structures which might be life-threatening when the failure occurs. At this point, SHM provides essential tools to engineers to improve sustainability and serviceability of existing structures by monitoring, analyzing and understanding the current health of

structures. An SHM system provides worthwhile information for quick assessment of damage levels of structures immediately after urban earthquakes, explosions or an accident. It may also provide an action to take precautions in case of life-threatening situations such as abrupt failures of structures by giving a knowledge of location and severity of structural damage. Furthermore, continuous SHM which is a long-term damage control, generally maintained for important structures such as long bridges, provides continuous control of structural safety and enables future plans for use and repairs as well as estimation of remaining lifetime of the structures (Johnson et al., 2004).

Since the civil engineering applications go back a long way in history, SHM is not actually a new topic around the world. People have always needed to know how healthy and reliable the structures are and needed to understand and repair damages of their structures. These requirements have led to developments in SHM strategies for centuries. Figure 1.1 shows, as an example, a testbed of a truss in England for a railway bridge in India (19th century). In those days, technological restrictions set bounds to the developments in SHM, so people had just visually inspected physical conditions of the structures to detect damage on them for years (Nagy-Grögy, 2012).

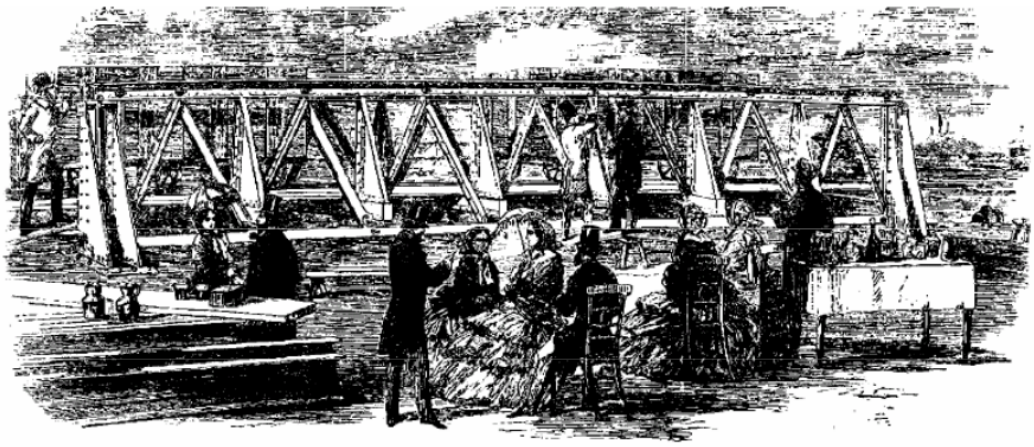

Figure 1.1. A testbed of a truss in England for a railway bridge in India (19th century) (Source: ISIS Canada Educational Module 5, Nagy-György, 2012)

As aforementioned, visual inspection has been used as an SHM technique for many years. It is still the predominant method in SHM to observe physical state of any structure just after a natural disaster such as a major earthquake or hurricane or tsunami, because visual inspection gives a sense about location and severity of damage.

However, visual inspection may be insufficient in the case when damage is less severe. Structures in high risk seismic zones might be subjected to medium or large scale ground motions for many times in their lifespans and many cracks with miscellaneous dimensions may occur on the structural elements. If the occurring damages on the structures are visible, then it can be made required provisions against damages. However, what if the damages are not visible on the structures? As an example to this, two hotels (Aslan Hotel and Bayram Hotel) which collapsed during a 5.6-magnitude earthquake in Van, a city of Turkey, can be considered. In October 2011, a major earthquake with a magnitude of 7.2 occurred in Van and these hotels did not collapse after this major earthquake. Damage detection of these hotels was performed with visual inspection. According to the visual inspection report of the hotels, there was no damage on the structures and so it was permitted to accommodate people in the hotels. However, in the following month of this major earthquake, a second earthquake with a magnitude of 5.6 occurred in the same region and the aforementioned hotels completely collapsed during such a minor earthquake. The cause of the failure was assumed that there had been severe damage on the structural elements of both hotels after the major earthquake, but it could not be realized by visual inspection. Damage may not be visible on the structural elements due to architectural covering elements such as walls and claddings, incapacitating the usage of visual inspection for damage detection purposes. Because it could tend to human error, it is clear that the reliability and accuracy of damage detection by visual inspection can be questioned. Furthermore, it might be difficult to access every structural element on extremely large and complex structures to visually inspect each element, making visual inspection time consuming. All these restrictions have forced researchers interested in SHM to develop more reliable, accurate and faster methods to detect damage on the structures. Developments towards more sophisticated methods in SHM will be discussed under the next subtitles.

Damage detection after the earthquakes seems to be attractive by using SHM techniques. However, the SHM techniques give information of current structural state only. The certain way to investigate structural changes is that current investigations of structural state should be compared with the previous ones to have a significant information of presence of any damage. In other words, identification results of structures which are obtained after a major earthquake are meaningless unless these results are compared with the identification results which are obtained before the earthquake. Thus, at least one reference measurement of dynamic response behavior is

required to compare with the further response measurements. Therefore, by using the SHM techniques, damage detection of a structure after an earthquake might be impossible unless any previous response measurement of the structure is available. Because of these reasons, continuous acquisition of response data of structures is more convenient for damage detection by the SHM techniques. However, continuous SHM requires large amount of data storage memories and so it is hard to save the response data obtained from all of the existing structures. Instead, important structures such as bridges, dams or hospitals could be continuously monitored to provide their sustainability after the disasters.

Furthermore, the SHM methods are called non-destructive testing methods and so a small amount of force is applied to the structures to acquire their response measurements. Since only small amount of forces are applied to the structures, the linear portion of the force-displacement curve could be observed in the analyses and therefore damage could not be detected even if it is present on the structure. In such conditions, destructive testing methods are more suitable. Since large amount of forces are applied to the structures in this type of methods, the nonlinear portion of the force-displacement curve could be observed and presence of any damage on the structure can be easily detected.

1.2. Developments in Structural Health Monitoring

Obtaining the physical response data from structures and conversion of the obtained data to essential information to be used in knowledge-based engineering decisions is a cornerstone for SHM implementations. Physical response data obtained from the structures include loads, deformations, strain, temperature, acceleration and so forth (Nagy-Grögy, 2012). Acquisition of such data from structures require the usage of relevant sensors and compatible data acquisition systems. Moreover, for the conversion of collected data to significant information for engineers, advanced computers and algorithms are the main essentials to cope with vast amount of collected data needed in applications of SHM. At the present time, immense developments in technology of data acquisition systems and computer processor capacities make it possible to deal with large amount of data in addition to developing sensor technology which makes it possible to obtain reliable response data from different type of structures. As a

consequence of ongoing developments of new sensor types and data acquisition systems as well as wireless and internet technologies, data transmission and archiving systems, researchers have been encouraged to develop new SHM techniques.

In the past two decades, an enormous effort has been placed on structural health monitoring in conjunction with technological developments, mainly to detect the possibility of damage in structures, but also to obtain a system model for structural control purposes. To this end, numerous SHM techniques have been developed until today. These developed techniques needed to be classified. However, these techniques not only have a specific parameter to classify in one group but also have different common parameters. Therefore, SHM techniques have several classifications according to different parameters. In the most general sense, there are two main types of SHM techniques which are local and global methods. In local SHM methods, knowledge of the location of damage in structures and access to the structural elements are prerequisites in detecting damage. On the other side, global techniques employ dynamic parameters of structures to detect damage in the structures without any access to the structural elements and there is no requirement to know whether the structural damage exists or not. Therefore, global techniques are mostly preferable for civil structures to reduce time and labor involvement which are needed in localized methods to identify damage location and to access to the structural elements.

Another classification of SHM techniques depends on the degree of the damage identification needed by researchers. According to this classification, there are four levels of damage detection (Caicedo, 2003 and Nagy-Grögy, 2012). In the first level of SHM techniques, it is investigated whether the damage is present in the structure or not. In the second level, damage in the structure is identified with its location on the structure. In the third level, presence and location of structural damage are determined with severity of identified damage. In the forth level, consequences of damage such as remaining lifetime of the structure or possibility of abrupt failures are assessed in addition to the identification of the presence, location and severity of the damage. Nagy-Grögy (2012) schematically represented the classification as in Figure 1.2.

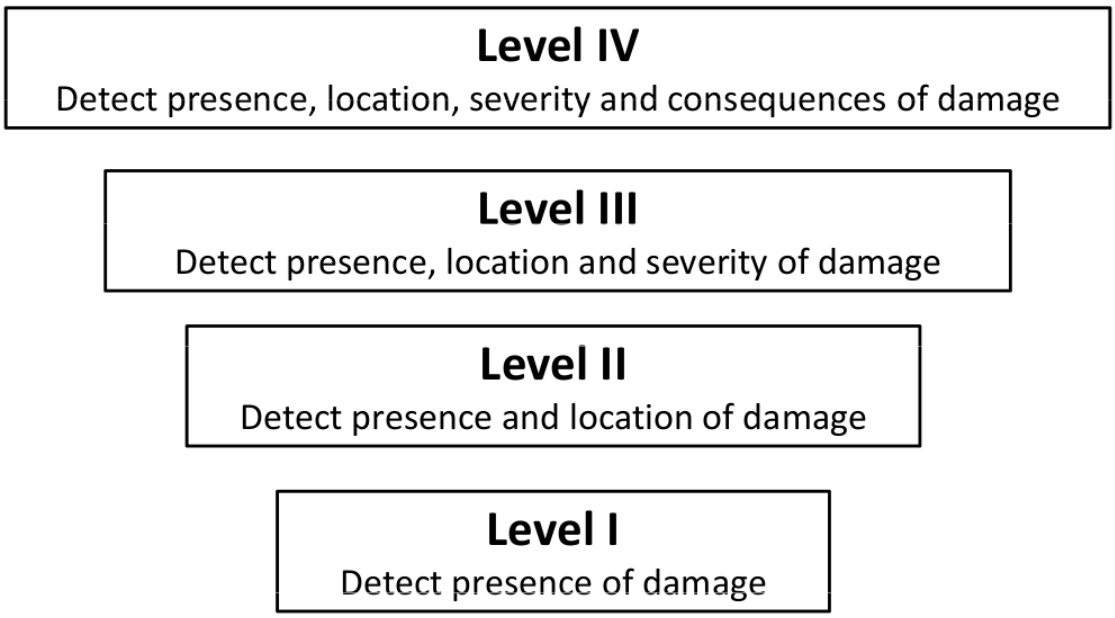

Figure 1.2. Classification of SHM techniques by level of identification
(Source: ISIS Canada Educational Module 5, Nagy-György, 2012)

When structural health monitoring techniques were started to be studied by researchers, different techniques were applied to different structures in various environments. These techniques included many variables which made it difficult to realize similarities and differences between each technique. In order to reduce the variety between the studies and to easily compare the advantages and disadvantages of each technique, in the late 1990s, a task group of the dynamics committee of the American Society of Civil Engineers (ASCE) and the International Association for Structural Control (IASC) developed a benchmark problem for structural health monitoring studies. It allowed researchers to work on the same structure in the same environmental conditions and to compare their newly developed structural health monitoring techniques with existing ones.

The benchmark problem was based on a 4-story, 2-bay by 2-bay steel-frame quarter-scale model structure existing in the Earthquake Engineering Research Laboratory at the University of British Columbia. The benchmark problem had two phases. The first phase was based on the analytical models of the structure and second phase was based on the experimental studies.

In the first phase (analytical phase), it was aimed that researchers would use the simulated data generated from the analytical models of the structure. Thus, they could

easily control the problems they might encounter at the beginning of their studies and have a better understanding of sensitivity of their techniques to various aspects such as modeling errors, noise in measured signals and incomplete sensor data. As a benchmark problem, an undamaged structure and six damage patterns were considered to experience the ability of various methods for detecting, localizing and quantifying the damage. Damage in the structure was simulated by removing braces or decreasing the stiffness of the floor beams. So as to perform these studies, two finite element models of the structure were analytically created to be utilized in structural health monitoring techniques. The first finite element model had a total of 12 DOF. The second one was considered to be more complex than the first one. The reason was that, in most engineering problems, structures might have many complex structural properties and there might be numerous model errors while modeling them. Thus, to be able to include the effects of these modeling errors in studying new structural health monitoring techniques, a second finite element model which had a total of 120 DOF was created. As a consequence, while 120 DOF model was used by researchers to investigate the sensitivity of the methods to modeling errors, the 12 DOF model was used as the identification model due to simplicity. More detailed definitions of the first phase of the benchmark problem together with the finite element models and excitation cases to generate response data were described by Johnson et al. (2004).

According to the researchers of the benchmark study, a positive feedback had been provided after the first phase studies. This promoted the Task Group to go one step forward and they commenced an experimental study of the benchmark problem in year 2002 (Dyke et al., 2004). The second phase was based on this experimental study which was performed to obtain acceleration response measurements from the physical benchmark structure located in the Earthquake Engineering Research Laboratory at the University of British Columbia. The aim for the second phase (experimental phase) was to focus on uncertainties in the structural parameters, less severe damage patterns and to conclude with some blind tests. Three types of excitations were used to generate responses in the experimental study, including ambient vibrations from the environment because of wind or pedestrians, a forced excitation induced by using an impact hammer and another forced excitation induced by an electrodynamic shaker. Nine different damage scenarios were considered in this study. Damage scenarios were simulated by removing braces in the structure or by loosening the bolts at beam-column connections.

More detailed definitions of the second phase of the benchmark problem were described by Dyke et al. (2004).

In this thesis, it has been focused on global SHM techniques which are based on dynamic characteristics of structures. In this type of SHM techniques, extraction of dynamic characteristics of structures is a prerequisite for damage identification purposes. For the extraction of dynamic characteristics, a system identification process has to be performed on structures. In the next section, basic information about system identification to obtain dynamic characteristics of the structural systems are discussed.

1.3. System Identification

SHM is the process of identification of damage in structures and a remarkable portion of this process consists of obtaining the required parameters for damage detection. These parameters are generally obtained from dynamic systems and gives information about dynamic characteristics of an individual system. Dynamic characteristics of a systems provide the information about its current internal working. A comparative study which is then performed between previous and current situations gives the damage information of the systems. This is the process for the most damage identification techniques in literature.

Obtaining an accurate system model of internal working of the systems, generally from experimental studies, is known as *system identification* (Yıldırım, 2014)

The required dynamic parameters to get an idea about current internal working of the systems are extracted by using the developed system identification techniques. Among these techniques, vibration-based system identification methods which take part in global damage identification techniques have been increasingly developed mostly around civil, mechanical and aerospace engineering communities to enable using vibrational response of the structures. The idea behind the vibration-based system identification is that changes in the structural properties such as stiffness, mass or damping also change modal parameters of the structures (natural frequencies, damping ratio or mode shapes) (Fan and Qiao, 2011). Among the vibration-based system identification techniques, methods which are based on extraction of modal parameters from measured vibration responses are known as modal-based system identification techniques (modal analysis techniques) and methods which are based on statistical

assessment of damage-sensitive properties of structures again using vibration response measurements are known as signal-based system identification techniques (Mahmood et al. 2014).

Modal-based system identification methods are the most preferred ones around engineering communities, because modal parameters of the systems can give full information about the existence, location and severity of the damage whereas the signal-based methods are capable of identifying the existence of damage only. (Mahmood et. al, 2014). Moreover, vibration response of a structure can be easily measured using the recent data acquisition and sensor technologies, and modal parameters of a structure from measured dynamic response data can be obtained more easily than other mathematical features of the structures.

In real life, obtaining the vibration response of existing structures always requires an in-situ experimental work, and so modal-based techniques are also known as *experimental modal analysis* among SHM communities. It should be noted that an accurate damage identification process based on experimental modal analysis might be only possible in case of obtaining accurate modal parameters (Moaveni, 2007). This, for example, depends on vibration measurements, because measurement process during the experimental works is directly affected by environmental conditions such as addition of measurement noise to data obtained or it may have some limitations due to technological restrictions. For instance, data acquisition systems always record structural vibration measurements in time domain only. However, it is generally difficult to deal with the response data in time domain for damage identification purposes. Hence, time domain data are generally transformed into frequency domain data which then can be used to obtain modal domain data to extract modal parameters of the systems in modal-based system identification techniques (Fan and Qiao, 2011). All three domains (time, frequency and modal domain) are being used by researchers, however each of these domains does not result in dependable system identification results for different types of structures.

Systems are generally considered as static or dynamic systems. For a system to be considered as dynamic, the system is required to have inputs and have outputs related with the dynamic characteristics of it. Therefore, having information about given inputs to the systems and outputs related with the given inputs can provide information about the dynamic characteristics of the systems. In some cases, having information of the outputs is sufficient to get dynamic characteristics of the systems. To this end,

modal-based system identification techniques have been categorized as input-output methods and output-only methods. In the input-output methods of modal identification techniques, vibration response output of a system is required together with the measurement of the input force to the system. On the other hand, output-only methods require measurement of the vibration response output of a system only. Both methods have implementations in literature, depending on type of the structure which is worked on and technological restrictions that researchers encounter.

1.4. Objective and Scope

This thesis involves two research studies conducted mainly to enhance the understanding of an output-only system identification technique. Within this scope, a combination of Natural Excitation Technique (NExT) and Eigensystem Realization Algorithm (ERA) (NExT-ERA) which is one of the output-only system identification techniques in the literature is used for modal parameter identification of two types of civil structures. Today, modal based system identification techniques are the most attractive ones around SHM communities, since changes in modal parameters can give a direct information on changes in structural conditions. Moreover, it is always difficult to excite civil structures by external forces in a controlled manner due to their large dimensions. Even if it is possible, researchers face difficulty of measuring such forces. With these pros and cons in mind, the aim of our decision to select NExT-ERA as the system identification method is that it is capable of identifying modal parameters of systems excited by ambient vibrations without having any knowledge of excitation forces.

The main objective of this thesis is to build an algorithm for the NExT-ERA method to obtain modal parameters of structures for determination of their structural reliability. For this purpose, an algorithm of NExT-ERA is coded within the Matlab environment. The NExT-ERA algorithm is used for identification of modal parameters and story mass changes of a three-story steel model building which is located in the Structural Mechanics Laboratory of Izmir Institute of Technology (IYTE). First, the methodology is numerically implemented on a mathematical model of the building. In addition to the NExT-ERA algorithm, a small program of a least squares approach is coded to assess the simulated changes in structural conditions. This numerical study

allow the verification of the coded algorithm of NExT-ERA. In addition, it reveals the capability of the method for detection of presence, location and severity of damage. Then, the methodology is experimentally implemented on the physical structure located in the laboratory. The objective herein is to implement the NExT-ERA method on an existing physical structure. This study allows us to deal with the difficulties encountered during in-situ applications and also allows us to modify the coded algorithm for real-life applications. Within the scope of this thesis, capability of the NExT-ERA algorithm is also assessed in case of acquiring measurements using a few sensors, only. For this objective, few sensors are used in a segmental way to measure a bridge type structure. A methodology is proposed to have measurements of the full bridge by using acquired segmental measurements, only.

CHAPTER 2

THEORETICAL BACKGROUND OF NExT-ERA

2.1. Introduction

In this chapter, some theoretical background information is provided, which is necessary to be able to understand the output-only system identification technique used in this thesis to obtain modal parameters of the structures.

The output-only system identification technique used is a combination of the Natural Excitation Technique (NExT) and the Eigensystem Realization Algorithm (ERA) (NExT-ERA). NExT-ERA is capable of identifying dynamic characteristics of structures by using ambient vibration responses without having knowledge of the excitation forces. To be able to analyze the acquired ambient vibration response data in NExT-ERA, the data have to be processed by signal processing techniques and must have some specific statistical properties. It should be noted here that it is impossible to have accurate identification results unless the convenient response signals are used in the identification processes. Therefore, a clear understanding of signal processing and statistical properties of signals acquired has a significant importance to make use of convenient response signals in the identification techniques. To this end, before discussing the methodology used in this thesis, some information about signal processing and statistical properties of signals are provided. Some basic definitions about signal processing are provided in Section 2.2. Then, specific statistical properties of the signals to be able to be used in NExT-ERA are provided in Section 2.3.

After providing information required to understand the methodology, NExT and ERA are discussed in detail in Section 2.4 and 2.5, respectively. In addition, a least squares approach is discussed to explain the identification process of changes in structural conditions after the identification of the modal parameters in Section 2.6.2.

2.2. Signal Processing

2.2.1. Basic Information

A signal is a function of one or more independent variables and comprises of information about behavior of incidents. A dynamic system is the system whose state varies with time and generally gives a response to a specific signal by generating another signal. Figure 2.1 shows a schematic representation of system-signal relationship. In the figure, $x(t)$ and $y(t)$ are mathematical representations of different

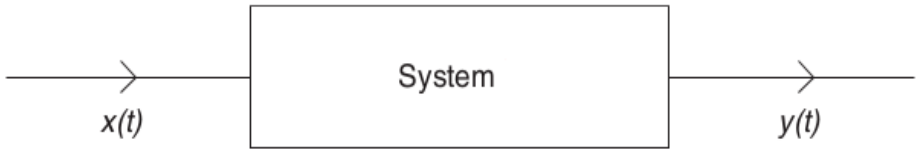

Figure 2.1. A schematic representation of system-signal relationship

signals which are input signal and output signal both in time domain, respectively. Since there is just one input and one output in this system, such systems are called single input single output (SISO) systems. Moreover, systems may give more than one output signal in spite of having just one input signal and such systems are called single input multi outputs (SIMO) systems or vice versa (MISO), or they may give multi outputs in response to multi inputs (MIMO). As an example, when a 3-story building is excited by an impact hammer at the top story and accelerations of each story are measured, this system is called a SIMO system.

2.2.2. Deterministic and Random Signals

In the most general sense, signals are classified as deterministic or random. A signal is deterministic if its value at any point in a time interval is foreseeable. Deterministic signals can be expressed by mathematical equations and they can be reproduced in case of meeting the same conditions. Once again considering a 3-story building model, solution of dynamic equation of motion of the model gives acceleration,

velocity and displacement response of the structure at any point in interested time interval for a specified set of initial conditions. Therefore, these response data are considered as deterministic signals.

A signal is random if its value at any point in a time interval is partially dependent on chance and unforeseeable. Random signals cannot be expressed by any mathematical equations and cannot be reproduced because of their randomness nature. Instead of mathematical equations, this type of signals are expressed by the concepts of probability and statistics. Random signals are obtained due to stochastic processes so they are also called stochastic signals. Stochastic processes gain an importance in SHM implementations of civil structures, especially in case of output-only identification processes. Because excitations due to ambient vibrations such as wind, traffic or ground motion loads on the structures are unpredictable and provide random signal inputs to the structures. The output-only system identification technique used in this thesis (NExT-ERA) employs ambient vibrations of the structures, thus understanding the stochastic processes and random signals is a fundamental tool to obtain successful identification results. Therefore, random signals are discussed in detail in the following sections. In the next section, classification of random signals is discussed as an introduction to statistical properties of this type of signals.

2.2.3. Classification of Random Signals

A random signal consists of a set of random values, usually in time domain. Statistically, each random value belongs to a probability distribution. If a random value on a distribution is independent from another one, the data are called independent. In general, each random value has a different probability distribution. However as a special case, when each probability distribution is identical, then the data are called identically distributed. When these two processes are present on the data, then the data are called independent and identically distributed. If this phenomenon is present on a random signal, just one probability distribution is needed to define the signal. For example, random signals based on a special probability distribution called Gaussian distribution have an importance from SHM engineering point of view. Because Gaussian distribution has constant statistical values which are its mean value and variance. Moreover, by the definition of central limit theorem, summation of independent random

values with different probability distributions approaches a Gaussian distribution. This makes the Gaussian distribution a powerful tool while modeling real-life SHM applications. Because in real-life, acquired data generally have measurement noises induced from different environmental sources with unknown different probability distributions. In the analysis, total measurement noise can be modeled as a Gaussian random signal as a result of the definition of central limit theorem. Figure 2.2 shows a representative Gaussian random signal over a time length of 100 seconds wit a sampling period of 0.01 sec.

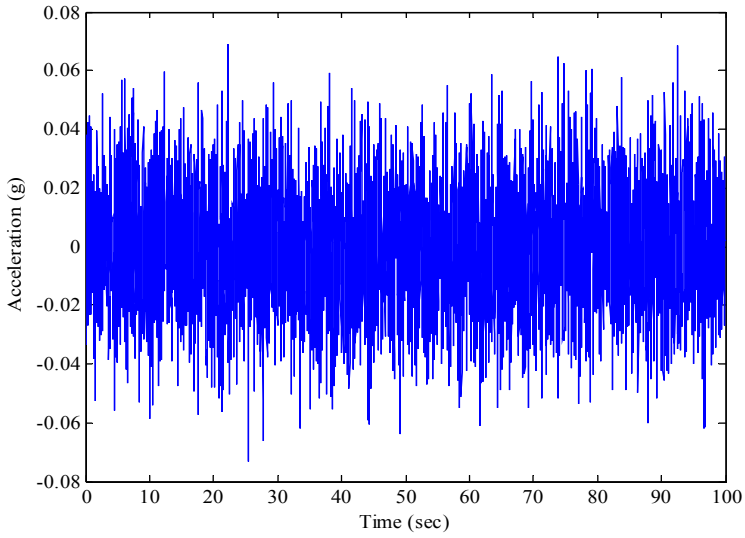

Figure 2.2. A representative Gaussian random signal over a time period of 100 s

Random signals can be classified as stationary or non-stationary. If a random signal has constant statistical values, the signal is called stationary. In random signals, if mean value and variance are the only constants, this type of random signals is called weakly stationary. In SHM applications, stationary signals are the most encountered signals because most physical events can be modeled as stationary. For example, ambient excitations due to rush hour traffic or long-continued wind can be modeled using stationary signals.

Some incidents such as breakdown of a sensor or a device during data acquisition may disturb stationarity of the signals. In this case, the mean or variance of the signal may vary with time. This type of signals are called non-stationary signals. Considering non-stationary signals has an importance in determining the failures in

acquisition process. Figure 2.3 (a) and (b) show representative stationary and non-stationary signals over a time period of 100 s, respectively.

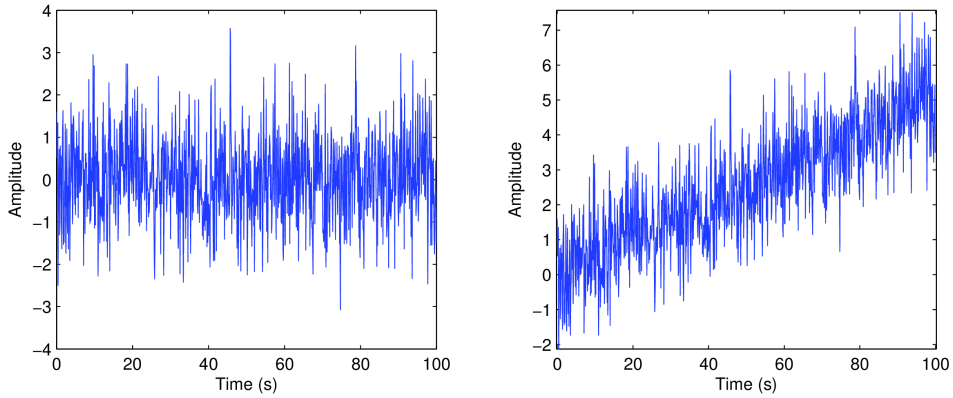

(a) *(b)*

Figure 2.3. Representative (a) stationary and (b) non-stationary signals over a time period of 100 s.

Random signals have numerous statistical features used in engineering applications. Among these features, some specific ones are the essentials to be able to understand the theoretical development of NExT which is provided in section 2.4. Some of these specific statistical concepts are based on the Fourier analysis of the signals and Fourier transform. Hence before discussing the statistical features, a short description of Fourier transform is provided in the following section.

2.2.4. Fourier Transform in Signal Processing

Before introducing the Fourier transform theory, it should be mentioned about continuous-time and discrete-time signals. Specified time can be continuous or discrete depending on type of the analysis performed. If the data used are analytical, then, the signal function could be continuous over time. If the signals are continuous, the signal can take values at any time instant and so continuous-time signals have an infinite number of values over time. Signals from analog systems are considered as continuous signals. On the other hand, if the data are obtained by data acquisition systems, each random signal value corresponds to a discrete time value. If the signals are discrete, the signals take values at specific time values and so discrete-time signals have finite

number of values over time. In real life, data acquisition systems always give discrete-time data.

In real life, data acquisition systems always acquire signals in time domain. If the signals of interest are especially random data, acquired time series do not provide any significant information by visually inspecting the data as a consequence of complex view of the signal. In such conditions, an effective tool to get significant information from the signal is to transform its domain into another one. As an example, for damage detection via vibration analysis, one of the attractive methods used for feature extraction is natural frequency-based methods. Such methods are based on the idea that change in natural frequencies gives information about damage occurred in structures (Fan and Qiao, 2011). To be able to analyze frequency content of the signals in this type of methods, the data in time domain have to be transformed into frequency domain. Thus the signal which already includes significant information but becomes meaningless when in time domain reaches significance when transformed into frequency domain. At this point, Fourier transform is used to decompose a signal of time into its frequency content.

For a continuous-time and non-periodic random signal $x(t)$ over the interval $[-\infty, +\infty]$, general definition of Fourier transform is as,

$$F[x(t)]=x(\omega)=\int_{-\infty}^{+\infty} x(t)e^{-i\omega t dt} \tag{2.1}$$

where *F[x(t)]* represents the Fourier transform of the signal $x(t)$. Inversely, the frequency-domain signal can be transformed into a signal of time by the inverse Fourier transform defined as,

$$F^{-1}[x(\omega)]=x(t)=\frac{1}{2\pi}\int_{-\infty}^{+\infty} x(\omega)e^{i\omega t}d\omega \tag{2.2}$$

where $F^{-1}[x(\omega)]$ represents the inverse Fourier transform of the frequency-domain signal $x(\omega)$. Inversely, x(t) is the corresponding time-domain signal of frequency-domain signal, x(ω).

However, acquired signals always have a finite duration in reality. In addition, they cannot be acquired in the form of continuous-time due to impossibility of computers to have infinite memory to store continuous functions even if they have a

finite duration. Instead, data acquisition systems and computers take measurements as discrete-time signals which have values just at certain time intervals, causing the signals to be sampled over time. Therefore, an acquired signal is actually a finite vector with N values. To be able to transform such discrete-time signals into frequency domain, Fourier transform defined above cannot be employed. For decomposition of discrete signals, definition of discrete Fourier transform (DFT) must be considered.

For a discrete-time signal $x_r=\{x_0, x_1, x_2,\ldots, x_N\}$ with a sampling period of dt where $x[t_0]=x_0$, $x[t_1]=x_1$ and $x[t_N]=x_N$, and $t_N=t_{N-1}+dt$, DFT is defined as,

$$X_n=\sum_{r=0}^{N-1} x_r e^{-i\frac{2\pi nr}{N}} \tag{2.3}$$

where X_n is the DFT of the signal x_r. Therefore, X_n is actually a finite vector containing the corresponding frequency-domain values of the signal of time x_r. To return the original time-domain signal from the frequency-domain, inverse discrete Fourier transform (IDFT) is defined in the similar manner with the Fourier transform for continuous signals as,

$$x_r=\frac{1}{N}\sum_{n=0}^{N-1} X_n e^{i\frac{2\pi nr}{N}} \tag{2.4}$$

However, calculations of DFT defined by equations 2.3 and 2.4 require a heavy computational afford and in order to overcome this difficulty, an algorithm has been developed called Fast Fourier Transform (FFT) to compute DFT in a timesaving way. Currently, most Fourier transform computations are carried out by FFT in many computer programs. FFT was also performed to calculate DFT of signals during the studies presented in this thesis. Development of FFT algorithm is provided by Bendat and Piersol (2010) and Farrar and Worden (2012) in detail.

It should be noted here that frequency content information which can be obtained from time-domain measurements depends on the sampling period of time-domain data. According to the Nyquist frequency theorem, the highest frequency information which can be obtained from time series is half of the sampling frequency of ($f_s=1/dt$, f_s is the sampling frequency of discrete time series) time-domain data. Thus,

this highest frequency is called the Nyquist frequency and has a great importance in signal processing.

2.3. Statistical Features of Random Signals

There are numerous statistical features in random signals, but only two major ones will be explained here, which are necessary to understand the concept in this thesis. These statistical features are the power spectral density functions and the correlation functions.

2.3.1. Power Spectral Density Function

The power spectral density function is a tool for the frequency analysis of stationary random signals. It demonstrates the variation of the mean square values which correspond to the related frequency values for stationary random signals.

Before introducing the estimation of the spectral density functions, a problematic situation associated with it should be firstly discussed. Finite duration random signals cannot represent the long-term frequency content unlike the infinite ones and they cause an error due to their finite duration nature (Farrar and Worden 2012). To overcome this issue, an averaging process is applied on the finite samples during the calculation of spectral density functions. Let x_T be a discrete-time signal with a finite duration and M samples, the frequency content of x_T is then expressed as

$$X(\omega)=E[X(\omega)]+E[\in_{\tau}(\omega)] \tag{2.5}$$

where E[] is the operator showing the expected value of its content, $\in_{\tau}(\omega)$ is the error term resulting because of the finite duration and $X(\omega)$ is the frequency-domain equivalent of the signal x_T. The averaging process is applied by employing N fragments of discrete-time signal x_T defining $X_n(\omega)=X(\omega)+\in_{\tau n}(\omega)$, then $X(\omega)$ is obtained as;

$$X(\omega)\approx E[X_n(\omega)]=\frac{1}{N}\sum_{n=0}^{N}X_n(\omega) \tag{2.6}$$

where $X(\omega)$ is the estimated frequency-domain signal without the error term included, X_n represents each term in the fragment for the values of n=1,2,...,N.

Then, the spectral density is estimated as,

$$S_{xx}(\omega)=E[|X(\omega)|^2]=E[X(\omega)X^*(\omega)] \tag{2.7}$$

where $S_{xx}(\omega)$ is the power spectral density function, $X^*(\omega)$ is the complex conjugate transform of $X(\omega)$.

The power spectral density is defined in three different ways:

I) Spectral density form correlation functions

II) Spectral density from finite Fourier transforms

III) Spectral density from filtering-squaring-averaging operations

2.3.1.1. Spectral Density Functions From Correlation Functions

As the first way, spectral density functions can be calculated from correlations as the Fourier transform of the correlation functions. For stationary continuous-time random signals x(t) and y(t), two-sided power spectral density functions are defined for ω over $(-\infty,+\infty)$ by

$$S_{xx}(\omega)=\int_{-\infty}^{+\infty} R_{xx}(\tau)e^{-j2\pi\omega\tau}d\tau \tag{2.8}$$

$$S_{yy}(\omega)=\int_{-\infty}^{+\infty} R_{yy}(\tau)e^{-j2\pi\omega\tau}d\tau \tag{2.9}$$

$$S_{xy}(\omega)=\int_{-\infty}^{+\infty} R_{xy}(\tau)e^{-j2\pi\omega\tau}d\tau \tag{2.10}$$

where S_{xx} and S_{yy} are the auto-spectral density functions of x(t) and y(t), respectively and S_{xy} is the cross-spectral density function between x(t) and y(t). R_{xx} and R_{yy} are the autocorrelation functions of x(t) and y(t), respectively and R_{xy} is the cross-correlation function between x(t) and y(t).

For stationary discrete-time random signals x_k and y_k, equations 2.8, 2.9, and 2.10 can be expressed as

$$S_{xx}(r)=\frac{1}{N}\sum_{k=1}^{N} R_{xx}(k)e^{\frac{-j2\pi rk}{N}} \tag{2.11}$$

$$S_{yy}(r)=\frac{1}{N}\sum_{k=1}^{N} R_{yy}(k)e^{\frac{-j2\pi rk}{N}} \tag{2.12}$$

$$S_{xy}(r)=\frac{1}{N}\sum_{k=1}^{N} R_{xy}(k)e^{\frac{-j2\pi rk}{N}} \tag{2.13}$$

where N is the number of points of the corresponding cross-correlation functions.

Assuming that the integral of the absolute values of R_{xy} has a finite duration which is defined as,

$$\int_{-\infty}^{+\infty} \left|R_{xy}(\tau)\right| d\tau < \infty \tag{2.14}$$

It reveals that the definition of the cross-spectral density function is also valid for finite record lengths. This is also true for the autocorrelation functions R_{xx} and R_{yy}.

2.3.1.2. Spectral Density Functions From Finite Fourier Transforms

As the second way, spectral density functions can be calculated from finite Fourier transform of the original data records. For stationary discrete-time random signals x_k and y_k in a finite time interval $0 \le t \le T$, define

$$S_{xy}(\omega,T,k)=\frac{1}{T}X_k^*(\omega,T)Y_k(\omega,T) \tag{2.15}$$

where

$$X_k(\omega,T)=\int_0^T x_k(t)e^{-j2\pi\omega t}dt \tag{2.16}$$

$$Y_k(\omega,T)=\int_0^T y_k(t)e^{-j2\pi\omega t}dt \tag{2.17}$$

In the equations above, $X_k(\omega,T)$ and $Y_k(\omega,T)$ demonstrate finite Fourier transforms of the signals x_k and y_k, respectively. In equation 2.15, $X_k^*(\omega,T)$ represents the complex conjugate of $X_k(\omega,T)$.

Then, the cross-spectral density function is defined by the expression

$$S_{xy}(\omega)=\lim_{T\to\infty} E[S_{xy}(\omega,T,k)] \tag{2.18}$$

where $E[S_{xy}(\omega,T,k)]$ is the expected value of $S_{xy}(\omega,T,k)$. Auto-spectral density functions $S_{xx}(\omega)$ and $S_{yy}(\omega)$ can be obtained in a similar way.

2.3.1.3. Spectral Density Functions From Filtering-Squaring-Averaging Operations

As the third way, the spectral density functions can be obtained by applying filtering, squaring and averaging operations on stationary random signals (Bendat and Piersol, 2010). For the stationary random signal x(t) with a record length T, the auto-spectral density function is estimated by using the following procedure;

- Frequency filtering is performed on the signal x(t) using a narrow bandpass filter whose bandwidth is B and center frequency is f_c in order to find $x(f_c, B, t)$.
- Squaring is then applied on the instantaneous value of the filtered signal.
- Next, averaging is applied on the squared value over T and as a result of averaging applied, a mean square value of the filtered signal is estimated.
- Then, the result is divided by bandwidth B to obtain the rate of change of the mean square value with the center frequency f_c.

Then, the auto-spectral density function of the signal $x(t)$ is mathematically defined as

$$G_{xx}(f)=\frac{1}{BT}\int_0^T x^2(f_c,B,t)dt \tag{2.19}$$

In the case of estimation of the cross-spectral density function, a similar procedure is performed. For stationary random signals $x(t)$ and $y(t)$ with a record length T, the cross-spectral density function is determined by the following procedure;

- Frequency filtering is applied on both the signals $x(t)$ and $y(t)$ by using narrow bandwidth filters whose bandwidths and center frequencies are the same, which are B and f_c, respectively. As a result of filtering, $x(f_c, B, t)$ and $y(f_c, B, t)$ are obtained.
- Then, the instantaneous values of the filtered signals are multiplied by each other without phase shifting to have the in-phase terms.
- The instantaneous values of the filtered signals are multiplied by $y(f_c, B, t)$ shifted 90° with respect to $x(f_c, B, t)$ to have the out-of-phase terms.
- Averaging is then applied on the above multiplication results over T and as a result of averaging, mean products of the in-phase and out-of-phase terms are estimated.
- Each mean product result is divided by bandwidth B to obtain $C_{xy}(f)$ and $Q_{xy}(f)$.

The cross-spectral density function between the signals $x(t)$ and $y(t)$ is mathematically defined as

$$G_{xy}(f) = C_{xy}(f) - jQ_{xy}(f) \tag{2.20}$$

where

$$C_{xy}(f) = \frac{1}{BT}\int_0^T x(f_c, B, t)\, y(f_c, B, t)\, dt \tag{2.21}$$

$$Q_{xy}(f) = \frac{1}{BT}\int_0^T x(f_c, B, t)\, y^{90}(f_c, B, t)\, dt \tag{2.22}$$

In equation 2.22, $y^{90}(f_c, B, t)$ represents a phase shift of 90° of the filtered signal $y(f_c, B, t)$.

2.3.2. Correlation Functions

Correlation functions are also important statistical features of random signals. A correlation function is a demonstration of how much similarity exists between the random signals. For stationary random signals x(t) and y(t), the correlation functions are defined as

$$R_{xx}(\tau)=E[x(t)x(t+\tau)] \tag{2.23}$$

$$R_{yy}(\tau)=E[y(t)y(t+\tau)] \tag{2.24}$$

$$R_{xy}(\tau)=E[x(t)y(t+\tau)] \tag{2.25}$$

where $R_{xx}(\tau)$ and $R_{yy}(\tau)$ denote the autocorrelation functions of x(t) and y(t), respectively. For the random signal x(t), the autocorrelation function demonstrates how much similarity exists between x(t) and $x(t+\tau)$ which is time shifted by an amount of τ. It shows how much similar a signal is to itself when shifted in time. $R_{xy}(\tau)$ represents the cross-correlation function between the random signals x(t) and y(t). A cross-correlation function demonstrates how much similarity exists between the signals x(t) and y(t).

In equations 2.23, 2.24 and 2.25, the mean values are constants for all values of t. The mean values are independent of t and they are defined as

$$\mu_x=E[x(t)]=\int_{-\infty}^{+\infty} xp(x)dx \tag{2.26}$$

$$\mu_y=E[y(t)]=\int_{-\infty}^{+\infty} yp(y)dy \tag{2.27}$$

where *p(x)* and *p(y)* are the probability density functions of random variables.

For arbitrary μ_x and μ_y, the covariance functions can be defined as the functions of correlation functions by the equations

$$C_{xx}(\tau)=R_{xx}(\tau)-\mu_x^2 \tag{2.28}$$

$$C_{yy}(\tau)=R_{yy}(\tau)-\mu_y^2 \tag{2.29}$$

$$C_{xy}(\tau)=R_{xy}(\tau)-\mu_x\mu_y \tag{2.30}$$

For equations 2.28, 2.29 and 2.30, correlation functions are equal to covariance functions when the mean values are zero. Two stationary random signals x(t) and y(t) become uncorrelated when $C_{xy}=0$ for all values of τ. According to equation 2.30, these two signals are uncorrelated when $R_{xy}(\tau)=\mu_x\mu_y$ for all values of τ. In this case, these two signals also become uncorrelated if $R_{xy}(\tau)=0$ for all values of τ when either μ_x or μ_y has a value of zero.

Correlation functions can be estimated directly from finite recorded data or from power spectral density functions. Using finite record data considering two discrete-time stationary random signals x_k and y_k with N samples for both, the correlation functions are defined as

$$R_{xx}(\tau)=\lim_{N\to\infty}\frac{1}{N}\sum_{k=1}^{N}x_k(t)\,x_k(t+\tau) \tag{2.31}$$

$$R_{yy}(\tau)=\lim_{N\to\infty}\frac{1}{N}\sum_{k=1}^{N}y_k(t)\,y_k(t+\tau) \tag{2.32}$$

$$R_{xy}(\tau)=\lim_{N\to\infty}\frac{1}{N}\sum_{k=1}^{N}x_k(t)\,y_k(t+\tau) \tag{2.33}$$

where $R_{xx}(\tau)$ and $R_{yy}(\tau)$ are the autocorrelation functions of $x_k(t)$ and $y_k(t)$, respectively. $R_{xy}(\tau)$ is the cross-correlation function between $x_k(t)$ and $y_k(t)$.

Using the power spectral density functions, the cross-correlation functions can be estimated as the inverse Fourier transform of the power spectral density functions based on equations 2.8, 2.9, and 2.10. For continuous-time stationary random signals x(t) and y(t), the correlation functions are defined as

$$R_{xx}(\tau)=\int_{-\infty}^{+\infty}S_{xx}(\omega)e^{j2\pi\omega\tau}d\omega \tag{2.34}$$

$$R_{yy}(\tau)=\int_{-\infty}^{+\infty} S_{yy}(\omega)e^{j2\pi\omega\tau}d\omega \tag{2.35}$$

$$R_{xy}(\tau)=\int_{-\infty}^{+\infty} S_{xy}(\omega)e^{j2\pi\omega\tau}d\omega \tag{2.36}$$

where $S_{xx}(w)$ and $S_{yy}(w)$ are the two-sided auto-spectral density functions and $S_{xy}(w)$ is the two-sided cross-spectral density function between x(t) and y(t). For discrete-time stationary random signals $x_k(t)$ and $y_k(t)$ with N samples for both, correlation functions are defined based on equations 2.11, 2.12, and 2.13 as

$$R_{xx}(r)=\frac{1}{N}\sum_{k=1}^{N} S_{xx}(k)e^{\frac{j2\pi rk}{N}} \tag{2.37}$$

$$R_{yy}(r)=\frac{1}{N}\sum_{k=1}^{N} S_{yy}(k)e^{\frac{j2\pi rk}{N}} \tag{2.38}$$

$$R_{xy}(r)=\frac{1}{N}\sum_{k=1}^{N} S_{xy}(k)e^{\frac{j2\pi rk}{N}} \tag{2.39}$$

Estimation of correlation functions using the power spectral density functions leads to averaging, filtering and windowing options during signal processing. Therefore, the cross-correlation functions which are essentials in the NExT method used in this thesis were estimated by the inverse Fourier transform of the cross-spectral density functions. The NExT method is based on the correlation functions of derivatives of random signals. To be able to have a better understanding of the methodology, it is necessary to present the derivative of random signals. In the following section, some basic theoretical background about the derivative of random signals are provided.

2.3.2.1. Derivative of Random Signals

In the most general sense, the derivative of any sample signal $x(t)$ in a random signal $X(t)$ is defined as

$$\dot{x}(t)=\frac{dx(t)}{dt}=\lim_{\epsilon\to 0}\left[\frac{x(t+\epsilon)-x(t)}{\epsilon}\right] \tag{2.40}$$

According to Bendat and Piersol, this derivative $\dot{x}(t)$ exists in two different ways. In the usual sense, $\dot{x}(t)$ exists if the limit has existence over all signals x(t) in the signal X(t). x(t) represents the fragmental signals that are obtained from the signal X(t). In the mean square sense, $\dot{x}(t)$ exists when

$$\lim_{\epsilon \to 0} E\left[\left|\frac{x(t+\epsilon)-x(t)}{\epsilon}-\dot{x}(t)\right|^2\right]=0 \tag{2.41}$$

Considering the mean square sense for a weakly stationary random signal, the required condition for $\dot{x}(t)$ to exist is that the first and the second order derivatives of autocorrelation function of x(t) which are $R'_{xx}(\tau)$ and $R''_{xx}(\tau)$ must exist. Here, $R'_{xx}(\tau)$ and $R''_{xx}(\tau)$ are defined as

$$R'_{xx}(\tau)=\frac{dR_{xx}(\tau)}{d\tau} \tag{2.42}$$

$$R''_{xx}(\tau)=\frac{d^2R_{xx}(\tau)}{d\tau^2} \tag{2.43}$$

For a weakly stationary random signal x(t), consider the following equations

$$R_{xx}(\tau)=E[x(t)x(t+\tau)]=E[x(t-\tau)x(t)] \tag{2.44}$$

$$R_{x\dot{x}}(\tau)=E[x(t)\dot{x}(t+\tau)]=E[x(t-\tau)\dot{x}(t)] \tag{2.45}$$

where

$$R_{x\dot{x}}(\tau)=R'_{xx}(\tau)=\frac{d}{d\tau}E[x(t)x(t+\tau)] \tag{2.46}$$

This expression is also equal to the following expression,

$$R'_{xx}(\tau)=\frac{d}{d\tau}E[x(t-\tau)x(t)]=-E[\dot{x}(t-\tau)x(t)]=-R_{\dot{x}x}(\tau) \tag{2.47}$$

The same expressions are valid for cross-correlation functions. By the definition in equation 2.45, the cross-correlation function between $\dot{x}(t)$ and y(t) can be defined as

$$R_{\dot{x}y}(\tau)=E[\dot{x}(t)\,y(t+\tau)]=E[\dot{x}(t-\tau)\,y(t)] \tag{2.48}$$

Using equation 2.40, equation 2.48 can be rewritten as

$$R_{\dot{x}y}(\tau)=E\left[\lim_{\epsilon\to 0}\left[\frac{x(t+\epsilon)-x(t)}{\epsilon}\right]y(t+\tau)\right] \tag{2.49}$$

It should be noted here that the expectation of a limit is equivalent to the limit of the expectation for random signal functions. By this definition, equation 2.49 can be expressed as

$$R_{\dot{x}y}(\tau)=\lim_{\epsilon\to 0}\frac{1}{\epsilon}E\left[x(t+\epsilon)\,y(t+\tau)-x(t)\,y(t+\tau)\right] \tag{2.50}$$

By using one of the properties of expectation operators such as $E[x(t)+y(t)]=E[x(t)]+E[y(t)]$, the last expression can be rewritten as

$$R_{\dot{x}y}(\tau)=\lim_{\epsilon\to 0}\frac{1}{\epsilon}\left[E\left[x(t+\epsilon)\,y(t+\tau)\right]-E\left[x(t)\,y(t+\tau)\right]\right] \tag{2.51}$$

By the definition of the cross-correlation function in equation 2.25,

$$R_{\dot{x}y}(\tau)=\lim_{\epsilon\to 0}\frac{1}{\epsilon}\left[R_{xy}(t+\epsilon,t+\tau)-R_{xy}(t,t+\tau)\right] \tag{2.52}$$

It should be noted that, autocorrelation and cross-correlation functions are independent of t for weakly stationary random signals and therefore,

$$R_{xy}(t,t+\tau)=R_{xy}(\tau) \tag{2.53}$$

Thus, equation 2.52 yields the following result;

$$R_{\dot{x}y}(t,t+\tau)=\frac{\partial}{\partial t}R_{xy}(t,t+\tau)=\dot{R}_{xy}(t,t+\tau) \tag{2.54}$$

Caicedo (2001) pointed out that the last expression can be written in the general form as

$$R_{x^m y^n}(t,t+\tau)=\frac{\partial^{m+n}}{\partial t^m \partial v^n}R_{xy}(t,t+\tau) \tag{2.55}$$

By considering equation 2.48 and the definition in equation 2.53, the cross-correlation function between $\dot{x}(t)$ and y(t) can be defined as

$$R_{\dot{x}y}(\tau)=-\frac{\partial}{\partial t}R_{xy}(\tau)=-\dot{R}_{xy}(\tau) \tag{2.56}$$

As a consequence, Caicedo (2001) came to the conclusion that, for weakly random signals, the cross-correlation function of derivatives in the mean square sense can be described as

$$R_{x^m y^n}(t,t+\tau)=R_{x^m y^n}(\tau)=(-1)^n\frac{\partial^{m+n}}{\partial \tau^{m+n}}R_{xy}(\tau) \tag{2.57}$$

The expression in equation 2.57 is the most important derivation to be able to understand the theoretical development of NExT. Theoretical background of NExT method which is the most important part of the output-only system identification technique used in this thesis is provided in the next section.

2.4. Natural Excitation Technique (NExT)

Natural Excitation Technique was developed by James et al. in 1993. According to James et al. the idea behind the technique is that vibration responses obtained from MIMO systems excited by random forces are used to obtain autocorrelation and cross-correlation functions. Cross-correlation functions between the responses obtained from different degrees-of-freedoms (DOFs) of the system and response of a selected reference DOF are equal to summations of decaying sinusoids. As a result, the

correlation functions have the same characteristics of a free vibration response of the system. Therefore, cross-correlation functions also satisfy the homogeneous equation of motion of the system. Since the cross-correlation functions are obtained from vibration responses only, there is no need to know the forces which excite the systems. This property makes NExT a powerful tool for output-only system identification of civil structures.

In the NExT method, excitation forces and responses of the systems should be second order weakly stationary random signals. In nature, ambient vibrations due to wind or traffic loads can be considered as weakly stationary random signals. Thus, vibration responses obtained from systems excited by ambient vibrations can be employed in NExT while estimating cross-correlation functions.

For a multi DOF structure, the equation of motion is defined as

$$\boldsymbol{M}\ddot{X}(t)+\boldsymbol{C}\dot{X}(t)+\boldsymbol{K}X(t)=\boldsymbol{F}(t) \tag{2.58}$$

where **M** is the mass matrix, **C** is the damping matrix and **K** is the stiffness matrix. $\ddot{X}(t), \dot{X}(t), X(t)$ are the vectors of weakly stationary random signals which correspond to acceleration, velocity and displacement response of the structure, respectively. **F**(t) is a vector of random force signals which excite the structure. Here, **F**(t) corresponds to ambient vibrations and it is assumed to be a broadband white noise signal. According to Caicedo (2001), the equation of motion in equation 2.58 is multiplied by the response of a selected reference DOF X_{REF}(t) and expectations of each term are obtained as

$$\begin{aligned}&\boldsymbol{M}E[\ddot{X}(t)X_{REF}(t-\tau)]+\boldsymbol{C}E[\dot{X}(t)X_{REF}(t-\tau)]+\boldsymbol{K}E[X(t)X_{REF}(t-\tau)]=\\&E[\boldsymbol{F}(t)X_{REF}(t-\tau)]\end{aligned} \tag{2.59}$$

In equation 2.59, **F**(t) is a white noise signal and therefore **F**(t) and $X_{REF}(t-\tau)$ become uncorrelated for all values of τ owing to the fact that the mean values of **F**(t) and $X_{REF}(t-\tau)$ are zero. For uncorrelated signals, the cross-correlation function between ***F(t)*** and *X(t)* is also zero ($R_{\boldsymbol{F}X_{REF}}=E[\boldsymbol{F}(t)X_{REF}(t-\tau)]=0$). In addition, the expectation terms on the left-hand side yield the definition of the cross-correlation function defined by equations 2.44, 2.45, and 2.48. Therefore, equation 2.59 can be rewritten as

$$\boldsymbol{M}\, R_{\ddot{X}X_{REF}}(\tau)+\boldsymbol{C}\, R_{\dot{X}X_{REF}}(\tau)+\boldsymbol{K}\, R_{XX_{REF}}(\tau)=0 \tag{2.60}$$

where $R_{\ddot{X}X_{REF}}(\tau)$, $R_{\dot{X}X_{REF}}(\tau)$, and $R_{XX_{REF}}(\tau)$ represent the correlation functions between the acceleration, velocity, and displacement response vectors and the selected reference signal, respectively. Then, using the derivative expression defined in equation 2.57 for cross-correlation functions, equation 2.60 can be expressed as

$$\boldsymbol{M}\, \ddot{R}_{XX_{REF}}(\tau)+\boldsymbol{C}\, \dot{R}_{XX_{REF}}(\tau)+\boldsymbol{K}\, R_{XX_{REF}}(\tau)=0 \tag{2.61}$$

This equation reveals the idea behind the NExT methodology used in this thesis as the first step of output-only system identification. According to this equation, cross-correlation functions between the displacement response signals and the response signal of a selected reference DOF satisfy the homogeneous equation of motion. Since the cross-correlation functions satisfy the homogeneous equation of motion, they can be considered as free vibration response of the structures. Caicedo (2001) demonstrated that equation 2.61 can be also used with acceleration response signals of the structures taking the derivative of the equation by fourth degree and thus the following expression is obtained as

$$\boldsymbol{M}\, \ddot{R}_{\ddot{X}\ddot{X}_{REF}}(\tau)+\boldsymbol{C}\, \dot{R}_{\ddot{X}\ddot{X}_{REF}}(\tau)+\boldsymbol{K}\, R_{\ddot{X}\ddot{X}_{REF}}(\tau)=0 \tag{2.62}$$

Consequently, the NExT method can be used to transform forced vibration responses into free vibration responses of the structures. The condition for doing so is that excitation forces should be uncorrelated with the vibration responses of the structures and the vibration responses should consist of stationary signals.

In the NExT method, cross-correlation functions are generally obtained via power spectral density functions in order to use the averaging, filtering and windowing options which provide useful advantages for signal processing of measurement response signals. At this point, the Welch-Bartlett method is used to obtain power spectral density functions by including the aforementioned advantageous signal processing options. In the next section, the Welch-Bartlett method is briefly provided.

2.4.1. Welch-Bartlett Method

The power spectral density of a random signal in the form of a sequence of time samples may be estimated in parametric and non-parametric ways. Autoregressive models are used in parametric estimation and non-parametric estimation of the spectral density is called *periodogram* (Manolakis and Proakis, 2007). The Welch-Bartlett method is one of the methods which is used for the estimation of the periodograms. This method is based on two main procedures. The first one is the Bartlett method. It is based on averaging of the periodograms. The second one is the Welch method and it is the modified form of the Bartlett method. The Welch method allows windowing and overlapping operations to apply on the data records before averaging of the periodograms.

2.4.1.1. The Bartlett Method

The Bartlett method is used to reduce the variance in the periodogram estimation. For this purpose, the data record is divided into smaller segments. The periodogram of each segment is calculated and calculated periodograms are then averaged.

Let the data record have a length of N samples. Then the total length is divided into K data segments which each has a length of M samples. Defining each data segment as $x_i(n)=x(n+i\mathrm{M})$ where i=0,1,...,K-1 and n=0,1,...,M-1, the periodogram for each segment is calculated as

$$P_{xx}^{(i)}(k)=\frac{1}{M}\left|\sum_{n=0}^{M-1} x_i(n)e^{-j2\pi kn}\right|^2 \tag{2.63}$$

where $P_{xx}^{(i)}(k)$ is the periodogram of i$^{\text{th}}$ segment. For K segments, K periodograms are calculated. Then, the calculated periodograms are averaged to obtain the spectral density estimation. The averaged periodogram is defined as

$$P_{xx}^{B}(k)=\frac{1}{K}\sum_{i=0}^{K-1} P_{xx}^{(i)}(k) \tag{2.64}$$

Since each data segment consists of less samples than the original data, the frequency resolution is reduced by a factor K. In addition, the variance of the periodogram estimation is

$$var[P_{xx}^{B}(k)]=\frac{1}{K}var[P_{xx}^{(i)}(k)] \tag{2.65}$$

As indicated in equation 2.65, the variance of the periodogram has been reduced by the factor K.

2.4.1.2. The Welch Method

The Welch method is the modified version of the Bartlett method. The method includes two main modifications to the Bartlett method.

It firstly allows data segments to overlap. Let overlapped data segments defined as $x_i(n)=x(n+iD)$ where $i=0,1,...,L-1$ and $n=0,1,...,M-1$. It should be noted here that the Bartlett method does not allow overlapping and so D becomes identical to M and the length of data segments L becomes equivalent to K in the Bartlett method. On the other hand, if D=M/2 , for example, it means that there is 50% overlapping between two consecutive data segments and in this situation, the length of data segments L is equal to 2K.

It secondly allows windowing of the data segments before calculating the periodograms. The modified periodogram is then defined as

$$\hat{P}_{xx}^{(i)}(k)=\frac{1}{MU}\left|\sum_{n=0}^{M-1}x_i(n)\omega(n)e^{-j2\pi kn}\right|^2 \tag{2.66}$$

where U represents the normalization factor in the windowing function $\omega(n)$ and it is expressed as

$$U=\frac{1}{M}\sum_{n=0}^{M-1}\omega^2(n) \tag{2.67}$$

Then, the calculated modified periodograms are averaged to obtain the spectral density estimation. The averaged modified periodogram is defined as

$$P_{xx}^{W}(k)=\frac{1}{L}\sum_{i=0}^{L-1}\hat{P}_{xx}^{(i)}(k) \tag{2.68}$$

It should be also mentioned that different overlapping ratios and different windowing function types can be used to have relevant characteristics of the spectral estimation. However, these also change the variance of the resulting periodogram.

2.5. Eigensystem Realization Algorithm (ERA)

Eigensystem Realization Algorithm (ERA) was developed by Juang and Pappa in 1985. They used the algorithm to obtain modal parameters of Galileo spacecraft. To this end, 162 acceleration sensors were used to evaluate impulse response functions to be employed in the algorithm. As a result, 34 modal frequencies, modal damping ratios and mode shapes were successfully identified from the experiments.

Juang and Pappa (1986) researched the effects of measurement noise on the results of the ERA method. They worked on simulated data and revealed that measurement noise has a higher effect on the higher modes of structures than the lower modes. They also showed that the identification process can be improved by using model reduction. They proposed a technique to determine the correct singular values to identify natural frequencies.

ERA is a time domain technique, which uses impulse response functions to identify modal parameters of MIMO systems from measurement data. The ERA method is based on the state-space representation of the linear dynamic system. Modal parameters are identified from the identified state-space matrices of the system. State-space matrices of the system are identified from singular value decomposition of the Hankel matrix. The Hankel matrix is a special type of matrix which is constructed by using Markov parameters of the system. Impulse response functions of the systems are employed as the Markov parameters while forming the Hankel matrix.

2.5.1. State-Space Representation of Linear Dynamic Systems

Consider an N DOF linear dynamic system. This system is represented by a second-order differential equation of motion which is defined as

$$\boldsymbol{M}\ddot{q}(t)+\boldsymbol{D}\dot{q}(t)+\boldsymbol{K}q(t)=\boldsymbol{V}f(t) \tag{2.69}$$

where **M**, **D** and **K** show (N x N) mass, damping and stiffness matrices, respectively. $q(t) \in \Re^{Nx1}$ represents the displacement response vector of the system. $f(t)$ denotes the excitation force vector and **V** matrix defines the spatial distribution of the excitation force $f(t)$. The response measurements which is acquired from this system is then expressed in equation as

$$y(t)=\bar{\boldsymbol{C}}\left[q(t)^T \quad \dot{q}(t)^T \quad \ddot{q}(t)^T\right] \tag{2.70}$$

where $y(t) \in \Re^{N_{out}x1}$ is the measured response output vector of the system and $\bar{\boldsymbol{C}}$ shows the linear distribution of the displacement, velocity and acceleration vectors in the measured response.

This continuous-time linear dynamic system is also represented by first-order differential equations in state-space form. This representation is more convenient for system control and identification purposes. The state-space representation is defined as

$$\begin{aligned}\dot{x}(t)&=\boldsymbol{A}_c x(t)+\boldsymbol{B}_c u(t)\\ y(t)&=\boldsymbol{C}_c x(t)+\boldsymbol{D}_c u(t)\end{aligned} \tag{2.71}$$

where

$x(t) \in \Re^{N_{in}x1}$ is the state vector and $x(t)=\begin{bmatrix}q(t)\\ \dot{q}(t)\end{bmatrix}$

$u(t) \in \Re^{N_{in}x1}$ is the input forcing vector and u(t)=f(t)

$y(t) \in \Re^{N_{out}x1}$ is the measured response output vector,

$\mathbf{A_c} \in \Re^{2N\,x\,2N}$, $\mathbf{B_c} \in \Re^{2N\,x\,N_{in}}$, $\mathbf{C_c} \in \Re^{N_{out}\,x\,2N}$ and $\mathbf{D_c} \in \Re^{N_{out}\,x\,N_{in}}$ are continuous time linear state-space matrices. N_{in} is the number of inputs and N_{out} is the number of outputs.

The linear state-space matrices are expressed as

$$\begin{aligned} \boldsymbol{A_c} &= \begin{bmatrix} \mathbf{0}_{N\,x\,N} & \boldsymbol{I}_{N\,x\,N} \\ -\boldsymbol{M}^{-1}\boldsymbol{K} & -\boldsymbol{M}^{-1}\boldsymbol{D} \end{bmatrix} \\ \boldsymbol{B_c} &= \begin{bmatrix} \mathbf{0}_{N\,x\,N_{in}} \\ -\boldsymbol{M}^{-1}\boldsymbol{I}_{N\,x\,N_{in}} \end{bmatrix} \\ \boldsymbol{C_c} &= \begin{bmatrix} \boldsymbol{I}_{N_{out}\,x\,N} & \mathbf{0}_{N_{out}\,x\,N} \end{bmatrix} \\ \boldsymbol{D_c} &= \begin{bmatrix} \mathbf{0}_{N_{out}\,x\,N_{in}} \end{bmatrix} \end{aligned} \tag{2.72}$$

If the system is a discrete-time dynamic system, the state-space representation of this system is defined as

$$\begin{aligned} x_{k+1} &= \boldsymbol{A}\,x_k + \boldsymbol{B}\,u_k \\ y_k &= \boldsymbol{C}\,x_k + \boldsymbol{D}\,u_k \end{aligned} \tag{2.73}$$

where x_k is the discrete state vector, u_k is the discrete input vector and y_k is the discrete output vector at time $t = kT_s$, T_s is the sampling time. **A**, **B**, **C** and **D** are the discrete state-space matrices in the same dimensions with their continuous ones.

The ERA method identifies an equivalent linear dynamic system by using the responses of the system due to impulse input. Since the response data are always acquired in discrete-time form, equivalent linear dynamic system which is identified by the ERA method is defined as

$$\begin{aligned} x_{k+1} &= \boldsymbol{A_{id}}\,x_k + \boldsymbol{B_{id}}\,u_k \\ y_k &= \boldsymbol{C_{id}}\,x_k + \boldsymbol{D_{id}}\,u_k \end{aligned} \tag{2.74}$$

where $\mathbf{A_{id}}$, $\mathbf{B_{id}}$, $\mathbf{C_{id}}$ and $\mathbf{D_{id}}$ are the identified state-space matrices. These matrices are identified by singular value decomposition (SVD) of Hankel matrix which consists of Markov parameters.

2.5.2. Construction of Hankel Matrix

The first fundamental step of modal identification via the ERA method is to construct the Hankel block matrix. The Hankel matrix is formed by using the Markov parameters of the dynamic system. The Hankel matrix is defined as

$$\boldsymbol{H}(k-1)=\begin{bmatrix} \boldsymbol{Y}(k) & \boldsymbol{Y}(k+1) & .... & \boldsymbol{Y}(k+c) \\ \boldsymbol{Y}(k+1) & \boldsymbol{Y}(k+2) & .... & \boldsymbol{Y}(k+c+1) \\ . & . & . & . \\ . & . & . & . \\ . & . & . & . \\ \boldsymbol{Y}(k+r) & \boldsymbol{Y}(k+r+1) & .... & \boldsymbol{Y}(k+c+r) \end{bmatrix} \tag{2.75}$$

where c and r represent the number of block columns and the number of block rows, respectively. $\mathbf{Y}(k)$ is the (m x d) matrix which consists of the Markov parameters at time step k. m and d represent the number of measurement stations and the number of reference DOFs, respectively. Matrix of the Markov parameters, $\mathbf{Y}(k)$ can be written as

$$\boldsymbol{Y}(k)=\begin{bmatrix} y_{1,1}(k) & y_{1,2}(k) & .... & y_{1,d}(k) \\ y_{2,1}(k) & y_{2,2}(k) & .... & y_{2,d}(k) \\ . & . & . & . \\ . & . & . & . \\ . & . & . & . \\ y_{m,1}(k) & y_{m,2}(k) & .... & y_{m,d}(k) \end{bmatrix} \tag{2.76}$$

where $y_{i,j}(k)$ represents the impulse response of the i^{th} DOF at time step k because of an impulse excitation at the j^{th} DOF. Therefore, the Hankel matrix is a block data matrix whose dimension is $m(r+1)$ x $d(c+1)$.

Obtaining the impulse response functions of the dynamic systems requires the knowledge of the input excitation force to the system. This property of the ERA method makes the methodology an input-output identification technique. However, the free vibration data can be also used as the Markov parameters in construction of the Hankel matrix. The NExT method computes the cross-correlation functions from the response data of the systems and these cross-correlation functions have the same characteristics with the free vibration data of the systems. By means of this property, the cross-

correlation functions that are found by the NExT method can be used as the Markov parameters in the Hankel matrix instead of the impulse responses. Thus, using the ERA method in conjunction with the NExT method does not require the knowledge of the input force to the system and this makes the NExT-ERA method an output-only system identification technique.

When the ERA method is used in conjunction with the NExT method, the elements of the $\mathbf{Y}(k)$ matrix in equation 2.76 are replaced by the cross-correlation function $\boldsymbol{R}_{\ddot{X}_{REF}\ddot{X}}(k)$ calculated between the i^{th} DOF and the reference DOF j at time step k. The $\mathbf{Y}(k)$ matrix in equation 2.76 also allows simultaneous usage of multi-reference DOFs while it allows the usage of a single reference DOF.

2.5.3. Singular Value Decomposition of the Hankel Matrix

The constructed Hankel block data matrix is decomposed into its singular values to identify the state-space matrices. Decomposition is performed for the Hankel matrix $\mathbf{H}(0)$ which is constructed at time step k=1. The singular value decomposition of the Hankel matrix $\mathbf{H}(0)$ is defined as

$$\boldsymbol{H}(0)=\boldsymbol{U}\boldsymbol{\Sigma}\boldsymbol{V}^{\boldsymbol{T}} \tag{2.77}$$

where $\mathbf{U}$ and $\mathbf{V}$ are the unitary matrices. $\boldsymbol{\Sigma}$ is the diagonal singular value matrix including positive numbers on the diagonal only. Superscript "T" denotes the transpose of the matrix. For ideal conditions, the number of the singular values on the diagonal of the matrix $\boldsymbol{\Sigma}$ should be equal to the number of system order (the number of poles of the system) and they should be monotonically decreasing. The matrix $\boldsymbol{\Sigma}$ can be expressed as

$$\boldsymbol{\Sigma}=\begin{bmatrix}\boldsymbol{\Sigma}_{NO} & \mathbf{0}\\ \mathbf{0} & \mathbf{0}\end{bmatrix} \tag{2.78}$$

where the subscript "NO" represents the number of system order. However, this is not the case in real life. Since the acquired data always contain measurement noise, all the diagonal terms become nonzero numbers due to the noisy response data and numerical truncation. Therefore, a minimum realization of the matrix $\boldsymbol{\Sigma}$ is performed by neglecting

the relatively smaller singular values. This means that a minimum system order is obtained so that it represents the real structure.

After the minimum realization of the singular value matrix $\mathbf{\Sigma}$, the unitary matrices are also realized for the same system order. Once the minimum realization of these matrices is performed, the state-space matrices can be identified as

$$\begin{aligned} \boldsymbol{A}_{id} &= \boldsymbol{\Sigma}_r^{(-1/2)} \boldsymbol{U}_r^T \boldsymbol{H}(1) \boldsymbol{V}_r \boldsymbol{\Sigma}_r^{(-1/2)} \\ \boldsymbol{B}_{id} &= \boldsymbol{\Sigma}_r^{(1/2)} \boldsymbol{V}_r^T \begin{bmatrix} \boldsymbol{I}_{NO\,x\,N_{in}} \\ \boldsymbol{0}_{(hc-NO)\,x\,N_{in}} \end{bmatrix} \\ \boldsymbol{C}_{id} &= \begin{bmatrix} \boldsymbol{I}_{N_{out}\,x\,NO} & \boldsymbol{0}_{N_{out}\,x\,(hr-NO)} \end{bmatrix} \boldsymbol{U} \boldsymbol{\Sigma}_r^{(1/2)} \\ \boldsymbol{D}_{id} &= \boldsymbol{Y}(0) \end{aligned} \tag{2.79}$$

where $\mathbf{A}_{id}$, $\mathbf{B}_{id}$, $\mathbf{C}_{id}$ and $\mathbf{D}_{id}$ are the identified state-space matrices, $\mathbf{U}_r$, $\mathbf{V}_r$ and $\mathbf{\Sigma}_r$ are the matrices obtained after the minimum realization of the matrices $\mathbf{U}$, $\mathbf{V}$ and $\mathbf{\Sigma}$. Here, the subscripts "*hc*" and "*hr*" represent the column number of the Hankel matrix which is $hc=d(c+1)$ and the row number of the Hankel matrix which is $hr=m(r+1)$.

It should be noted here that when the ERA method is used in conjunction with the NExT method, the input force to the system is unknown and therefore $\mathbf{B}_{id}$ and $\mathbf{D}_{id}$ matrices cannot be identified since they are related with the input force $u(t)$ in state-space form. As a result, only $\mathbf{A}_{id}$ and $\mathbf{C}_{id}$ matrices can be identified by the NExT-ERA method and these two matrices are sufficient for the identification of the modal parameters of the dynamic systems.

Since the $\mathbf{A}_{id}$ and $\mathbf{C}_{id}$ matrices are identified by using the response measurement data, these matrices are in discrete-time form. In order to identify the modal parameters from these identified state-space matrices, the identified system needs to be transformed to the continuous-time form.

Eigenvalues of the identified matrix $\mathbf{A}_{id}$ gives complex conjugate pairs which are equivalent to the poles of the dynamic system. Each pair gives information about one mode of vibration. Consider the eigenvalues and eigenvectors of the identified matrix $\mathbf{A}_{id}$. The relationship between them is defined as

$$\boldsymbol{A}_{id} = \boldsymbol{\Psi}\,\boldsymbol{\Lambda}\,\boldsymbol{\Psi}^{-1} \tag{2.80}$$

where $\boldsymbol{\Psi}$ and $\boldsymbol{\Lambda}$ are eigenvector and eigenvalue matrices of $\mathbf{A}_{id}$. The diagonal terms of the eigenvalue matrix gives the poles of the system as complex conjugate pairs. Consider the poles of the system are defined as ($\sigma_i \pm j\Omega_i$). Thus, the damped natural frequencies and the modal damping ratios can be found as

$$\begin{aligned} \omega_{d,i} &= imag(\sigma_i \pm j\Omega_i) \\ -\zeta_i . \omega_{n,i} &= real(\sigma_i \pm j\Omega_i) \end{aligned} \tag{2.81}$$

where $\omega_{d,i}$ and $\omega_{n,i}$ represent the damped and undamaped natural frequency of the i^{th} mode, respectively. "*imag*" and "*real*" denote the imaginary part and the real part. ζ_i represents the modal damping ratio of the i^{th} mode. The mode shapes of the system can be found as

$$\boldsymbol{\Phi}_i = \boldsymbol{C}_{id} . \boldsymbol{\Psi}_i \tag{2.82}$$

where $\boldsymbol{\Phi}_i$ and $\boldsymbol{\Psi}_i$ are the mode shape vector and eigenvector of the i^{th} mode, respectively.

2.6. Identification Procedure

2.6.1. Modal Identification Procedure

The output-only system identification technique, NExT-ERA, consists of two sections which are NExT and ERA because they are actually two separate methods. ERA employs impulse response functions of systems for identification of dynamic characteristics. It can be also used by employing the free vibration response of the systems. Thus, ERA has been used for input-output system identification purpose in the literature, as well. On the other hand, NExT is used to obtain cross-correlation functions which have the same characteristics with the free vibration response of the systems. The cross-correlation functions of the structural responses can be then employed in ERA for the identification of the dynamic characteristics. Therefore, NExT is the main section that makes the NExT-ERA method an output-only system identification technique.

In this thesis, the cross-correlations have been obtained by discrete IFFT of the cross-spectral density functions. Therefore, as the first step of the identification process, it has been focused on estimation of the cross-spectral density functions. A successful identification is possible only if high quality cross-correlation functions can be obtained. Therefore, parameters that affect the calculation of the cross-spectral density functions directly affect the quality of the cross-correlation functions. It should be noted here that the identification procedure has been considered in the light of the practical guidelines for NExT-ERA which are recommended by Caicedo (2011). In the studies provided within the scope of this thesis, the cross-spectral density functions have been calculated by using the Welch's method. In this method, the response data are divided into smaller frames. FFT of the data in each frame is then calculated and squared magnitudes of calculated FFTs are averaged. While averaging, the frames are overlapped onto each other with a specific ratio to improve averaging of the FFTs. In addition, a windowing function such as Hanning or Hamming window is applied on the data in each frame to prevent data from the leakage effects when overlapped (Farrar and Worden, 2012). This procedure produces the cross-spectral density functions of the response data. According to Caicedo (2011), number of points of the data in each frame and overlapping ratio between the frames affect the identification process. In addition, record length of the response data affects the process because longer records provides more precise averaging in calculation of the cross-spectral density functions. Sampling frequency of records also specifies the quality of the cross-correlation functions since the sampling frequency determines the frequency bandwidth of the correlations.

Since the cross-spectral density functions are obtained between two signals, it is required to select a reference signal (also called reference channel) for the calculation of the cross-spectral density functions. Selection of this reference channel is also a critical step for a successful identification. Since there is no motion on the nodal points of the modes of structures during their vibrations, the signals on or near the nodal points of the mode of interest cannot have any information on that mode. Therefore, this mode cannot be identified as long as the signals on its nodal points are selected as reference channel. As a result, the signals which are far from the nodal points of the modes of interest should be selected as reference signals in the calculation of the cross-spectral density functions. However, it is generally difficult to perceive the node locations of the modes of large structures such as bridges. In this situation, the cross-spectral density functions

are calculated by selecting the response measurement of each DOF as reference channel one by one and identification process is repeated for each selection.

Once the cross-spectral density functions are evaluated, the cross-correlation functions are obtained by inverse IFFT of the cross-spectral density functions. The resulting cross-correlation functions have the same length with the data frame used in the calculation of the cross-spectral density functions and their sampling frequency is equal to the sampling frequency of the response records. NExT section ends with the determination of the cross-correlation functions.

In the ERA section, the first step is to form the Hankel matrix by using the cross-correlation functions. The number of rows and columns of the Hankel matrix determines how much portion of the cross-correlation functions will be included in the identification process. Therefore, determination of the size of the Hankel matrix plays an important role for a successful identification. Although various recommendations for determination of the size are found in the literature, Caicedo (2011) recommends that number of columns of the Hankel matrix should be equal to twice the number of expected poles of the system. For determination of the number of rows, the data which include the frequency content of interest should be used as much portion as possible. According to Caicedo (2011), at least a few cycles of the cross-correlation functions which also represent the free vibration behavior should be used to successfully determine dynamic characteristics of the system. This leads to the fact that longer response records are required for determination of low frequency behavior since the periods of such behavior are longer.

This recommendation for determination of the size of the Hankel matrix requires prior knowledge of the number of poles (twice the number of modes) of the system. However, system dynamics may not be estimated for large and complex structures. In this situation, different number of poles (model order) of the systems are designated and the Hankel matrix is reconstructed for the new model order. The identification process is then repeated for each model order. At this point, stabilization diagrams are effectively used to visually investigate the change of identified modes for different model orders. Stabilization diagrams can be also obtained for different reference signals which are used in the calculation of the cross-spectral density functions. Different studies provided in the literature have revealed that using too high model orders results in the occurrence of computational modes in the stabilization diagrams. Similarly, using too low model orders results some modes not to be identified and they cannot be

observed in the stabilization diagrams. On the other hand, true modes of the system show consistency for appropriate model orders and reference signals in the stabilization diagrams. In this way, true modes can be identified in addition to the determination of the true model orders and the true reference channel for the system.

As the next step of ERA, the constructed Hankel matrix is decomposed into its singular values. One alternative way to estimate the model order is to visually check the number of high singular values. Because there has been generally a jump between the singular values of true modes and the computational ones.

2.6.2. Identification Procedure of Changes in Structural Conditions

In reality, damage in structures generally means stiffness change of the structural elements. Changes in stiffness values affect the dynamic characteristics of the structures by changing the modal parameters of the structures. Mass changes also result in changes in the modal parameters of the structures but damage in structures may not occur because of mass changes in real life.

In this thesis, a least squares approach is used to identify changes in structural conditions. In the least squares approach, the stiffness matrix can be identified by using the modal parameters of a specific shear frame structure. In this approach, the stiffness matrix can be found only if the mass matrix is known. The problem may be considered inversely. The mass matrix can be identified by using the modal parameters and in this situation, the mass matrix can be found only if the stiffness matrix is known. In the studies conducted in the scope of this thesis, change in structural conditions is represented by means of changes in story masses. The stiffness matrix is considered to be known.

Consider an N DOF lumped mass shear frame model structure. Then, the mass matrix and the stiffness matrix of the structure can be described as follows;

$$\boldsymbol{M}=\begin{bmatrix} m_1 & 0 & . & . & 0 \\ 0 & m_2 & 0 & . & 0 \\ 0 & 0 & m_3 & . & 0 \\ . & . & . & . & . \\ 0 & 0 & . & . & m_N \end{bmatrix} \tag{2.83}$$

$$\boldsymbol{K}=\begin{bmatrix} k_1+k_2 & -k_2 & . & . & 0 \\ -k_2 & k_2+k_3 & -k_3 & . & 0 \\ 0 & 0 & . & . & 0 \\ . & . & . & . & -k_N \\ 0 & 0 & . & -k_N & k_N \end{bmatrix} \tag{2.84}$$

Then, the eigenvalue problem of this system can be expressed as,

$$(\boldsymbol{K}-\lambda_i \boldsymbol{M})\phi_i=0 \tag{2.85}$$

This expression can be also written as,

$$\phi_i^T \boldsymbol{K}=\phi_i^T \lambda_i \boldsymbol{M} \tag{2.86}$$

where λ_i is the i'th eigenvalue and ϕ_i is the i'th eigenvector of the structure. The least squares approach then determines the lumped mass values of each story as follows;

$$\begin{Bmatrix} m_1 \\ m_2 \\ . \\ . \\ m_N \end{Bmatrix}=\frac{1}{N}\begin{bmatrix} I_N & I_N & . & . & I_N \end{bmatrix}_{Nx(NxN)}\begin{bmatrix} \delta_1 & & & & \\ & \delta_2 & & & \\ & & . & & \\ & & & . & \\ & & & & \delta_N \end{bmatrix}^{-1}\begin{bmatrix} \Delta_1 \\ \Delta_2 \\ . \\ . \\ \Delta_N \end{bmatrix}\begin{Bmatrix} k_1 \\ k_2 \\ . \\ . \\ k_N \end{Bmatrix} \tag{2.87}$$

where

$$\delta_i=\begin{bmatrix} \phi_{1i}\lambda_i & 0 & . & 0 & 0 \\ 0 & \phi_{2i}\lambda_i & . & 0 & 0 \\ . & . & . & 0 & 0 \\ 0 & 0 & 0 & . & 0 \\ 0 & 0 & 0 & 0 & \phi_{Ni}\lambda_i \end{bmatrix} \tag{2.88}$$

$$\Delta_i=\begin{bmatrix} \phi_{1i} & \phi_{1i}-\phi_{2i} & . & . & 0 \\ 0 & \phi_{2i}-\phi_{1i} & \phi_{2i}-\phi_{3i} & . & 0 \\ . & . & . & . & . \\ 0 & 0 & 0 & \phi_{(N-1)i}-\phi_{(N-2)i} & \phi_{(N-1)i}-\phi_{Ni} \\ 0 & 0 & 0 & 0 & \phi_{Ni}-\phi_{(N-1)i} \end{bmatrix} \tag{2.89}$$

$\mathbf{I}_N$ is a N x N identity matrix and ϕ_{ji} is the i'th mode shape amplitude at the j'th story. m_j and k_j are the mass and stiffness value of the j'th story (j=1,2,...,N).

2.7. Previous Studies of NExT-ERA

James et al. (1993) used the NExT on three different structures for modal parameter identification. The first structure was the DOE/Sandia vertical axis wind turbine located in Bushland, Texas. It was a 34-m high structure used to convert the wind energy into electricity. An analytical model of this turbine was set to generate the response data to be used in the method. Modal parameters (natural frequencies and modal damping ratios) identified using NExT were compared with the ones of the analytical model and the modal parameters were in good agreement with each other. In addition to this analytical study, the method was implemented on the physical turbine while it was rotating in order to demonstrate the capabilities of the NExT from an experimental point of view. As the second structure, a 19-m FloWind Corporation vertical wind turbine was used for the implementation of the method. Unlike the previous study, this turbine was parked (not rotating) while the response data was collecting. The turbine was tested using conventional modal techniques as well as using the NExT for modal parameter identification and identification results of both techniques were in good agreement. As the third structure, a tractor trailer vehicle was also tested with the NExT to obtain its natural frequencies and modal damping ratios.

Caicedo (2001) studied the first phase of the benchmark problem in his M.Sc thesis. He used a combination of NExT and ERA methods to identify modal parameters and damage cases of the analytical phase of the problem. Caicedo numerically constructed both 12 DOF and 120 DOF finite element models of the benchmark structure to generate acceleration response data. To do so, two excitation cases were applied to each model. In the first excitation case, he simulated ambient wind vibration by exciting the structure with Gaussian white noise forces and in the second one, he simulated the forced vibration of a shaker on the roof by exciting it again with a Gaussian white noise force. As aimed in the benchmark problem, he used 12 DOF model as an identification model to study the sensitivity of NExT-ERA to the record length, effect of sensor noise and modeling errors and used 120 DOF model to investigate the effects of modeling errors in the identification process. In his study, he

firstly used the NExT-ERA methodology to identify natural frequencies, damping ratios and mode shapes of the structure by investigating the influencing factors of each modal parameter during the identification process. Thereafter, six damage patterns as described in the first phase of the benchmark problem were studied to be identified. To this end, stiffness coefficients were obtained by a least squares solution to identify severity and location of stiffness changes in each pattern. He compared the translational natural frequency results and the stiffness changes obtained from NExT-ERA with the reported ones of the actual structure by Johnson et al. (2000). For the 12 DOF model, every identified modal parameter as well as the identified stiffness changes were in a good agreement with that of the actual structure, demonstrating the accuracy of the NExT-ERA method for modal parameter and damage identification. However, for the 120 DOF, the identification of the stiffness coefficients resulted in high errors in identifying stiffness coefficients. It was considered that these high errors were caused by the introduced modeling errors in the 120 DOF model, showing the sensitivity of the NExT-ERA methodology to the modeling errors.

Nayeri et al. (2009) used NExT together with three different methods which are ERA, ERA with data correlations (ERA/DC) and the least squares algorithm (LS) so as to identify modal parameters of the New Carquinez suspension bridge located in the vicinity of San Francisco. The bridge was instrumented with 64 accelerometers to measure ambient and forced vibration responses to be used in the NExT. In the study, various factors that influence the identification process such as selection of a proper reference DOF and giving the right decisions about user-selectable parameters of, especially in the experimental applications, the aforementioned algorithms were discussed. Unlike Caicedo (2001), Nayeri et al. (2009) simultaneously used all DOFs of the system as the reference channel instead of using a single reference channel to be able to distinguish the true modes from computational modes. Results of the three identification techniques were compared with each other and with results of a stochastic subspace identification (SSI) study. It was concluded that the results of identified natural frequencies using NExT/ERA and NExT/ERA-DC were in a very good agreement with the SSI results and with each other while NExT/LS resulted in some deficient information of the frequencies. In contrast, identified modal damping ratios resulted in substantially different values in each method and it was reached the fact that modal damping values could not be identified as accurately as natural frequencies using such methods.

Caicedo (2011) published a paper including practical guidelines for the NExT and the ERA for modal parameter identification using ambient vibrations. In this study, Caicedo worked on the experimental phase of the IASC-ASCE benchmark problem and identified the modal parameters of the physical structure using the NExT and the ERA to illustrate the usage of the methodology. The actual aim of the study was to focus on the steps of the NExT-ERA by analyzing parameter selection criteria for each step. The effects of record length and record sampling frequency, number of points for the FFT on the calculation of cross-correlation functions in NExT as well as the effects of the number of rows and columns of constructed Hankel matrix and number of expected modes in ERA were some of the discussion topics in the paper. Six natural frequencies of the structure were successfully identified using the presented criteria of NExT-ERA.

Mahmood et al. (2014) implemented the combination of NExT and ERA with a least squares solution on the analytical phase I and experimental phase II of the IASC-ASCE benchmark problem for identification of modal parameters and stiffness changes. In their study, they emphasized the limitations of using a single reference channel and a specific order of the system in NExT-ERA. In their opinion, closely spaced true and computational modes might be available after identification process, making it impossible to distinguish the true modes from the computational ones by using a single reference and a true mode might also be available up to a certain model order of the system. Again making it impossible to identify the true mode when just a specific model order was used. In order to cope with these limitations, Mahmood et al. (2014) proposed a new multi-reference-based mode selection approach by including an autonomous algorithm. In this approach, it was preferred to use all DOFs of the system as the reference channel, one at a time unlike Nayeri et al. (2009) who used all DOFs as reference channel simultaneously, making the computational issues hard to handle. They used all reasonable model orders of the system to be able to see all true modes by presenting the results via stabilization diagrams. The identification results of the modal parameters were in good agreement with the exact results reported by Johnson et al. (2004) as the error between them was within 0.5%. The methodology was found to have the accuracy of about 90% in damage localization. Emerging errors were interpreted as the methodology being sensitive to the modeling errors, which was also revealed by (Caicedo, 2001).

CHAPTER 3

IMPLEMENTATIONS OF NExT-ERA

3.1. Introduction

Within the scope of this thesis, two different research studies were carried out for the implementation of the NExT-ERA method. In the first study, a three-story steel model building located in the Structural Mechanics Laboratory of Civil Engineering Department of Izmir Institute of Technology was used in the implementation. In the second study, NExT-ERA was implemented on a numerical model of a continuous beam bridge by employing the grouped response measurements of the model. The NExT-ERA algorithm were programmed within Matlab environment to be used as the output-only system identification technique in the aforementioned studies.

The first study consists of a numerical and an experimental phase. In the experimental phase, NExT-ERA was implemented on the physical structure in the laboratory. To do so, 10 different scenarios of structural changes were added to the structure in addition to the unchanged state. To simulate the changes in structural conditions, four different mass blocks were added on the floors of the structure in 10 different combinations. In this study, change in structural conditions was represented by means of changes in story masses instead of stiffness changes because in this way, it was possible to repeat the tests exactly. For each structural condition, the acceleration response of each floor were recorded. The acceleration response data obtained for each structural condition were then employed in the NExT-ERA in order to estimate modal parameters of the physical structure for each condition. Then, the identified modal parameters were used to calculate changes in story masses in order to identify structural changes. A least squares approach was used to identify the story mass changes.

In the numerical phase, the three-story physical structure was numerically modeled within the Matlab environment including exactly the same structural conditions used in the experimental study. It was excited by generated white noise signals to obtain ambient vibration responses of the model. The modal parameters were evaluated from the mathematical model by using the programmed NExT-ERA algorithm

and simulated structural changes of the model were tried to be identified using a least squares approach. The aim to perform this numerical study was to verify the coded NExT-ERA algorithm and also to verify the results which were obtained from the experimental study.

In the second study, NExT-ERA was implemented on the numerical model of a continuous beam bridge to identify the modal parameters of the model by employing grouped response measurements. A methodology was proposed to have measurements of whole structure by using acquired grouped measurements. In this study, although NExT-ERA was used for modal parameter identification of the bridge model, the main focus of this study was actually on the modal parameter identification by using the proposed methodology and therefore this study has been provided in detail as an independent study in Chapter 4.

The first study is discussed in the following section. The physical model structure which was used in the first study is firstly described. Then, implementation process of the NExT-ERA method has been comprehensively explained in later sections.

3.2. First Study: Implementation on the 3-story Model Building

3.2.1. Description of the Model Building

The structure used for application of the identification technique is a three-story, one-bay steel shear frame model building which is located in the Structural Mechanics Laboratory of the Civil Engineering Department of Izmir Institute of Technology (İYTE). This structure was constructed within the scope of a research project supported by TUBITAK Engineering Research Group. Physical and dynamic properties of the structure were described in a report published by Turan and Aydın (2011). According to this report, the structure has story heights of 80 cm. The lateral stiffness of the building was provided by four columns located at the corners with a cross-sectional area of 1^{cm} x 10^{cm}. Beams of type HE100B were placed at the story levels in both the x and y directions. The column sizes were determined such that the first period of the structure became around 0.5 seconds. The physical structure is illustrated in Figure 3.1.

To be used in the numerical study, a finite element model of the physical structure was constructed. Turan and Aydın (2011) modeled the structure by using 3-D

beam elements. They initially defined a total of 96 DOFs in the finite element model and then reduced the system by the following assumptions;

- Motion of the nodal points on the base of the structure was considered to be constrained.
- The story floors were assumed as rigid diaphragms.
- Vertical deflections were assumed to be zero and motion along the strong direction of the columns was also assumed to be zero, and therefore they were eliminated from the system equations.
- The beams were assumed to be rigid in their longitudinal direction and their rotational DOFs were reduced by static condensation.

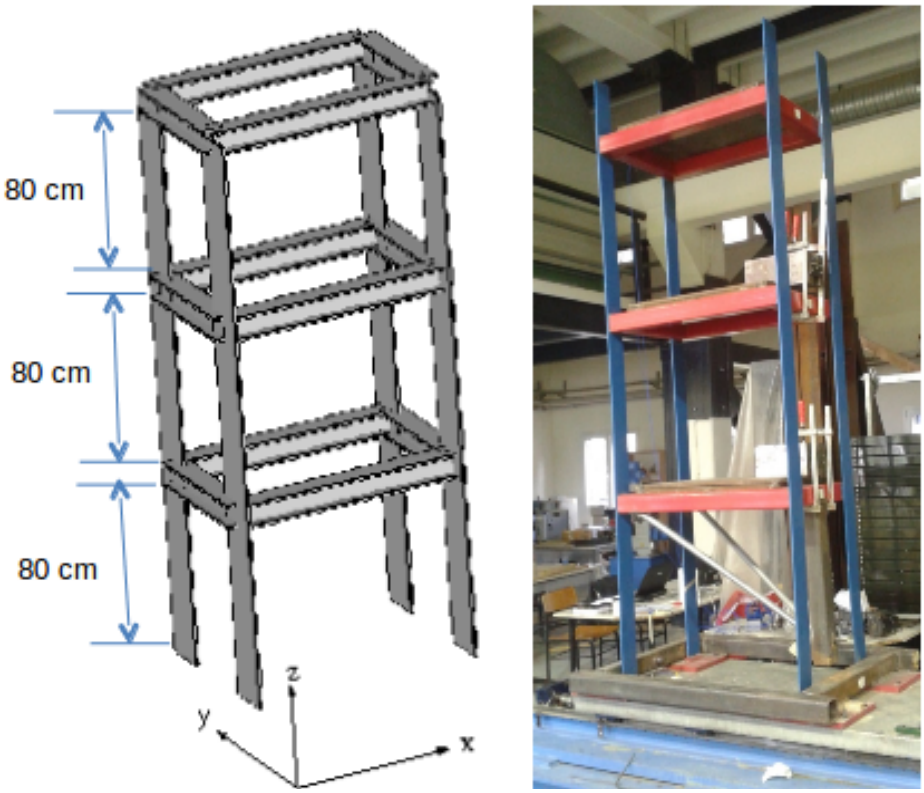

Figure 3.1. Three-story steel shear frame model structure in the Structural Mechanics Laboratory of Izmir Institute of Technology

As a result of the assumptions described above, a 3-DOF mathematical model of the structure was obtained. In the model, the story masses were considered to be lumped on the story levels. Figure 3.2 shows the lumped mass model used to extract system matrices of the structure.

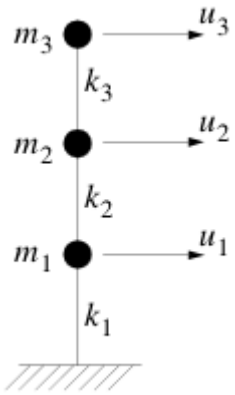

Figure 3.2. Lumped mass model of the structure

Since the ratio of the beam stiffness to the column stiffness was very high (the ratio was 540), it was assumed that there would be no rotation at the nodal points. Thus, the lateral stiffness of the first story was calculated as

$$k_1 = 4 * \left(\frac{12\,E\,I}{L^3} \right) \tag{3.1}$$

where E is the elasticity modulus of steel (E=2 ·10^{11} N/m^2), I is the moment of inertia in the direction of motion (I= 8.333 ·10^{-9} m^4) and L is the clear length of a column (L=0.80 m). Since each story has four columns, stiffness of a column was multiplied by four in order to obtain the total stiffness of a story. Since all the columns have identical dimensions, the stiffness of each story is also identical with that of the first story. The total stiffness of a story was then found as

$$k_{story} = k_1 = 156250\,N/m \tag{3.2}$$

This value was verified by a pull test by Turan and Aydın (2011) . They applied a force on the first story and both the resulting displacement and the applied load were measured. The ratio of these measured values was close to the value given in equation 3.2. Thus, this stiffness value was used as the story stiffness in the mathematical model. The stiffness matrix of the model was constructed in the light of the provided information as

$$K = \begin{bmatrix} 312500 & -156250 & 0 \\ -156250 & 312500 & -156250 \\ 0 & -156250 & 156250 \end{bmatrix} N/m \tag{3.3}$$

Steel slabs were placed on the beams of the structure to include story masses. By geometrical measurements of the steel components, story masses were determined as 194 kg, 194 kg and 190 kg for the first, second and third stories, respectively. By considering the lumped mass configuration, the mass matrix of the model was constructed as

$$M = \begin{bmatrix} 194 & 0 & 0 \\ 0 & 194 & 0 \\ 0 & 0 & 190 \end{bmatrix} kg \tag{3.4}$$

Turan and Aydın (2011) also determined the free vibration characteristics of the model. They had performed a number of numerical simulations before determining the actual free vibration characteristics of the model by experiments. Free vibration periods of the three modes of the structure were estimated by experiments performed on the physical structure. Modal damping ratios of the three modes of the structure were also estimated by these experiments. Each damping ratio was calculated by using the logarithmic decrement method. Theoretical results were then compared to the results of the experiments. Theoretical and experimental free vibration characteristics of the structure are represented in Table 3.1.

Table 3.1. Free vibration characteristics of the model structure

	Free vibration period (s)			**Damping Ratio (%)**		
	T_1	T_2	T_3	ξ_1	ξ_2	ξ_3
Theoretical	0.498	0.177	0.122	-	-	-
Experimental	0.525	0.186	0.125	0.58	0.53	0.57

A classical damping coefficient matrix was constructed by using the Rayleigh damping approach (Chopra, 2012). While evaluating the damping coefficient matrix, the damping ratios were considered to be 0.005 for the first and second mode as obtained

from the experimental analysis. In the light of this information, the damping coefficient matrix of the model was constructed as

$$C = \begin{bmatrix} 82.9574 & -32.4036 & 0 \\ -32.4036 & 82.9574 & -32.4036 \\ 0 & -32.4036 & 50.1796 \end{bmatrix} Ns/m \quad (3.5)$$

3.2.2. Numerical Study

In the numerical study, NExT-ERA was implemented on the constructed mathematical model of the physical structure described in the previous section. The mathematical model were constructed within Matlab environment including the scenarios of structural changes to be identified. The unchanged state and each structural condition of the model were excited by generated white noise signals to obtain ambient vibration responses from each state. The modal parameters of the mathematical model were estimated by using the NExT-ERA method and simulated structural changes in the mathematical model were tried to be identified using the least squares approach which will be discussed section 3.2.2.5 on page 66. In the following section, each structural condition is described in detail.

3.2.2.1. Structural Conditions

Various scenarios were considered as changes in structural conditions to be able to verify the identification algorithm. Changes in structural conditions were simulated by means of changes in story masses. The reason to prefer mass changes as the structural changes instead of stiffness changes was that it was possible to repeat the tests exactly when needed. To this end, a total of 10 different mass combinations was used to simulate the change in structural conditions in addition to the unchanged state. In order to organize the mass combinations, four different mass blocks with a mass of 40 kg, 43 kg, 46 kg and 19 kg were considered to be added on the floors of the structure. The first three blocks which have considerably close mass values to each other and the last one with a relatively less mass value were selected to be able to investigate the sensitivity of the identification technique in the identification of structural changes. For the first

condition, no mass was added to the structure representing that the structure was initially in the unchanged state. Table 3.2 shows all the structural conditions, or in this case the mass combinations by representing the additional mass block locations on the structure.

Since the mass blocks were considered to be added on the story floors, they change the total story mass on which they are added. For instance, there is an additional mass only on the first story in the second structural condition. The story mass which is 194 kg in the unchanged state increases to 240 kg in the second condition because of an additional mass block of 46 kg. Similarly, the remaining structural conditions imply additions in story masses which result in reduced frequencies of the structure.

Table 3.2. Representation of mass locations for each structural condition

Structural Condition	**Story I**	**Story II**	**Story III**
1 (unchanged)	0	0	0
2	46 kg	0	0
3	46 kg	43 kg	0
4	46 kg	43 kg	40 kg
5	0	43 kg	40 kg
6	46 kg	0	40 kg
7	0	0	40 kg
8	0	43 kg	0
9	19 kg	0	0
10	0	19 kg	0
11	0	0	19 kg

3.2.2.2. Generation of Response Data from the Mathematical Model

Ambient ground motions were generated and the resulting vibrational story responses of the mathematical model were used in the implementation of NExT-ERA. Ambient ground motions were formed by using normally distributed Gaussian white noise signals by using *randn.m* function of Matlab. Each generated white noise signal had a sampling frequency of 1000 Hz and a duration of 300 seconds. Since the highest

modal frequency of the model was not exceeding 10 Hz, there was no need for excitation signals to have a frequency content higher than 20 Hz. For this reason, the excitation signals were filtered by using a 6th order low-pass Butterworth filter with a cutoff frequency of 20 Hz. Unchanged state and all the other structural conditions of the model were excited by using white noise signals with the same properties as described above, but with different seeds. In other words, all excitations had the same statistical properties, but they were different signals. A representative white noise signal which was used to excite the unchanged state of the model is illustrated in Figure 3.3. The figure illustrates the first 50 seconds of the signal.

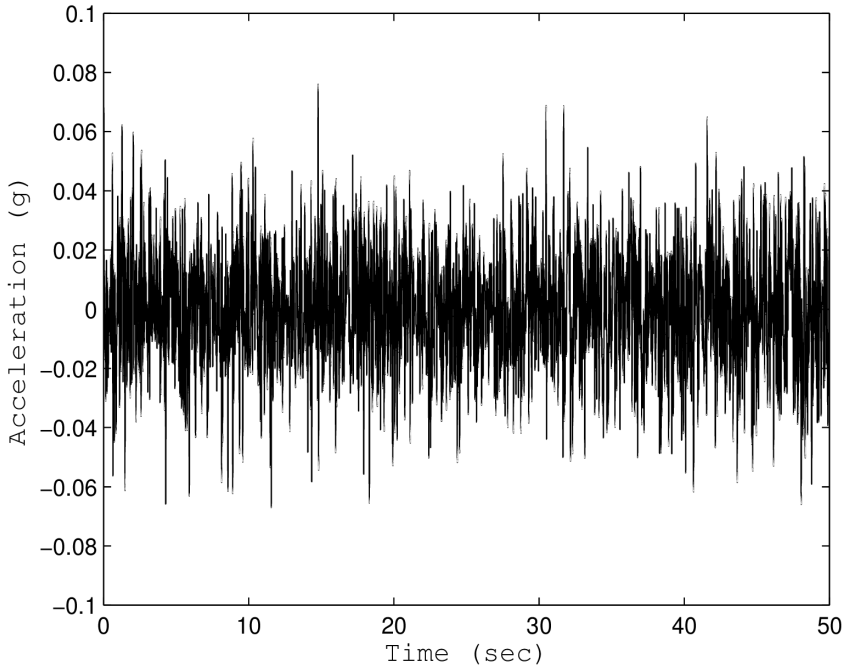

Figure 3.3. White noise signal used to excite the unchanged state of the model

Acceleration response data of each structural condition of the model were obtained by using the Newmark-Beta method with constant average acceleration approach (Chopra 2012). In the simulations, initial conditions were considered to be zero. In order to imitate measurement noise effects as encountered in real life, random noise is added to the acceleration response of each story by using the Matlab *randn* function. The noise was set for each acceleration response to have a root mean square (RMS) of %70 of the RMS of the response itself. Acceleration response data had a sampling frequency of 1000 Hz and have a duration of 300 seconds as the excitation signals had.

The vibrational frequencies of the first, second and third modes of the mathematical model are around 2 Hz, 5 Hz and 8 Hz for all structural states, respectively. These frequencies were expected to show up in the response data in addition to the forced excitation responses, which would have frequencies up to 20 Hz. Therefore, the frequency response of interest for the identification procedure was much lower in bandwidth than the provided 1000 Hz. As a consequence of this, the acceleration response data were down-sampled to 100 Hz by using the *resample.m* function of Matlab. This function also passes the data through a low pass anti-aliasing filter prior to the re-sampling process. This re-sampling procedure resulted in a Nyquist frequency of 50 Hz, which was higher than twice the largest value of the natural and excitation frequencies of the structure. This complied with the Nyquist theorem. Re-sampling process of the data also reduced the number of points in the acceleration signals. This significantly shortened the computation time of the identification algorithm. Figure 3.4 shows the re-sampled acceleration response data obtained from the unchanged state of the mathematical model.

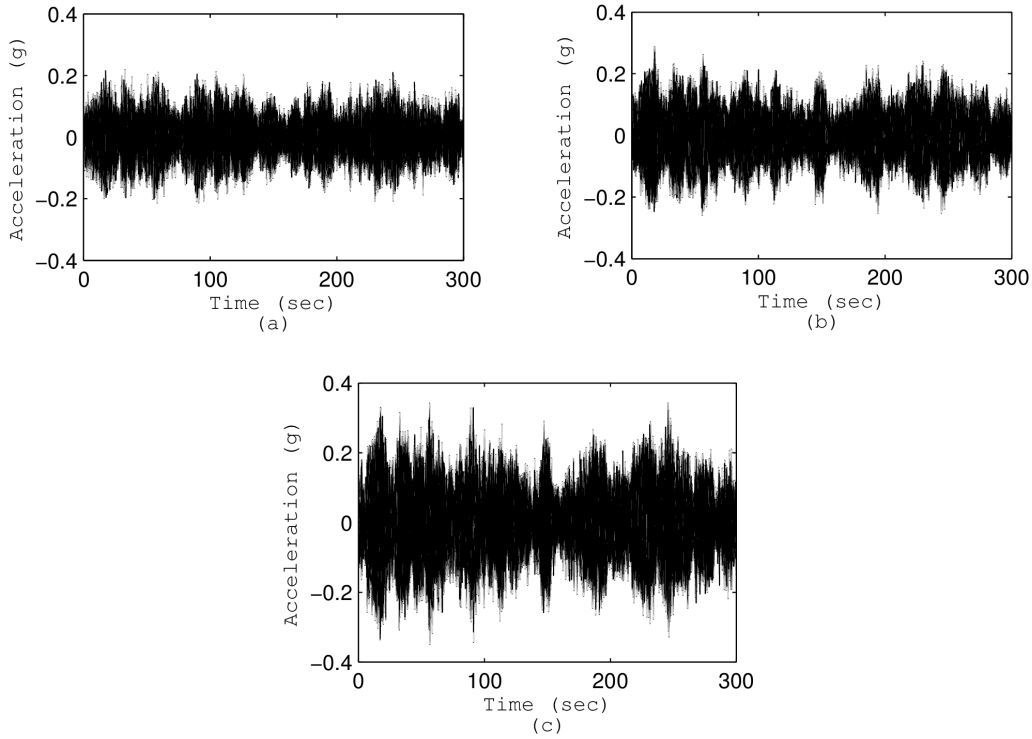

Figure 3.4. Re-sampled acceleration response of a) the first b) the second and c) the third story obtained from the unchanged state of the mathematical model

3.2.2.3. Identification Process

The guidelines provided in section 2.6 of the previous chapter have been followed for the identification process of the mathematical model. Once the re-sampled acceleration response data were obtained for each structural condition of the model, they were firstly processed by NExT to obtain the cross-correlation functions. The cross-correlation functions were evaluated by the discrete IFFT of the cross-spectral density functions. Therefore, the first step was to obtain the cross-spectral density functions. To this end, the cross-spectral density functions were evaluated by using *cpsd.m* function of Matlab. This function uses the Welch's method during the calculation of the cross-spectral density functions. In the calculations, each data frame consisted of 1024 points of the acceleration data. The overlapping ratio between two consecutive frames were taken as 50%. It should be noted that these values were determined by trial and error repeating the identification process for several times. To prevent the leakage effects for overlapped frames, a Hamming window with a length of 1024 points was also applied on the data in each frame.

The dynamic system of the model structure was priorly known since it was a simple structure. Therefore, the appropriate reference channel to be used for the determination of high quality cross-spectral functions were easily determined by trial and error. In case the previous knowledge of the dynamic system is unknown, the stabilization diagrams could be employed to ensure a successful identification process. The stabilization diagrams will be explained in the following paragraphs. Each acceleration response signal was selected as the reference channel and thus a total of three identification processes were performed. At the end of these identification processes, the stable results were obtained when the acceleration response of the second story was selected as the reference channel. Therefore, acceleration response of the second story was considered as the true reference channel for the identification process. The cross-spectral density function (CPSD) of the first story response of the unchanged state is illustrated in Figure 3.5. Frequency content of 20 Hz is represented in the figure to visually focus on the peaks although the CPSDs were obtained within the Nyquist frequency range (50 Hz). In the figure, peak values of the evaluated cross-spectral density functions were also compared with the peak values of the FFT plot of the re-sampled acceleration response of interest. By doing so, it was verified that the cross-

spectral density functions were successfully estimated to have the information on the three modes of the model.

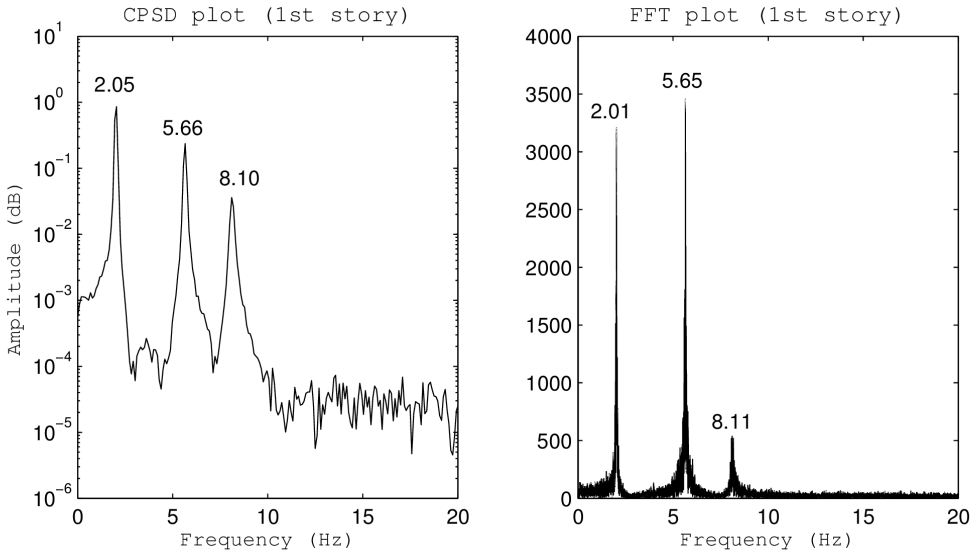

Figure 3.5. The CPSD of the acceleration response data [Reference channel: 2nd story] (Left), FFT plot of the acceleration response data (Right)

Once the cross-spectral density functions were successfully evaluated, the cross-correlation functions were easily obtained by taking the discrete IFFT of the cross-spectral density functions. To do this, the *ifft.m* function of Matlab was employed. Figure 3.6 illustrates the cross-correlation functions (x-corr) obtained from the cross-spectral density functions illustrated in Figure 3.5. The NExT section ended with the evaluation of the correlation functions.

The correlation functions were then employed in ERA to identify modal parameters of the model structure. As the first step of ERA, the Hankel matrix was constructed by using the obtained correlation functions. The constructed Hankel matrix consisted of 32 columns and 144 rows. While constructing the Hankel matrix, block matrices were firstly constructed (Nayeri et al. 2009). Each block matrix with a size of 48x32 were constructed to have information from the correlation functions of the first, second and third story. Thus, in each block matrix a total of 0.79 seconds of the correlation functions were used. Then, the constructed three block matrices were added one under the other, which forms the Hankel matrix with a size of 144x32.

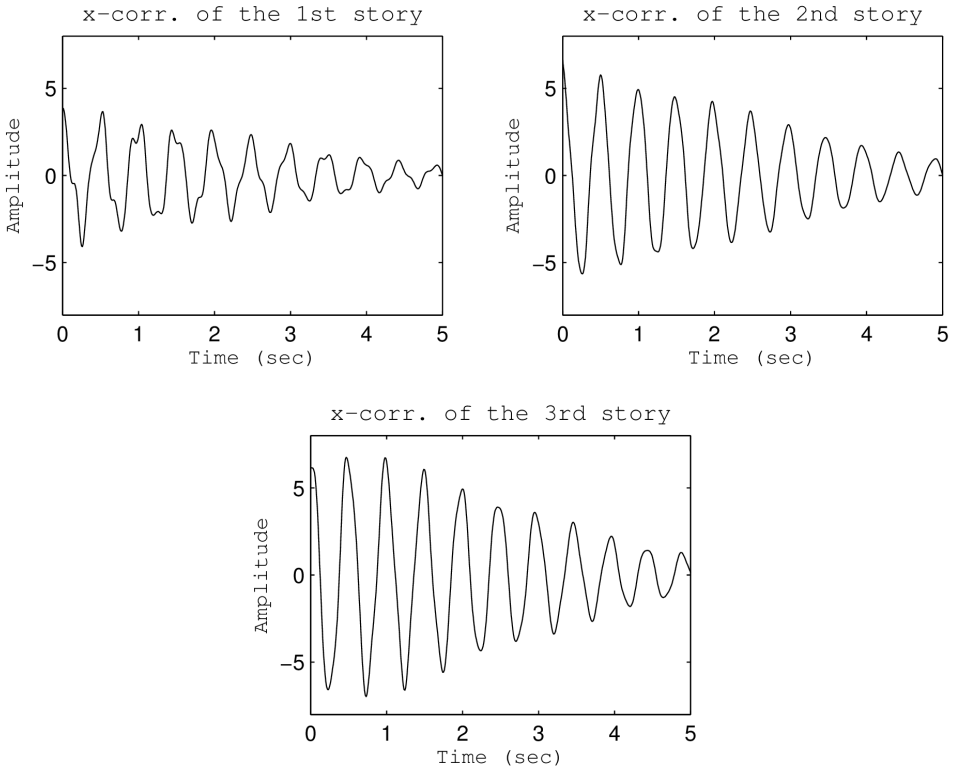

Figure 3.6. The correlation functions [Reference channel: 2nd story]

As the next step, the Hankel matrix were decomposed into its singular values. The singular values of the constructed Hankel matrix are illustrated in Figure 3.7. As shown in the figure, the first 6 points have significantly high singular values when compared to the remaining ones. This means that the system may have 6 poles of vibration (3 modes of vibration). Besides, the singular values should not be only the criterion to determine the number of poles.

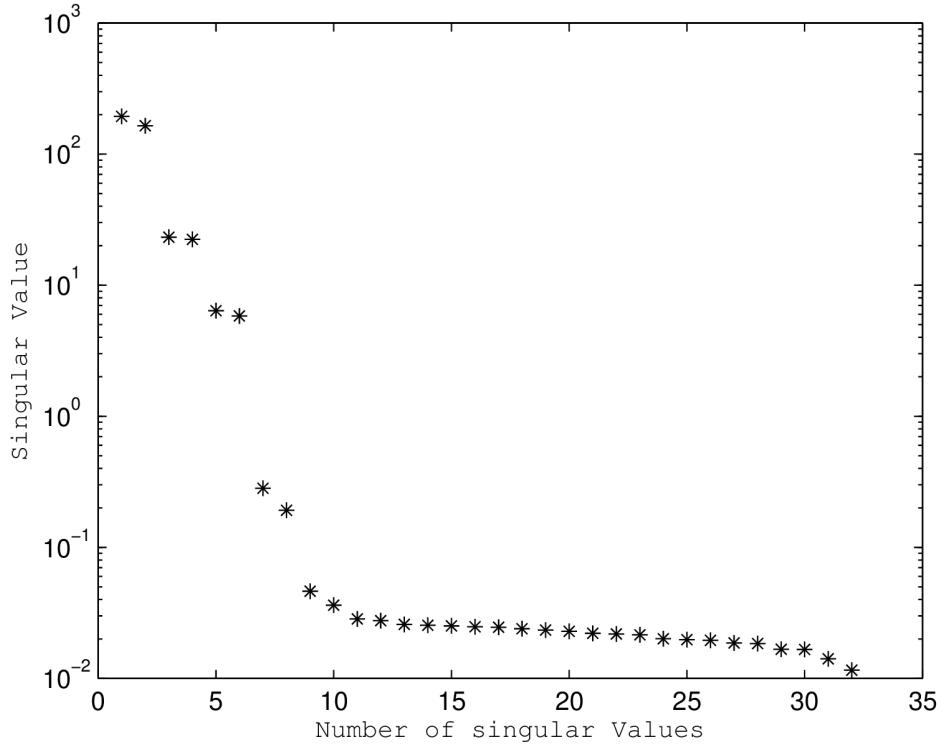

Figure 3.7. Singular values of the constructed Hankel Matrix

Since there are infinite numbers of system matrices in the state-space representation, the identification process by ERA is based on the minimum realization to obtain the system matrices in the state-space representation (Caicedo 2011). In the light of this fact, system matrices in the state-space representation were obtained by using a model order of 6 as the minimum realization of these matrices. Thus, the true modes of the system were successfully identified at the end of the identification process. The reason to select the model order to be 6 was that the poles of the model structure had been already known from the dynamics of the model. However, if the model order of the structure had not been known, the stabilization diagrams and the modal assurance criterion (MAC) should have been then employed to distinguish the true modes from the computational ones. To be able to see the effect of the selection of model order on the identification process, we obtained the stabilization diagrams by changing the model order of the structure from 2 to 20. Moreover, we obtained the stabilization diagrams by changing the reference channel in the calculation of the cross-spectral density functions to be able to see the effect of the selection of reference channel on the identification process. The stabilization diagrams which were obtained by selecting the acceleration

response signal of the first, second and third story of the unchanged state are illustrated in Figure 3.8.

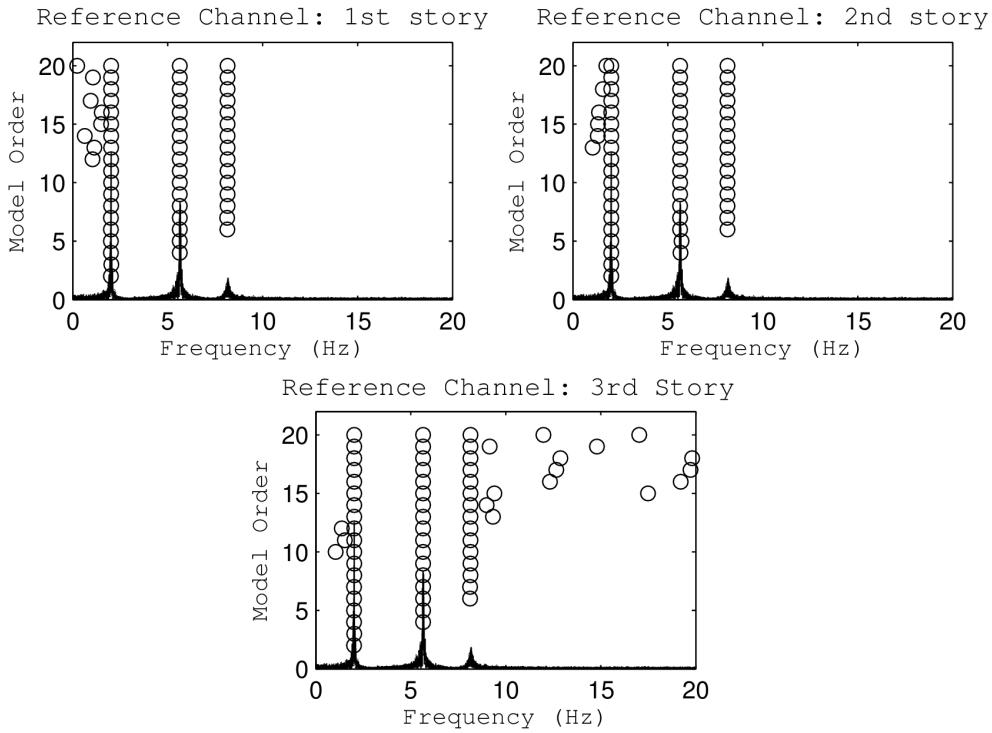

Figure 3.8. Stabilization diagrams obtained by different reference channels

The stabilization diagrams were provided with the CPDS plot of the acceleration response of the first story for the verification purpose. As seen in the figure, the modal frequencies of the first, second and third mode (2.02 Hz, 5.65 Hz and 8.64 Hz, respectively) stably show up in all the three stabilization diagrams. All three modes appear in the model order range from 6 to 20. On the contrary, the third mode does not appear for model orders that have smaller values than 6. The second and third mode does not also appear for model orders that have smaller values than 4. In addition, some unstable modes are clearly seen after the model order value of 10. These are the computational modes which have nothing to do with the structure under investigation.

3.2.2.4. Modal Identification Results

It should be noted again that the model order value of 6 was used in the identification process of all the structural conditions of the model. After the system matrices in the state-space representation had been evaluated with a minimum realization, modal parameters of the mathematical model were obtained by the eigenvalue analysis of the evaluated system matrices. To be able to verify the modal identification results, modal parameters of the mathematical model were also obtained by the eigenvalue analysis of its stiffness and mass matrix. These were considered as the exact modal parameters of the mathematical model.

As a result of the identification process provided in the previous section, the identified modal frequencies of all the structural conditions of the model by using NExT-ERA are shown in Table 3.3. According to the results, modal frequencies of the mathematical model have been successfully identified with a maximum error of 0.24%.

The identified modal damping ratios of all the structural conditions of the model by using NExT-ERA are shown in Table 3.4. According to the results, the minimum error for the identification of the modal damping ratios is 0.5% while the maximum error is 66%. The identification results of the damping ratios were incorrect, but as many researchers have also encountered the same issue, the incorrectness was considered normal for the identification process by NExT-ERA.

Table 3.3. Comparison of the Modal Frequencies

Modal Frequencies (Hz)						
	Exact (by eigenvalue analysis)			**Identified by NExT-ERA**		
Case	f_1	f_2	f_3	f_1	f_2	f_3
1	2.022	5.653	8.148	2.019	5.649	8.142
2	1.996	5.310	7.902	1.991	5.304	7.886
3	1.922	5.285	7.456	1.921	5.281	7.452
4	1.832	5.105	7.360	1.828	5.105	7.346
5	1.852	5.384	7.681	1.849	5.380	7.673
6	1.894	5.149	7.803	1.892	5.147	7.798
7	1.891	5.436	8.060	1.888	5.435	8.058
8	1.946	5.589	7.747	1.947	5.591	7.739
9	2.011	5.506	8.028	2.012	5.514	8.024
10	1.988	5.625	7.951	1.987	5.625	7.940
11	1.969	5.561	8.108	1.968	5.556	8.115

Table 3.4. Comparison of the Modal Damping Ratios

Modal Damping Ratios (%)						
	Exact (by eigenvalue analysis)			**Identified by NExT-ERA**		
Case	ξ_1	ξ_2	ξ_3	ξ_1 ***(Error)***	ξ_2 ***(Error)***	ξ_3 ***(Error)***
1	0.5 for all modes			0.539 **(7%)**	0.580 **(16%)**	0.674 **(34%)**
2				0.502 **(0.5%)**	0.477 **(4%)**	0.743 **(48%)**
3				0.477 **(4%)**	0.581 **(16%)**	0.637 **(27%)**
4				0.693 **(38%)**	0.447 **(10%)**	0.548 **(9%)**
5				0.548 **(9%)**	0.496 **(0.6%)**	0.613 **(22%)**
6				0.527 **(5%)**	0.512 **(2%)**	0.832 **(66%)**
7				0.664 **(32%)**	0.450 **(10%)**	0.669 **(33%)**
8				0.557 **(11%)**	0.525 **(5%)**	0.667 **(33%)**
9				0.545 **(9%)**	0.533 **(6%)**	0.639 **(27%)**
10				0.648 **(29%)**	0.503 (**0.6%)**	0.597 **(19%)**
11				0.594 **(18%)**	0.535 **(7%)**	0.734 **(46%)**

For the verification of the mode shape identification, MAC values were calculated between the identified and exact mode shapes of the mathematical model. This criterion is based on the modal orthogonality principle. Therefore, MAC values take values between 0 and 1. Accordingly, if the identified modes are consistent with the exact modes of the system, the MAC values converge to 1. To the contrary, for inconsistent modes, the value converges to 0. The MAC values are calculated by using the following expression;

$$MAC_{i,j} = \frac{(\Phi_i^T \Phi_j)^2}{(\Phi_i^T \Phi_i)(\Phi_j^T \Phi_j)} \tag{3.6}$$

where Φ_i and Φ_j are the two mode shape vectors. Superscript T represents the transpose of the vector. The identified mode shapes of the unchanged state are illustrated with their MAC values in Figure 3.9. Calculated MAC values and visual inspection have been revealed that the mode shapes of all the structural conditions of the mathematical model were successfully identified.

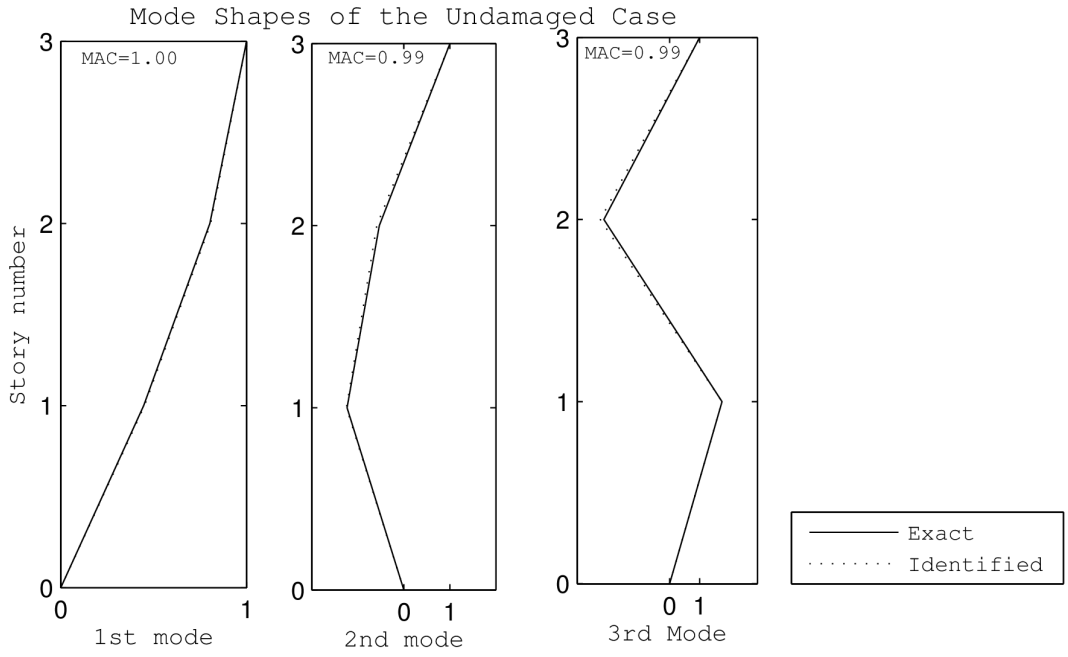

Figure 3.9. Comparison of the mode shapes of the unchanged state

3.2.2.5. Identification Results of Changes in Structural Conditions

After the modal parameters of the mathematical model had been identified, the story masses in each structural condition were able to be evaluated by using the least squares approach. In the least squares approach for this specific shear frame structure, the mass matrix can be identified only if the stiffness of each floor is known, or vice-versa, the stiffness matrix can be identified if the mass in each story is known (Caicedo, 2001). Although the stiffness matrix was available in the numerical model, it was considered that it should be obtainable from an unknown structure as well. Therefore, the stiffness matrix was firstly evaluated for the unchanged state by employing the modal parameter identification results of this state in the least squares approach. In the calculation of the stiffness matrix, the mass matrix of the mathematical model which was provided in equation 3.4 was used. From this point on, the stiffness matrix is assumed to be constant, while the changed mass matrix is being evaluated as

$$\begin{Bmatrix} m_1 \\ m_2 \\ m_3 \end{Bmatrix} = \frac{1}{3} \begin{bmatrix} I_3 & I_3 & I_3 \end{bmatrix} \begin{bmatrix} \delta_1 & & \\ & \delta_2 & \\ & & \delta_3 \end{bmatrix}^{-1} \begin{bmatrix} \Delta_1 \\ \Delta_2 \\ \Delta_3 \end{bmatrix} \begin{Bmatrix} k_1 \\ k_2 \\ k_3 \end{Bmatrix} \tag{3.7}$$

where

$$I_3 = \begin{bmatrix} 1 & 0 & 0 \\ 0 & 1 & 0 \\ 0 & 0 & 1 \end{bmatrix}, \quad \delta_i = \begin{bmatrix} \phi_{1i}\lambda_i & 0 & 0 \\ 0 & \phi_{2i}\lambda_i & 0 \\ 0 & 0 & \phi_{3i}\lambda_i \end{bmatrix}, \quad \Delta_i = \begin{bmatrix} \phi_{1i} & \phi_{1i}-\phi_{2i} & 0 \\ 0 & \phi_{2i}-\phi_{1i} & \phi_{2i}-\phi_{3i} \\ 0 & 0 & \phi_{3i}-\phi_{2i} \end{bmatrix} \tag{3.8}$$

I_3 is a 3 x 3 identity matrix, λ_i is the i'th eigenvalue, and ϕ_{ji} is the i'th mode shape amplitude at the j'th story (j=1,2,3) which are calculated by the NExT-ERA method. The identification results of the story masses obtained by this technique are given in Table 3.5. According to the identification results, the mass of the second story in condition 10 was identified with a minimum error of 0.01%. In contrast, the mass of the first story in condition 6 was identified with a maximum error of 2.80%. As a conclusion, changes in story masses have been successfully identified with the changes in modal parameters of the mathematical structure by using an output-only system identification technique.

Table 3.5. Comparison of the Story Masses

Case		Values of the Story Masses (kg)				
		Exact			Identified	Error (%)
		Story Mass	Additional mass	Total story mass		
1	Story 1	194	-	194	196.40	1.23
	Story 2	194	-	194	195.56	0.80
	Story 3	190	-	190	190.70	0.37
2	Story 1	194	46	240	246.12	2.55
	Story 2	194	-	194	196.84	1.46
	Story 3	190	-	190	191.99	1.04
3	Story 1	194	46	240	244.19	1.74
	Story 2	194	43	237	239.43	1.02
	Story 3	190	-	190	192.26	1.19
4	Story 1	194	46	240	240.07	0.03
	Story 2	194	43	237	240.20	1.35
	Story 3	190	40	230	230.06	0.02
5	Story 1	194	-	194	198.04	2.08
	Story 2	194	43	237	236.40	0.25
	Story 3	190	40	230	230.27	0.11
6	Story 1	194	46	240	246.73	2.80
	Story 2	194	-	194	196.13	1.10
	Story 3	190	40	230	230.40	0.17
7	Story 1	194	-	194	196.25	1.16
	Story 2	194	-	194	196.49	1.28
	Story 3	190	40	240	240.09	0.04
8	Story 1	194	-	194	199.25	2.70
	Story 2	194	43	237	234.92	0.87
	Story 3	190	-	190	190.80	0.42
9	Story 1	194	19	213	214.24	0.58
	Story 2	194	-	194	195.16	0.59
	Story 3	190	-	190	191.54	0.81
10	Story 1	194	-	194	193.46	0.27
	Story 2	194	19	213	213.01	0.01
	Story 3	190	-	190	192.17	1.14
11	Story 1	194	-	194	198.62	2.38
	Story 2	194	-	194	193.44	0.28
	Story 3	190	19	209	212.17	1.52

3.2.3. Experimental Study

In the experimental study, NExT-ERA was implemented on the physical structure described in Section 3.2.1. To this end, acceleration sensors were placed on each story level of the structure and ambient vibration responses were acquired. The aim was to perform identification of modal parameters and changes in structural conditions exactly the same with the identification process conducted in the numerical study. However, reasonable data could not be acquired for changes in structural conditions of the structure possibly due to an unexpected failure of acceleration sensors. Therefore, the experimental study is presented here for only unchanged state of the physical structure.

Once the reasonable results of structural changes could not be identified, the stiffness matrix and the mass matrix of the physical structure were recalculated. For the stiffness matrix determination, constant external forces were applied to each story one at a time. The displacement response of each story under the each applied force was recorded with the value of applied force to determine the stiffness value of each story. The mass matrix was determined by detailed geometrical measurements of all structural elements of the physical structure. According to these processes, the stiffness matrix (K_{new}) and the mass matrix (M_{new}) of the structure were found as

$$K_{new} = \begin{bmatrix} 289640 & -144390 & 0 \\ -156250 & 283270 & -138870 \\ 0 & -138870 & 138870 \end{bmatrix} N/m \tag{3.9}$$

$$M_{new} = \begin{bmatrix} 189 & 0 & 0 \\ 0 & 190 & 0 \\ 0 & 0 & 192 \end{bmatrix} kg \tag{3.10}$$

3.2.3.1. Data Acquisition from the Physical Structure

Ambient vibration response data of the physical structure were acquired to be used in NExT-ERA in order to identify modal parameters of the structure. To do so, the physical structure was firstly fixed on the ground. Three piezoelectric acceleration

sensors were placed on each story level of the structure. The specifications of acceleration sensors are provided in Appendix A.

Acceleration response data were measured with a duration of 1 hour without applying any external force to the structure. The acceleration sensors had a noise level proportional with the frequency bandwidth and so the noise level was independent from the acceleration response amplitude. Noise-to-signal ratio was probably high since the amplitude of the acceleration response data was very small due to absence of any external force. This was the reason that the acceleration response data were measured with a duration of 1 hour, because long duration measurement allows to eliminate noise in the response signal by allowing more averaging in the NExT part. Data acquisition system which had a sampling frequency of 1000 Hz were used during the measurement. Figure 3.10 shows the physical structure with the acceleration sensors on each story and the data acquisition system.

(a) (b)

Figure 3.10. (a) Data acquisition system and (b) acceleration sensor placement on the physical structure

When the raw response signals were checked, it was seen that the signals were non-stationary and there were extraordinary peaks at some specific sections of the signals. However, response data should be stationary to be used in the NExT-ERA method. To this end, non-stationary response signals firstly needed to be transformed to the stationary signals. For this purpose, the signals were divided into smaller frames which overlap on each other. Each frame was having a duration of 5 seconds. As an example, the first frame had response values between 0 and 5 seconds, the second frame had response values between dt and (5 + *dt*) seconds and the third frame had response values between 2**dt* and (5 + 2*dt*). Then, the n^{th} frame had response values between (*n*-1)*dt* and 5+(*n*-1)*dt* seconds. Here, *dt* is the sampling period of the signals (*dt* = 0.001 sec.). The mean value of the signals in each frame were then subtracted from response value at the midpoint of the frame. For example, mean value of the signal in the first frame was subtracted from the response value at t=2.5 sec. and mean value of the signal in the second frame was subtracted from the response value at t=2.5+*dt* sec. To cut down relatively small frequencies, the data were also filtered by a high-pass 5^{th} order Butterworth filter with a cut-off frequency of 0.3 Hz. The extraordinary peaks were also truncated from the signal. The first and the last 3 minutes of the signals were not taken account to ensure the stationary data. By applying this process for whole signal, stationary response data were obtained with a duration of 50 minutes. Figure 3.11 shows the stationary response signal obtained from the first story of the physical structure.

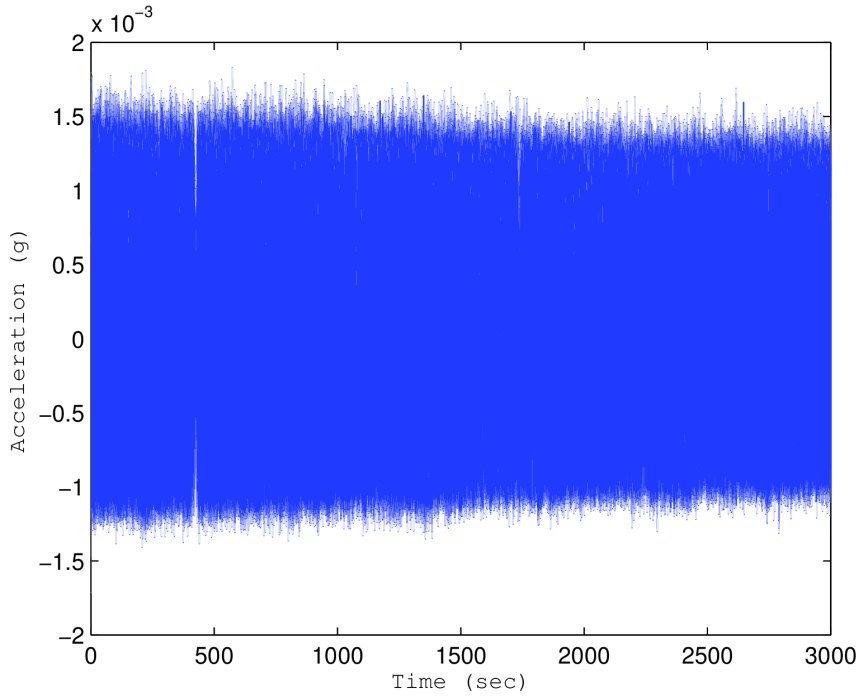

Figure 3.11. A representative ambient response data obtained from the first story of the physical structure

The vibrational frequencies of the first, second and third modes of the physical structure which were calculated by using K_{new} and M_{new} are evaluated as 1.94 Hz, 5.41 Hz and 7.86 Hz, respectively. These frequencies were expected to show up in the response data in addition to the forced excitation responses, which would have frequencies up to 20 Hz. Therefore, the frequency response of interest for the identification procedure was much lower in bandwidth than the provided 1000 Hz by the data acquisition system. Therefore, the acceleration response data were down-sampled to 50 Hz by using the *resample.m* function of the Matlab program. Thus, this re-sampling procedure resulted in a Nyquist frequency of 25 Hz, which was higher than twice the largest value of the vibrational frequencies of the structure. This complied with the Nyquist theorem. In addition, the sample size were reduced to shorten the computation time of the identification process. Figure 3.12 shows the re-sampled acceleration data obtained from the first story of the physical structure (re-sampled form of the provided data in Figure 3.11)

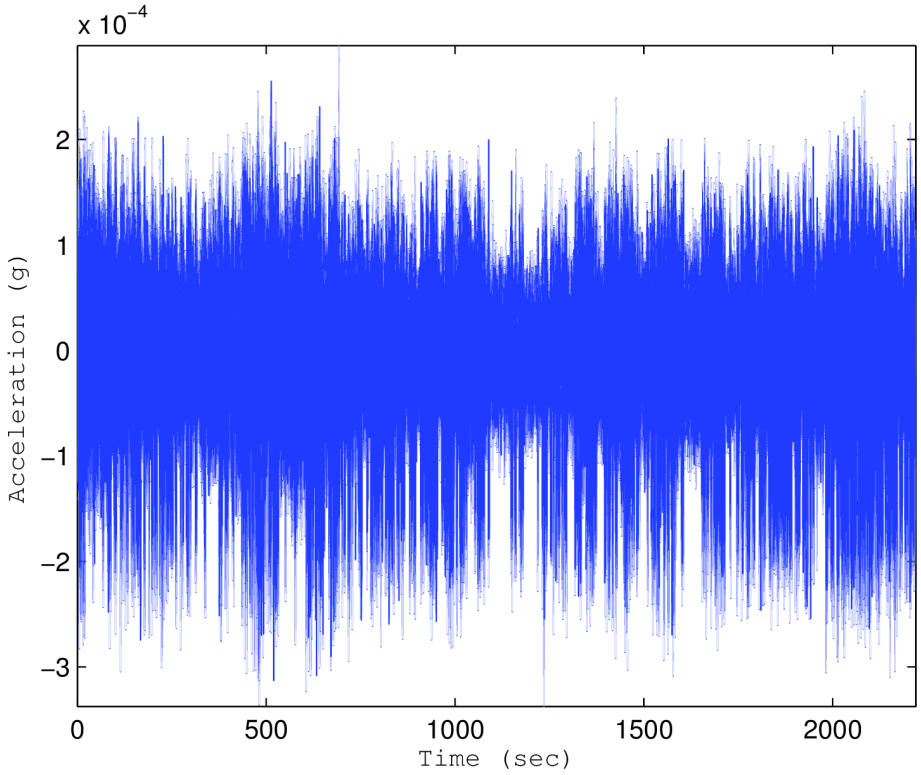

Figure 3.12. A representative re-sampled ambient response data obtained from the first story of the physical structure

3.2.3.2. Identification Process

The guidelines provided in section 2.6 have been followed for the identification process of the physical structure. Once the re-sampled acceleration response data were obtained, they were firstly processed by NExT to obtain the cross-correlation functions. The cross-correlation functions were evaluated by the discrete IFFT of the cross-spectral density functions. Therefore, the first step was to obtain the cross-spectral density functions. To this end, the cross-spectral density functions were evaluated by using *cpsd.m* function of Matlab. Caicedo (2001) recommended to use long data frames in case of using noisy data to be able to identify mode shapes in high accuracy. In the light of this recommendation, re-sampled data were divided into data frames of 10240 points. The overlapping ratio between two consecutive frames were taken as 50%. It should be noted that the number of points in data frames and overlapping ratio were determined by trial and error. To prevent the leakage effects for overlapped frames, a Hamming window with a length of 10240 points was also applied on the data in each frame.

The appropriate reference channel to be used for the determination of high quality cross-spectral functions were determined by trial and error. Each acceleration response signal was selected as the reference channel and thus a total of three identification processes were performed. At the end of these identification processes, the stable results were obtained when the acceleration response of the third story was selected as the reference channel. Therefore, acceleration response of the third story was considered as the true reference channel for the identification process of the physical structure. The cross-spectral density function (CPSD) is calculated by using the aforementioned parameters. Once the CPSD were successfully evaluated, the cross-correlation functions were easily obtained by taking the discrete IFFT of the cross-spectral density functions. To do this, the *ifft.m* function of Matlab was employed. Figure 3.6 illustrates the cross-correlation functions (x-corr) obtained from the cross-spectral density functions illustrated in Figure 3.5. The NExT section ended with the evaluation of the correlation functions. The CPSD and the x-corr of the first story response is illustrated in Figure 3.13(a) and (b), respectively. Frequency content of the Nyquist frequency (25 Hz) is represented in the figure (a).

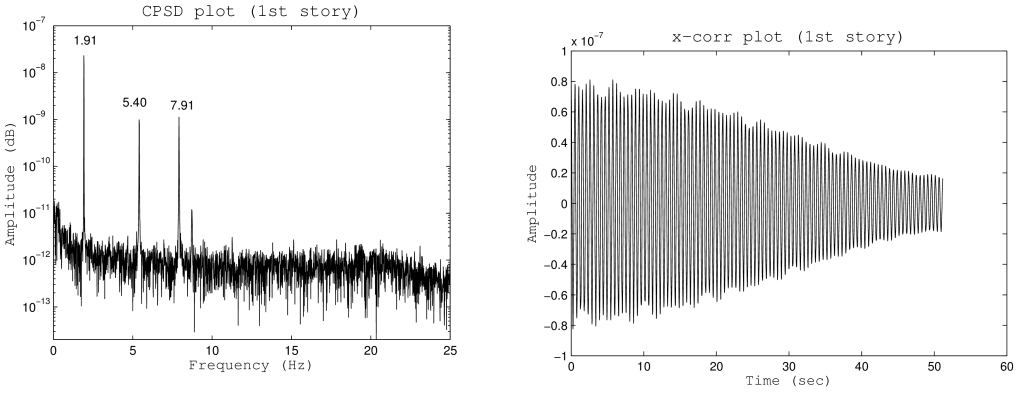

(a) *(b)*

Figure 3.13. (a) The CPSD and (b) the correlation function of the re-sampled acceleration data of the 1st story [Reference channel: 3rd story]

The correlation functions were then employed in ERA to identify modal parameters of the physical structure. As the first step of ERA, the Hankel matrix was constructed by using the obtained correlation functions. The constructed Hankel matrix consisted of 120 columns and 2160 rows. While constructing the Hankel matrix, block matrices were firstly constructed (Nayeri et al., 2009). Each block matrix with a size of

720x120 were constructed to have information from the correlation functions of the first, second and third story. Thus, in each block matrix a total of 16.78 seconds of the correlation functions were used. Then, the constructed three block matrices were added one under the other, which forms the Hankel matrix with a size of 2160x120. It should be noted here that the size of the constructed Hankel matrix was much larger than the Hankel matrix constructed in the numerical study. The reason was to include more data from the correlation function into the identification process to eliminate noisy data and to ensure having all possible modes of vibration.

The next step was to decompose the Hankel matrix into its singular values. The singular values of the constructed Hankel matrix are illustrated in Figure 3.14. As shown in the figure, the first 6 points have significantly high singular values and also the first 6 points seem to constitute 3 pairs when compared to the remaining ones. This means that the system may have 6 poles of vibration (3 modes of vibration). Besides, the singular values should not be only the criterion to determine the number of poles.

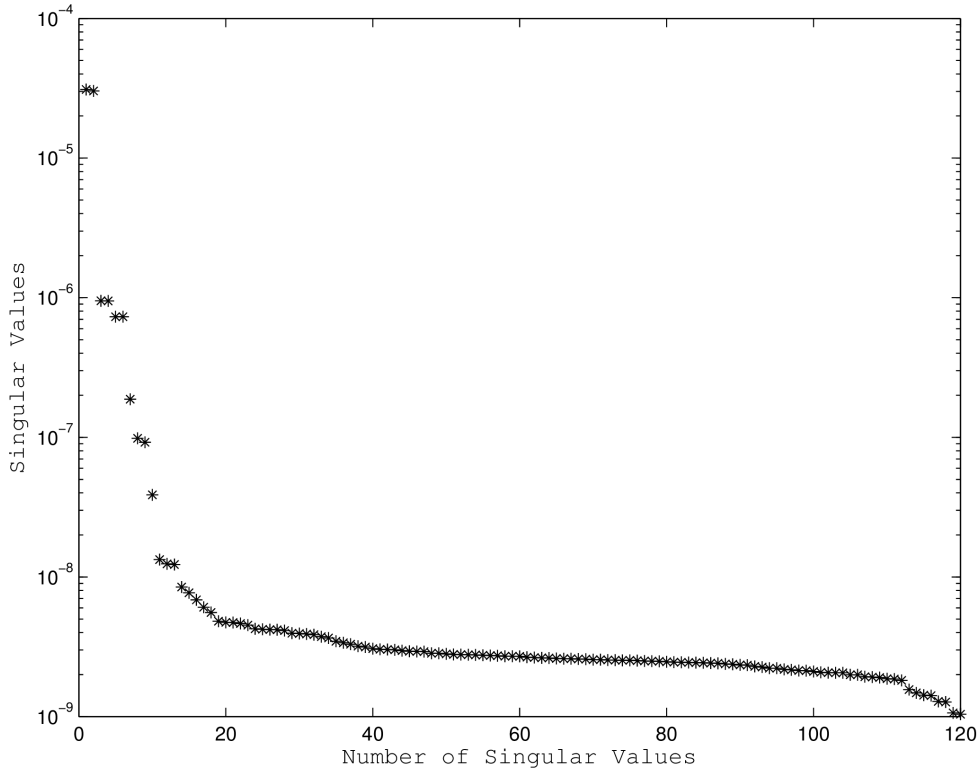

Figure 3.14. Singular values of the constructed Hankel matrix

The identification process by ERA is based on the minimum realization to obtain the system matrices in the state-space representation as discussed in section 2.5. In the light of this fact, system matrices in the state-space representation were obtained by using a model order of 6 as the minimum realization of these matrices. Thus, the true modes of the system were successfully identified at the end of the identification process. The reason to select the model order to be 6 was that the poles of the physical structure had been already known from the dynamics of the numerical model. To be able to see the effect of the selection of model order on the identification process, we obtained the stabilization diagrams by changing the model order of the structure from 2 to 20. Moreover, we obtained the stabilization diagrams by changing the reference channel in the calculation of the cross-spectral density functions to be able to see the effect of the selection of reference channel on the identification process. The stabilization diagrams which were obtained by selecting the acceleration response signal of the first, second and third story are illustrated in Figure 3.15.

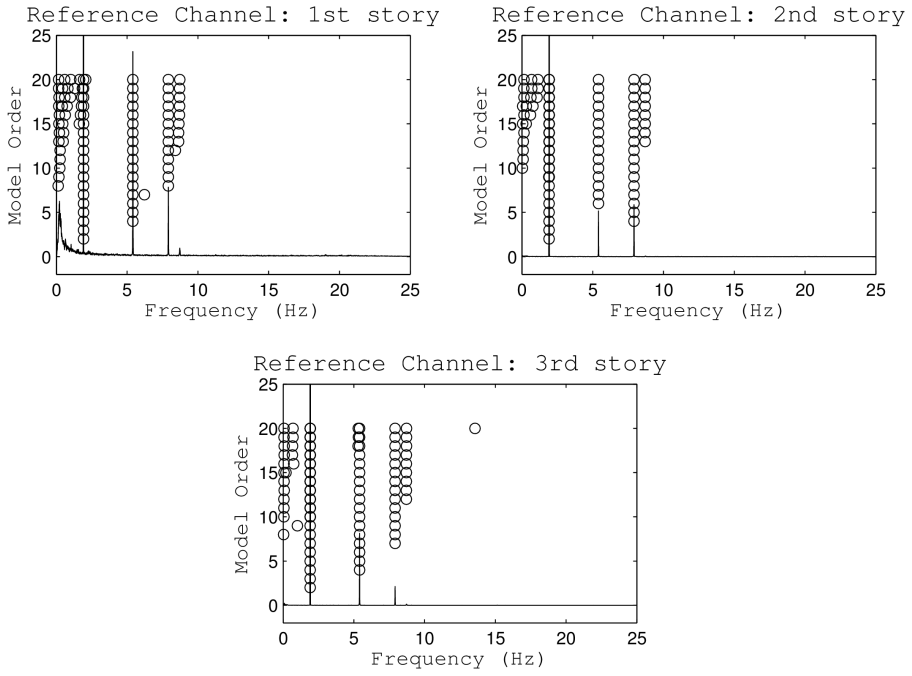

Figure 3.15. Stabilization diagrams obtained by using different reference channels

The stabilization diagrams were provided with the CPSD plots of the acceleration response of the first story for the verification purpose. As clearly seen in the figure, some modes stably show up for specific numbers of model order and they are

also stable in all the three stabilization diagrams. These stable modes correspond to the modal frequencies of the first, second and third mode (1.94 Hz, 5.41 Hz and 7.86 Hz, respectively) of the physical structure. All three modes appear in the model order range from 6 to 20. For smaller values of the model order than 6, some modes does not appear on the stabilization diagrams. In addition, many unstable modes are clearly seen in the range of 0 – 1 Hz. Since these modes have an unstable behavior, they may be considered as computational modes by visual inspection of the stabilization diagrams. However, if the diagrams are checked in detail, there is a stable mode on the frequency of 9 Hz. The certain way to distinguish the true modes of vibration from the computational ones is to calculate MAC values of the identified mode shapes between the same modes identified by different model order. On the other hand, the MAC values can bu calculated between the identified mode shapes from the physical model and the mode shapes of the mathematical model which are found from the eigenvalue analysis. In this study, we calculated the MAC values between the identified mode shapes and the mode shapes of the mathematical model which are obtained from the eigenvalue analysis.

3.2.3.3. Modal Identification Results

The model order value of 6 was used to present the identification results. After the system matrices in the state-space representation had been evaluated with a minimum realization, modal parameters of the physical structure were obtained by the eigenvalue analysis of the identified system matrices. To be able to verify the modal identification results, modal parameters of the mathematical model which was reconstructed by using K_{new} and M_{new} were obtained by the eigenvalue analysis. These were considered the exact modal parameters of the physical structure.

The identification results of the first, second and the third modal frequencies and modal damping ratios of the physical structure are presented in Table 3.6. Modal frequencies have been successfully identified with a maximum error of 0.2%.

Table 3.6. Comparison of the modal frequencies and the modal damping ratios

	Modal frequencies (Hz)			**Damping Ratio (%)**		
	f_1	f_2	f_3	ξ_1	ξ_2	ξ_3
Exact	1.94	5.41	7.86	0.5		
Identified	1.91	5.40	7.91	0.54	0.64	0.44

The minimum error for the identification of the modal damping ratios is 8% while the maximum error is 28%. The identification results of the damping ratios can be considered as incorrect but as discussed in the results of the numerical study, many researchers have also encountered the same issue. The numerical study was also resulted in such high errors in identification of modal damping ratios. Therefore, the incorrectness of the identified modal damping ratios of the physical structure was considered normal for the identification process by NExT-ERA.

For the verification of the mode shape identification, MAC values were calculated between the identified and exact mode shapes of the physical structure. The identified mode shapes and the mathematical mode shapes are illustrated with their MAC values in Figure 3.9. Calculated MAC values and visual inspection have been revealed that the mode shapes of the physical structure were successfully identified.

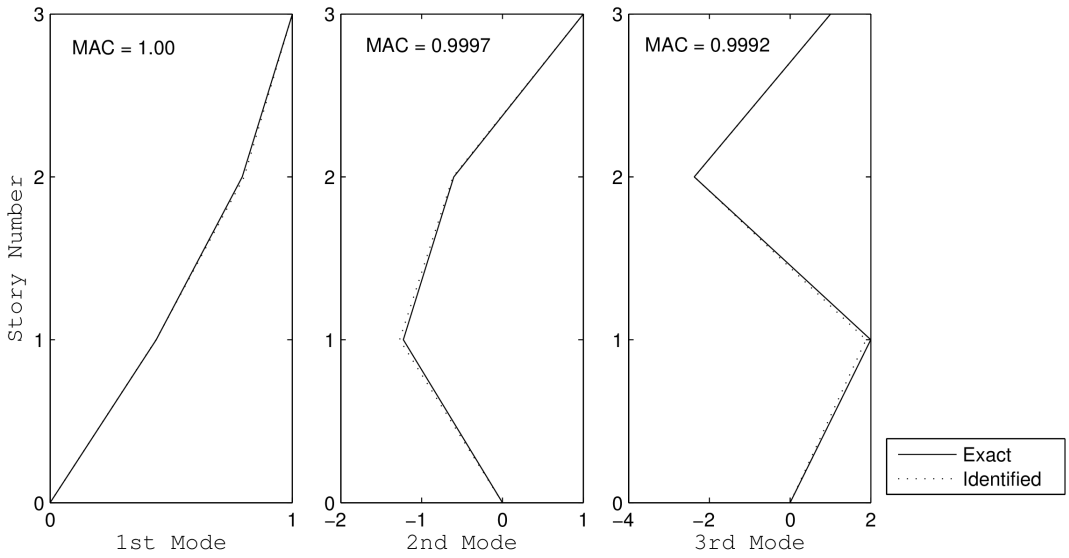

Figure 3.16. Comparison of the mode shapes of the physical structure

3.2.3.4. Results of Story Mass Identification

In the beginning of the experimental study, the aim was to perform identification of modal parameters and changes in structural conditions exactly the same with the identification process conducted in the numerical study. For this purpose, structural condition 2 was tried on the physical structure by adding a 46 kg block only on the first story. However, reasonable data could not be acquired for structural condition changes of the structure possibly due to an unexpected failure of acceleration sensors. Therefore, identification of structural changes could not be performed for the experimental study. Instead, the mass value of each story was identified for only unchanged state of the physical structure by using the least squares approach discussed in section 2.6.2. Identification results of the mass value of each story were presented in Table 3.7. According to the identification results of the story masses, story masses have been identified with a maximum error of 2.75% and with a minimum error of 1%.

Table 3.7. Comparison of story masses of the physical structure (unchanged)

	Story Mass Values (kg)		
	m_1	m_2	m_3
Exact	189	190	192
Identified	187	195	195

CHAPTER 4

MODAL PARAMETER IDENTIFICATON BY USING GROUPED RESPONSE MEASUREMENTS

4.1. Introduction

Experimental modal analysis of large civil structures such as bridges requires measurements of the bridge vibrations, which are generally arduous to obtain. Response measurements have been obtained with wired communication for years and today it is also possible to acquire such measurements with wireless communication by means of ongoing technological developments in wireless sensors. In the case of wired communication in long structures, environmental noise is very likely to enter the measured response signals. This means that acquired response measurements could not represent the actual structural response behavior when long signal cables are used. One way to reduce the noise in long cables is to use multiple data acquisition systems in the structure and have shorter distances to the sensors. On the other hand, when wireless sensors are used, the cable noise problems are resolved, but a few other problems are added. Since wireless communication bandwidth is very limited, all the wireless sensors cannot communicate with a central data acquisition unit. Thus, several data acquisition units need to be set up to acquire measurement data from distant sensors that are placed within a long or tall structure. As a result, the communication bandwidth of wireless sensors will stay in limited range (Basten and Schiphorst, 2012).

The usage of multi-centered data acquisition units increases the cost for both wired and wireless communication. In addition to this, usage of a large amount of sensors requires to use a large number of channels on data acquisition systems. This has a drawback on the maximum sampling rate of the data acquisition system. The maximum sampling rate of the measurement data decreases with the same proportion of increment in the number of channels used on data acquisition systems (Beyen et al., 2011). Fortunately, civil structures do not possess vibrational modes with high frequencies. To make it more precise, structural modes that have frequencies beyond 50 Hz are generally not opted for in experimental modal analysis. The main reason for this

fact can be based on the frequency bandwidth of the recorded past earthquakes. There is generally no significant ground motion at frequencies that are larger than 50 Hz (Besides, this seems to be the reason why earthquakes are generally recorded at a sampling rate of 200 Hz). Thus, it can be assumed that the structure will not be excited by larger frequencies. To conclude the sampling rate issue, it can be said that the larger amount of sensors are used during measurements, the lower will be the sampling frequency. As a consequence of this, it will be difficult to identify higher modal frequencies of the structures using response measurements with a low sampling frequency.

All the aforementioned problems arise due to the usage of large numbers of sensors during measurements and therefore using smaller number of sensors for response measurements of structures can be considered as a solution for such problems. In the study provided in this chapter, modal parameter identification of a model bridge was tried to be performed using grouped response measurements which were obtained with a limited number of sensors. To illustrate the procedure, a continuous beam bridge was numerically modeled within Matlab environment. Simulation responses of the model bridge was then obtained in groups of which each is considered to be acquired at different times and due to different excitations. However, in order to employ the measurement data in NExT, the responses of all DOFs should be measured at the same time. To this end, the grouped simulation responses were obtained at different times, but then each group responses were transformed into a single time interval. In order to obtain the transformed responses, transfer functions are employed between two consecutive groups. Once the equivalent response data was obtained, they were employed in the NExT-ERA method to extract modal parameters of the model bridge. In this study, the aim was to be able to estimate the first 10 modes of the model bridge and compared them to the results of the eigenvalue analysis of the numerical model.

In the next section, the finite element model of the bridge is described. Simulations performed on the numerical model and the methodology used for transformation of the grouped measurements into the equivalent response data were provided in later sections. Results of the study are discussed in the last section followed by a summary of this chapter.

4.2. Finite Element Model

In order to implement the methodology, a two dimensional finite element model of a continuous beam bridge was setup in a Matlab program. The model bridge has a total length of 180 meters which is composed of five spans of which each has a different length. The idea in assigning various lengths for the individual spans is to make it more complex for the system identification process. Then the total length is divided into 36 equal pieces of elements and each node in-between these elements has a vertical translational DOF and a rotational DOF. The structural stiffness matrix has a total of 74 DOFs, which consists of 37 vertical translational DOFs and 37 rotational DOFs. Axial deformations and second order effects were neglected in the analysis. The 6 support conditions and each DOF of the finite element model of the bridge used for implementation of the methodology are presented in Figure 4.1.

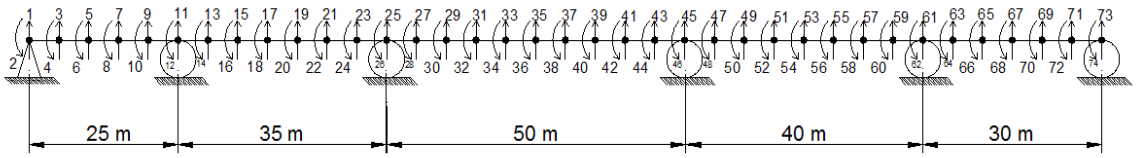

Figure 4.1. Finite element model of the bridge

The moment of inertia of the cross-section around the bending axis of the beams was considered to be 0.0731 m^4 in the analysis. Dimensions of the cross-section were determined so that the maximum vertical displacement of midspan would be 6 cm.

The mass, damping, and stiffness matrices required for dynamic analysis were numerically obtained with the dimensions of 68x68. These are the structural DOFs, after the vertical support DOFs were removed. In this study, we aimed to be able to estimate the first 10 modes of the numerical model. For this purpose, we applied a modal condensation on the obtained system matrices and we obtained the generalized system matrices with the reduced dimensions of 10x10. The damping matrix was constructed by using the mass-proportional damping formulation that is based on the Rayleigh Damping approach (Chopra, 2012) and the modal damping ratio was considered to be 2% for all modes of the structure.

4.3. Implementation of the Methodology

The methodology was tested on the numerical bridge model that is described in section 4.2. The 31 vertical unrestrained DOFs of the bridge model were aimed to be measured by using only a group of four sensors. The group of sensors was then shifted on the model in order to obtain the response measurements from all DOFs. For each shifting operation, the location of one sensor in each group was unchanged and this sensor was considered to be a reference sensor between the two consecutive groups. In Figure 4.2, the placement of the sensors in the first three groups is represented on the model bridge.

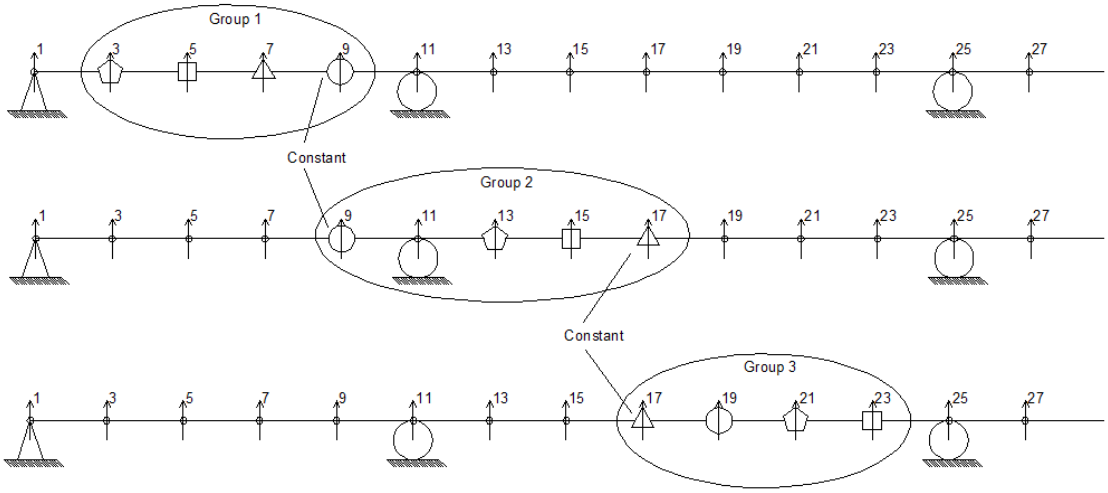

Figure 4.2. Placement of the sensor groups on the model bridge

As it is clearly shown in the figure, the rightmost sensor in each group was assigned as the reference sensor and thus a reference signal was obtained between two consecutive groups. According to the figure, the reference signal between group 1 and group 2 was obtained by the circle-shaped sensor on the 9^{th} DOF. Similarly, the reference signal between group 2 and group 3 was obtained by the triangle-shaped sensor on the 17^{th} DOF. All the other groups are placed on the model in the same sense. As a result, ambient vibration responses of each DOF of the model are obtained by a total of 10 group measurements by using four sensors, only. In the following section, the generation of numerical ambient vibration signals for each group measurements discussed in detail.

4.3.1. Generation of Response Data for Group Measurements

Since there is a total of 37 vertical translational DOFs in the numerical model, it is impossible to obtain response measurements from all DOFs at the same time by using 4 sensors only. Therefore, response measurements in each group should be considered to be obtained at different time intervals. In order to have ambient vibration responses at different time intervals for each group, the bridge model was excited by 10 different generic signals. To this end, 10 different white noise excitations were generated. It should be noted here that according to Caicedo (2003), it is required to use long durational response measurement records for system identification using NExT-ERA in order to identify low mode frequency behavior of structures such as bridges. For this purpose, 10 different white noise excitation signals with a duration of 30 minutes are generated. Even though there is a need for long measurement records in NExT-ERA to obtain low frequency behavior, there is no need to acquire the data with a high sampling rate. Here, the generated white noise excitation signals have a sampling frequency of 200 Hz. These white noise signals are different along the time line, but they are stationary signals which have a constant mean and standard variation – statistically they are identical. In order to obtain non-stationary excitation signals, 10 different ground motion records with reduced amplitudes were included into the white noise signals. Since none of the recorded ground motions have a duration of 30 minutes, each ground motion signal is added to the end of itself until the total duration becomes 30 minutes. As an example, the process of generating the excitation signal used for group 1 is represented in Figure 4.3. To generate the excitation signal used for group 1, the ground motion record of the Duzce Earthquake which was recorded at the Bolu Station on the 12th_of November 1999 was employed with a reduced amplitude. Figure 4.3(a) displays the ground motion signal of the selected earthquake with rectangular block that is zoomed in and shown in Figure 4.3(b). Figure 4.3(c) shows the generated white noise excitation and Figure 4.3(d) shows the combination of the ground motion and the white noise signal which is eventually used as the ambient excitation force to obtain ambient vibration response data for group 1. Excitation signals for the 9 remaining groups were generated using the similar procedure by using different earthquake records and different white noise signals.

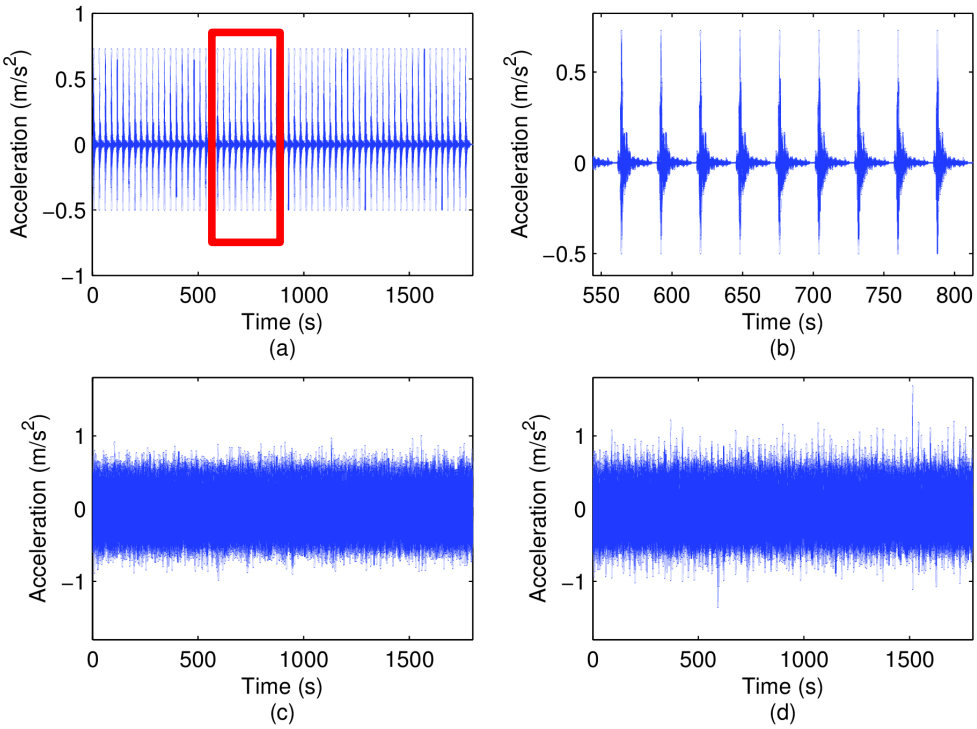

Figure 4.3. (a) ground motion excitation with a duration of 30 minutes, (b) zoomed view of the ground motion signal (in the squared portion), (c) white noise excitation with a duration of 30 minutes, (d) the combination of the ground motion and white noise excitations

Once 10 different excitation signals were generated, the numerical model was excited by each of the generated excitation signals so that 10 different simulations were performed by using the Newmark β method with the constant average acceleration approach (Chopra, 2012). As a result, acceleration response of each DOF was obtained as if the response data in a simulation were measured at a different time with respect to another simulation. Acceleration response data were obtained with a duration of 30 minutes and with a sampling frequency of 200 Hz like the excitation signals. However, in order to focus on the identification of lower modes of the numerical model using NExT-ERA method, acceleration response data were down-sampled to a lower sampling frequency. In this study, it was aspired to determine the first 10 modes of the model bridge. According to the eigenvalue analysis of the numerical model, the resonant frequency of the 10th mode has a value of 23.58 Hz. Therefore, in order to successfully identify the first 10 modes of the model, the acceleration response data were down-sampled to 50 Hz. It was expected to be able to identify the first 10 modes of the model, since the down-sampled data has a Nyquist frequency of 25 Hz which covers the

resonant frequencies up to the 10th mode. The response signals were down-sampled by first applying a low-pass anti-aliasing filter. This filter was necessary so that the modal responses with higher frequencies would be completely removed from the signals. From this point on, the term "acceleration response data" refers to the term "down-sampled acceleration response data."

Once 10 different acceleration response data were generated with 10 different simulations, the data obtained from each simulations were grouped in the configuration shown in Figure 4.2. For example, the acceleration response signals of 3rd, 5th 7th and 9th DOF obtained in the 1st simulation were used as the response measurements of group 1. Similarly, the acceleration response signals of 9th, 13th, 15th and 17th DOF obtained in the 2nd simulation were used as the response measurements of group 2. Consequently, all the acceleration response measurements in the groups were obtained with the same procedure in accordance with the sensor placement represented in Figure 4.2. As an example, the acceleration response signals of the reference sensor on the 9th DOF between group 1 and group 2 are illustrated in Figure 4.4(a) and (b). Figure 4.4(a) shows the acceleration response signal obtained in group 1 by using the reference sensor on the 9th DOF while Figure 4.4(b) shows the acceleration response signal obtained in group 2 by using the reference sensor on the 9th DOF. Similarly, acceleration response signals of the reference sensor on the 17th DOF between group 2 and group 3 are illustrated in Figure 4.4(c) and (d). Figure 4.4(c) shows the acceleration response signal obtained in group 2 by using the reference sensor on the 17th DOF while Figure 4.4(d) shows the acceleration response signal obtained in group 3 by using the reference sensor on the 17th DOF.

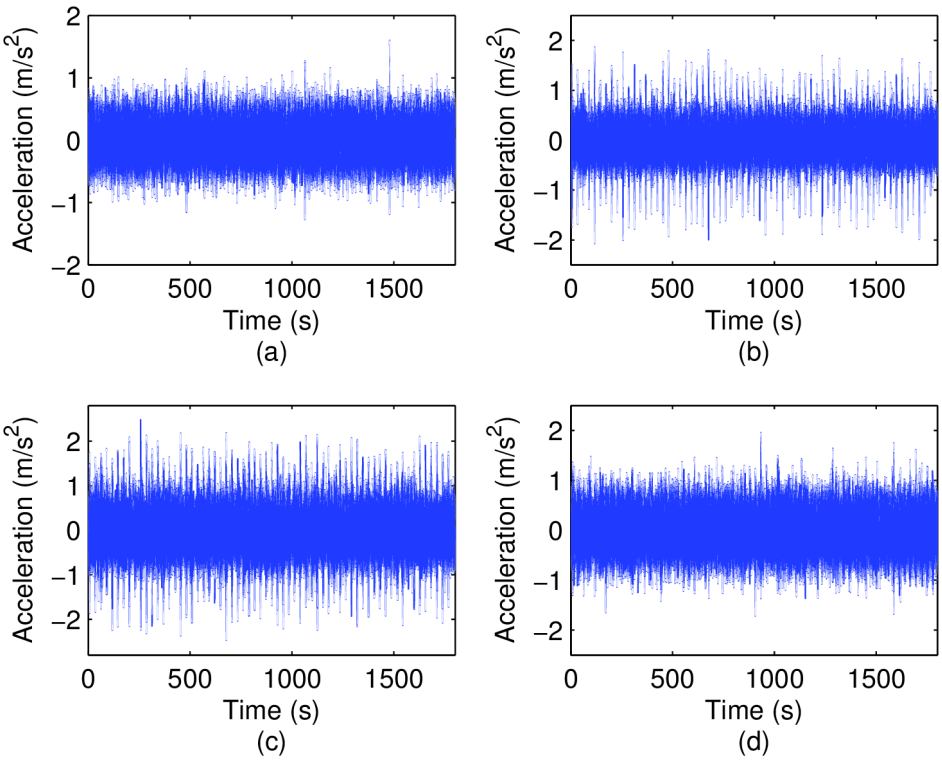

Figure 4.4. (a) acceleration response of 9th DOF in group 1, (b) acceleration response of 9th DOF in group 2, (c) acceleration response of 17th DOF in group 2, (d) acceleration response of 17th DOF in group 3

4.3.2. Transformation of Grouped Response Measurements into the Equivalent Response Data

In order to obtain correlations between the response measurements obtained from different DOFs of a structure, all the response signals which will be used to obtain cross-correlation functions should be measured at the same time to be employed in NExT. Therefore, response measurements in groups, of which each is obtained in a different time interval, should be transformed into an equivalent response time frame to be used in NExT. As discussed in the previous section, the location of one sensor was kept fixed between two consecutive groups while the remaining sensors were being shifted towards the next group measurement. Thus, there are actually two different response measurements for a reference sensor between two consecutive groups. In order to perform the transformation of signals, the reference signals between the groups were employed. By using the transfer function between two response measurements on a reference sensor, response measurements in a group can be transformed into their

equivalents in another group. In order to obtain transfer functions between two consecutive groups, all the acceleration response signals in the time domain were transformed into the frequency domain by applying Fast Fourier Transforms (FFT). In this study, the target was to estimate the response data which are equivalent to the response data obtained in the 1st simulation. Therefore, all grouped measurements were transformed into their equivalent responses with the 1st simulation. It should be noted here that since the response measurements in group 1 are the portion of the response measurements in the 1st simulation, the transformed response measurements of the remaining groups were expected to become as if measured at the same time with the response measurements in group 1.

In order to formulate the transformation procedure according to the sensor configuration shown in Figure 4.2, let the FFTs of the acceleration response signals obtained from 3rd, 5th 7th and 9th DOF in group 1 be $u_3{}^1(w)$, $u_5{}^1(w)$, $u_7{}^1(w)$ and $u_9{}^1(w)$, respectively. Also, let the FFTs of the acceleration response signals obtained from 9th, 13th, 15th and 17th DOF in group 2 be $u_9{}^2(w)$, $u_{13}{}^2(w)$, $u_{15}{}^2(w)$ and $u_{17}{}^2(w)$, respectively. The transformation between group 1 and group 2 is derived by the function expressed in equation 4.1.

$$\alpha_{21}(w) = \frac{u_9{}^1(w)}{u_9{}^2(w)} \tag{4.1}$$

In the equation, the subscript of *u(w)* represents the DOF number from which u(w) was obtained and superscript of *u(w)* represents the group number to which u(w) belongs to. $\alpha_{21}(w)$ is the transformation coefficient to transform the response measurements of group 2 into the equivalent response measurements of group 1.

Then, each response measurement in group 2 was multiplied by $\alpha_{21}(w)$ to obtain the response measurements of group 2 which are equivalents of the response measurements in group 1 as shown in the expressions

$$u_{13}{}^1(w) = \alpha_{21}(w) \bullet u_{13}{}^2(w) \tag{4.2}$$

$$u_{15}{}^1(w) = \alpha_{21}(w) \bullet u_{15}{}^2(w) \tag{4.3}$$

$$u_{17}{}^1(w) = \alpha_{21}(w) \bullet u_{17}{}^2(w) \tag{4.4}$$

According to the above expressions, $u_{13}{}^{1}(w)$, $u_{15}{}^{1}(w)$ and $u_{17}{}^{1}(w)$ represent the response measurements of group 2 which are transformed into the equivalents in group 1.

By using the similar procedure, $\alpha_{31}(w)$ is obtained which is the transformation function used to transform the response measurements of group 3 into the equivalents in group 1 and it is calculated using the following expression

$$\alpha_{31}(w) = \alpha_{32}(w) \bullet \alpha_{21}(w) \tag{4.5}$$

where $\alpha_{32}(w)$ is the transformation coefficient which was used to transform response measurements from group 3 into the equivalents in group 2 and it is defined as

$$\alpha_{32}(w) = \frac{u_{17}{}^{2}(w)}{u_{17}{}^{3}(w)} \tag{4.6}$$

As it can be clearly understood from the expression 4.5, while performing the transformation, the response measurements in group 3 were firstly transformed into their equivalents in group 2 and then these transformed equivalents were transformed into their equivalents in group 1. Calculating the transformation function $\alpha_{31}(w)$, each response measurement in group 3 was multiplied by $\alpha_{31}(w)$ to obtain the response measurements of group 3 which are equivalents of the response measurements in group 1 as shown in the expressions

$$u_{19}{}^{1}(w) = \alpha_{31}(w) \bullet u_{19}{}^{3}(w) \tag{4.7}$$

$$u_{21}{}^{1}(w) = \alpha_{31}(w) \bullet u_{21}{}^{3}(w) \tag{4.8}$$

$$u_{23}{}^{1}(w) = \alpha_{31}(w) \bullet u_{23}{}^{3}(w) \tag{4.9}$$

In the above expressions, $u_{19}{}^{1}(w)$, $u_{21}{}^{1}(w)$ and $u_{23}{}^{1}(w)$ represent the response measurements of group 3 which are transformed into the equivalents in group 1.

Using the same procedures provided above, response measurements in all groups were transformed into their equivalents in group 1. Since the transformed results obtained by the above procedures are in the frequency domain, they were transformed

into the time domain by the Inverse Fast Fourier transform (IFFT) in order to be employed in NExT. As a result, the equivalent time-domain response data of the bridge model which were expected to be equivalent with the response data in the 1st simulation were obtained using the grouped response measurements. Thus, the equivalent response data obtained by the transformation process were able to be employed in NExT-ERA in order to estimate modal parameters of the bridge model. The results of the study are presented in the next section.

4.4. Conclusion and Discussion of the Results

Before employing the equivalent response data obtained by the transformation process in NExT, it was checked whether the transformed responses reflect the actual response behavior of the bridge model or not. In order to make this check, transformed response of each DOF were compared with the response measurement of the corresponding DOF obtained in the 1st simulation. Since the response measurements in each group were transformed into their equivalent responses in the 1st simulation, it is expected that a transformed response signal of a specific DOF should match up with the response signal of the same DOF in the 1st simulation. In Figure 4.5, comparison between the transformed response signals obtained by the grouped measurements and the response signals in the 1st simulation which are ungrouped is illustrated. As seen in the figure, the equivalent response signals obtained by the transformation of the grouped measurements are very close to the ungrouped response signals in the 1st simulation. This result provides a successful verification of the equivalent response data obtained by transformation process and demonstrates that the transformed responses reflect the actual response behavior of the bridge model and so they can be employed in NExT to estimate modal parameters of the bridge model.

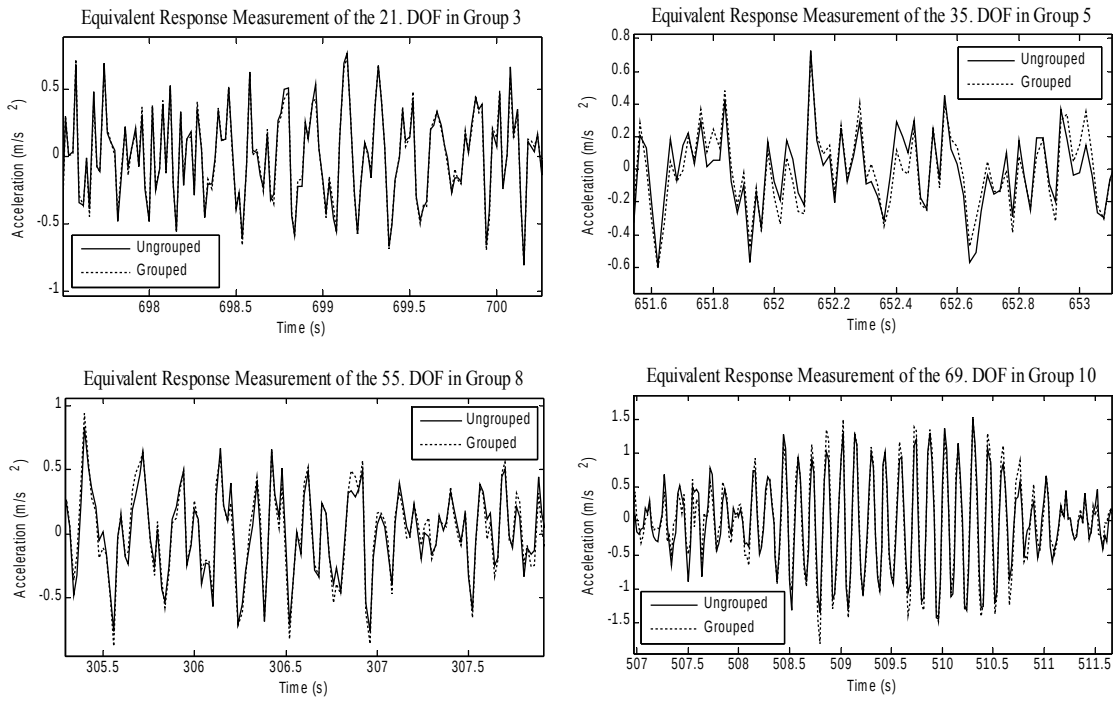

Figure 4.5. Comparison of grouped and ungrouped measurement data

Once the transformation process was successfully verified, the equivalent response data were employed in NExT-ERA to identify the modal parameters of the model. The equivalent measurement of each DOF was used as a reference channel one by one also changing the model order of the system during the identification process and so many different identification processes were performed in order to be able to separate the true resonant frequencies of the model from computational frequencies. So as to visually inspect consistency of the true modes when different model orders were used with different reference channels, stabilization diagrams were also plotted within Nyquist frequency range for each identification process. While plotting the stabilization diagrams, model order of the system was changed from 10 to 32. True modes of the numerical model were expected to be consistent in almost all the stabilization diagrams. Figure 4.6 demonstrates four of the plotted stabilization diagrams in the identification process. Stabilization diagrams shown in the figure were selected among the midspan DOFs since the vertical motion is maximum at the midspan. As seen from the diagrams in the figure, specific frequencies show a high consistency when a different reference channel was selected for the identification process and therefore the frequencies which

are consistent in almost all the stabilization diagrams were selected as the true modal frequencies of the numerical model.

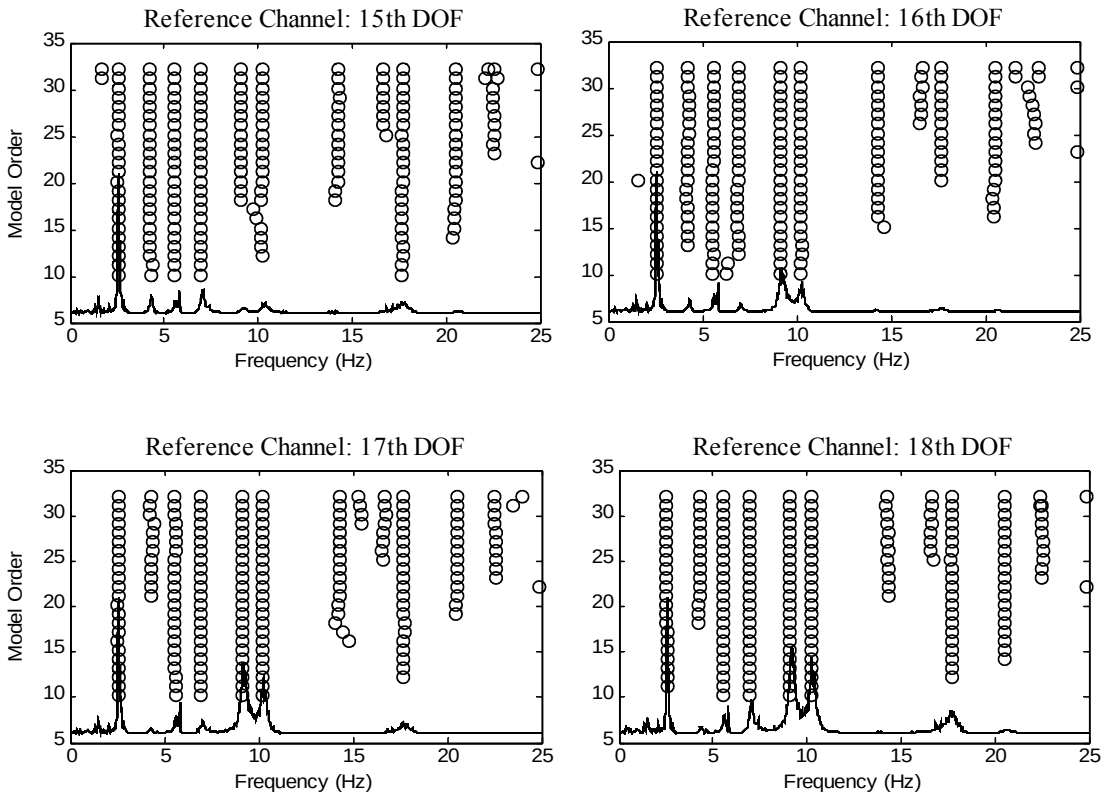

Figure 4.6. Stabilization Diagrams within the Nyquist Frequency Range

To be able to verify the modal parameters obtained by using the equivalent response data in NExT-ERA, modal parameters (modal frequencies, modal damping ratios and mode shapes) of the numerical model were calculated by an eigenvalue analysis and were considered as the true modal parameters of the bridge model. In Table 4.1, the modal frequencies identified by using the equivalent response data in NExT-ERA were compared with the actual modal frequencies of the first 10 modes of the model. According to the results of the modal frequency identification represented in the table, the first 10 modal frequencies of the model have been successfully identified with a maximum error of 2.905% by using the equivalent response data obtained by the transformation process.

Table 4.1. Comparison of modal frequencies of the model bridge

Mode Number	Actual Frequencies (Hz)	Identified Frequencies (Hz)	Error (%)
1	2.654	2.634	0.75
2	4.322	4.340	0.416
3	5.644	5.657	0.230
4	7.052	7.024	0.397
5	9.256	9.193	0.681
6	10.425	10.320	1.000
7	14.646	14.403	1.659
8	18.251	17.774	2.614
9	21.375	21.719	1.609
10	23.583	22.898	2.905

In Table 4.2, the modal damping ratios estimated by using the equivalent response data in NExT-ERA were compared with the actual modal damping ratios of the first 10 modes of the model. According to the results of the modal damping ratio identification presented in the table, although some identification results have minor errors within the acceptable limits, many of the results have major errors above the acceptable limits such as the identification result of the modal damping ratio of the 1st mode which has a maximum error of 53.5%. A large error in modal damping ratio estimation such as the case in this study is a well known fact among system identification researchers. Nayeri et al. (2009) explained this problem as “modal damping estimation is always crude and not as accurate as the modal frequency estimation” in the system identification methods including NExT-ERA. In addition, Moaveni (2007) observed that “the natural frequencies using different methods are reasonably consistent while the identified damping ratios exhibit much larger variability across system identification methods.”

Table 4.2. Comparison of modal damping ratios of the model bridge

Mode Number	Actual Modal Damping Ratios (%)	Identified Modal Damping Ratios (%)	Error (%)
1	2	3.07	53.5
2		2.41	20.5
3		2.18	9
4		2.62	31
5		1.96	2
6		1.93	3.5
7		2.18	9
8		1.92	4
9		2.66	33
10		2.93	46.5

Nonetheless, for the validation purpose and to examine whether the major errors in identification of the modal damping ratios are caused by the transformed responses or not, the response measurements of the 1st simulation which are ungrouped measurements were directly employed in NExT-ERA and modal parameters of the numerical model were also identified in this way. The identification results have demonstrated that using the direct response measurements also results in similar major errors in identification of the modal damping. Thus, this result has validated that major errors in identified modal damping ratios are independent of using grouped measurements in the identification process.

The first 6 mode shapes of the numerical model were successfully identified in NExT-ERA by using the equivalent response measurements. The identified mode shapes were verified by comparing with the actual mode shapes obtained from eigenvalue analysis of the numerical model. They were also compared with the mode shapes identified by using the direct response measurements of the 1st simulation in NExT-ERA. Comparison of the first 10 mode shapes of the bridge model are represented in Figure 4.7.

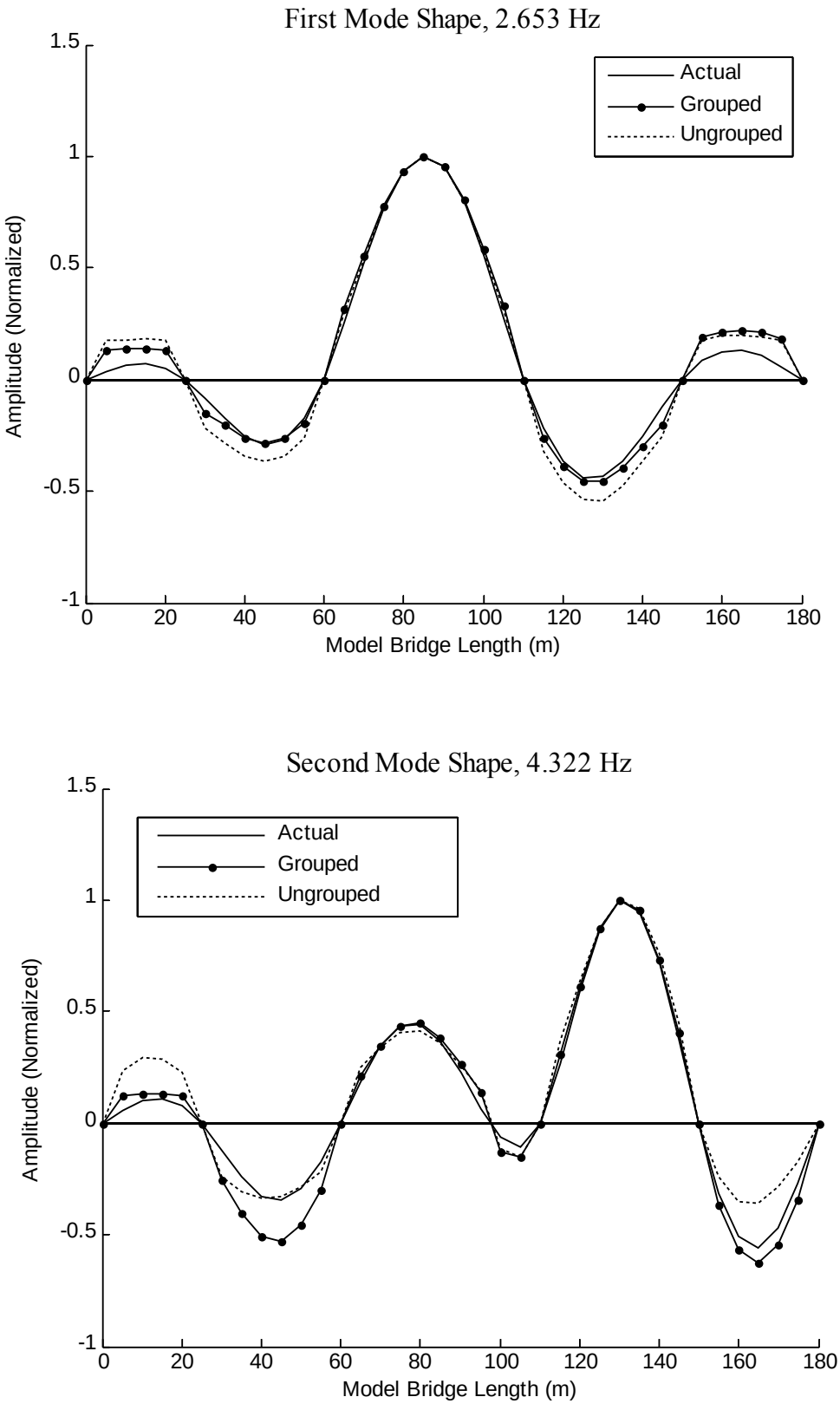

Figure 4.7. Comparison of the first 10 modes shapes of the numerical model

(Cont. on the next page)

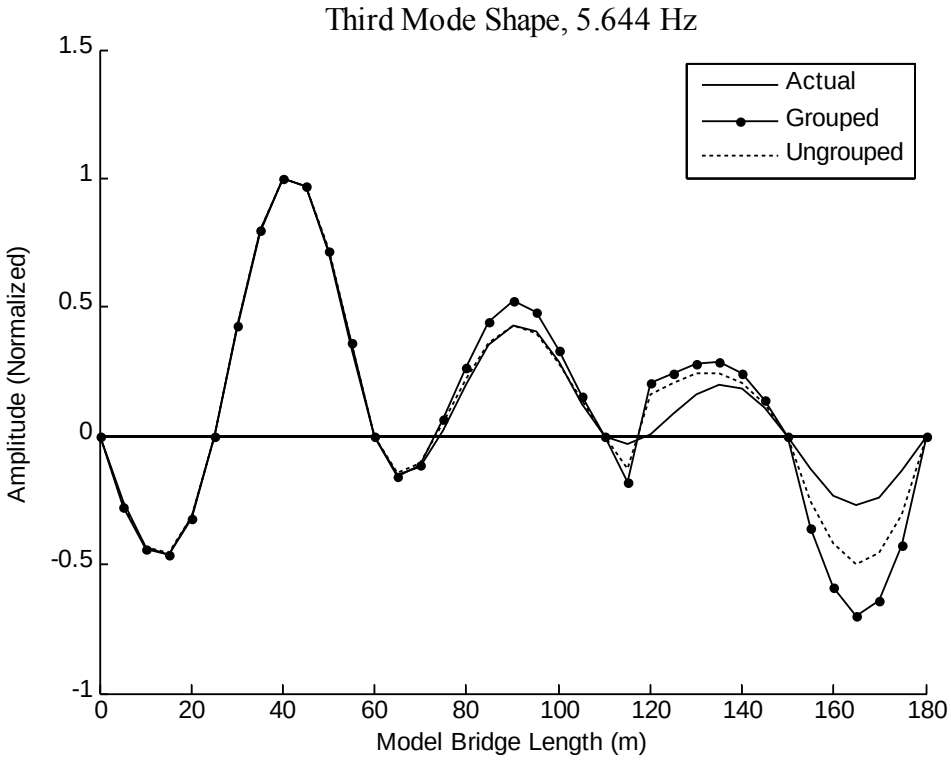

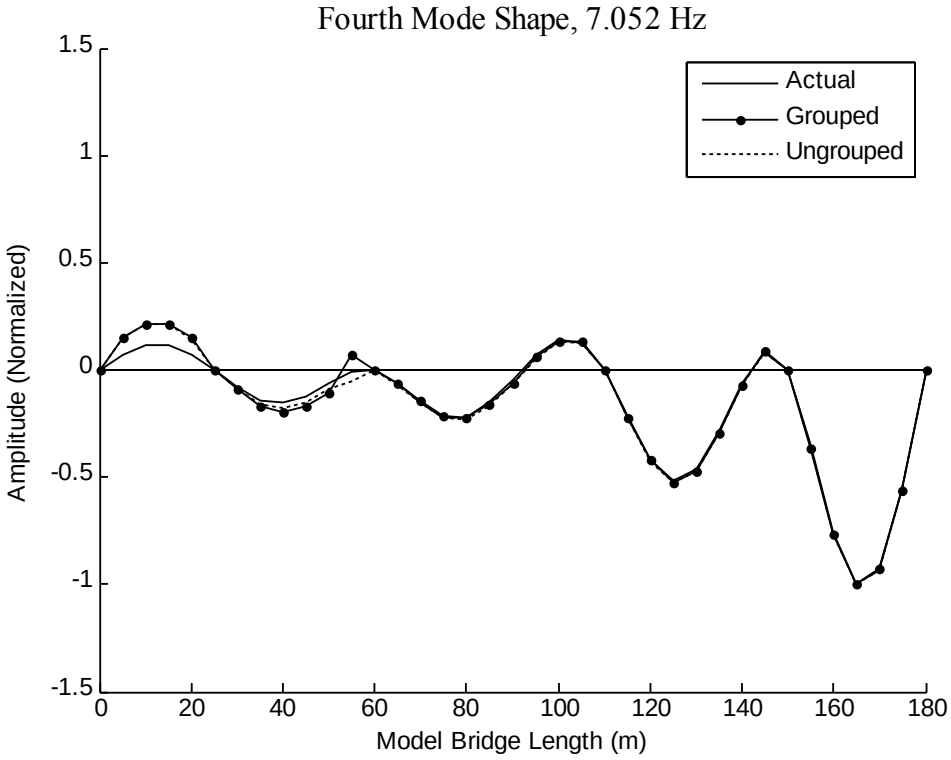

Figure 4.7. (Cont.)

(Cont. on the next page)

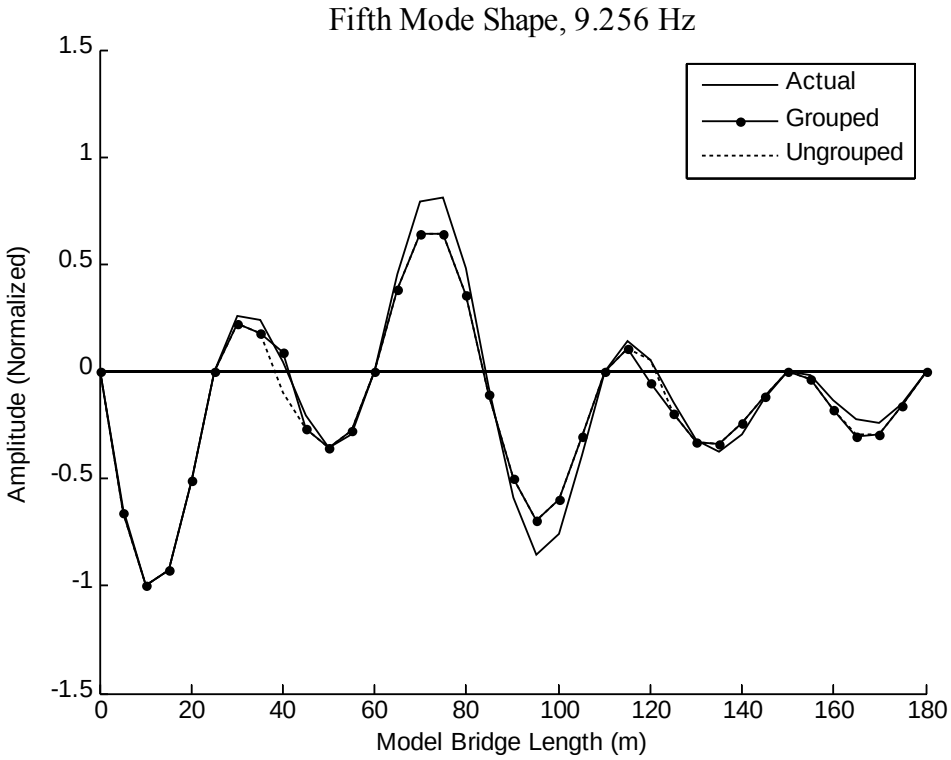

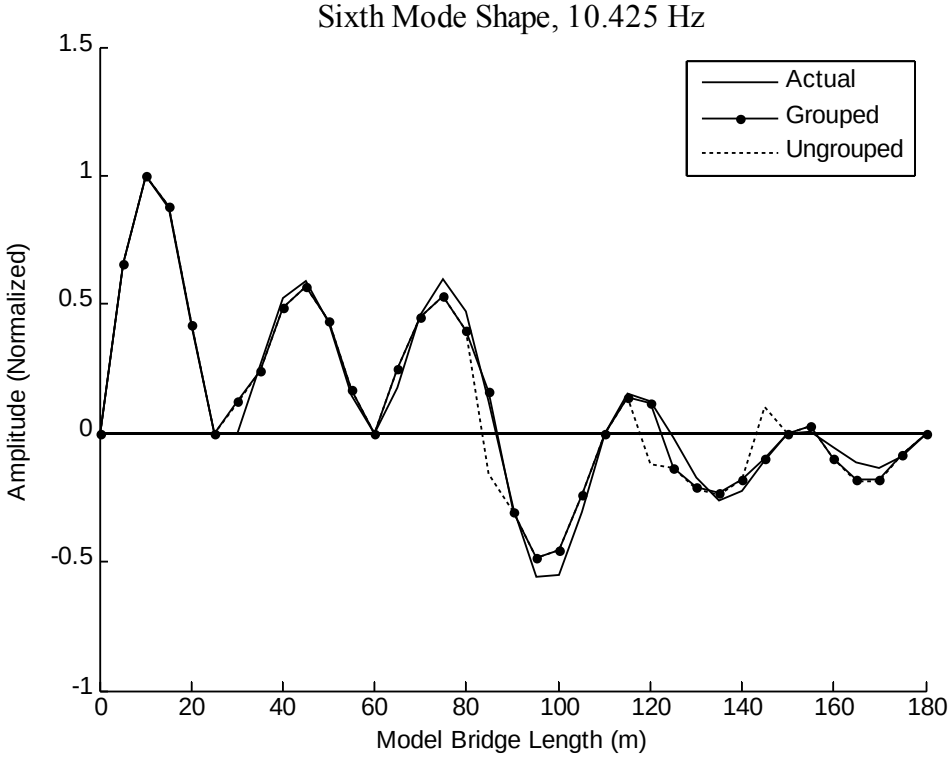

Figure 4.7. (Cont.)

(Cont. on the next page)

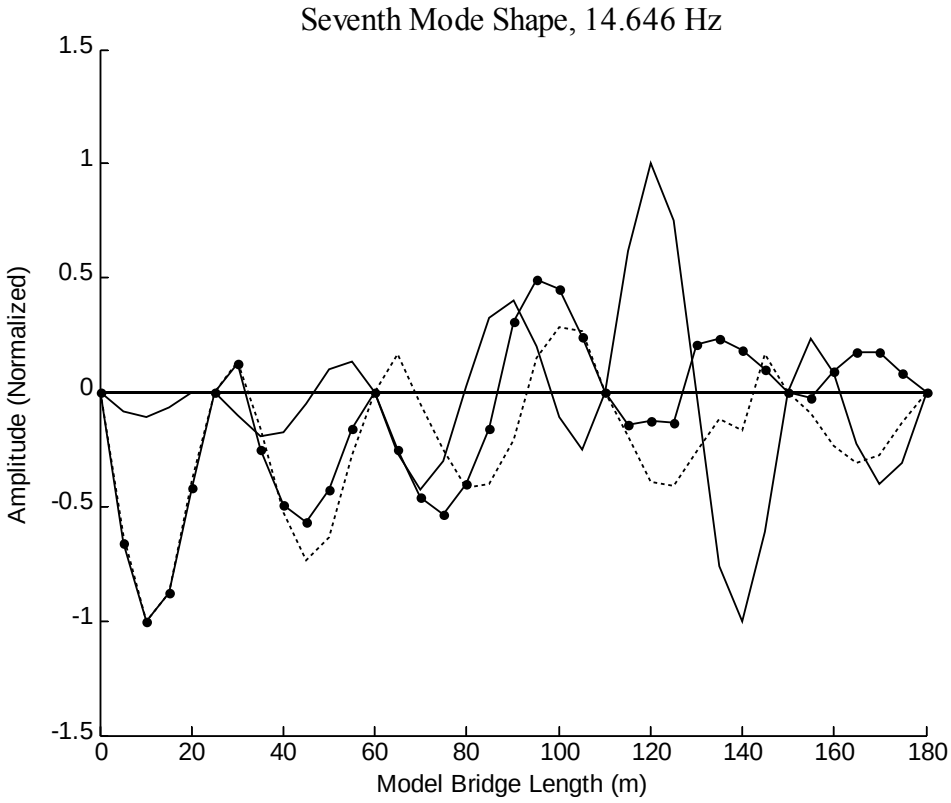

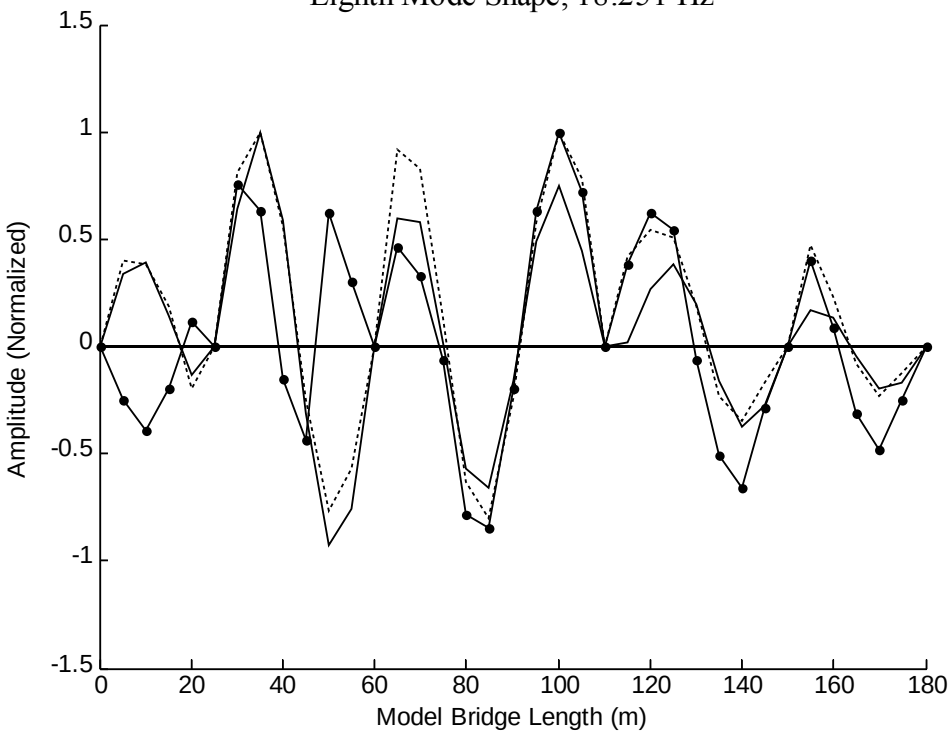

Figure 4.7. (cont.)

(Cont. on the next page)

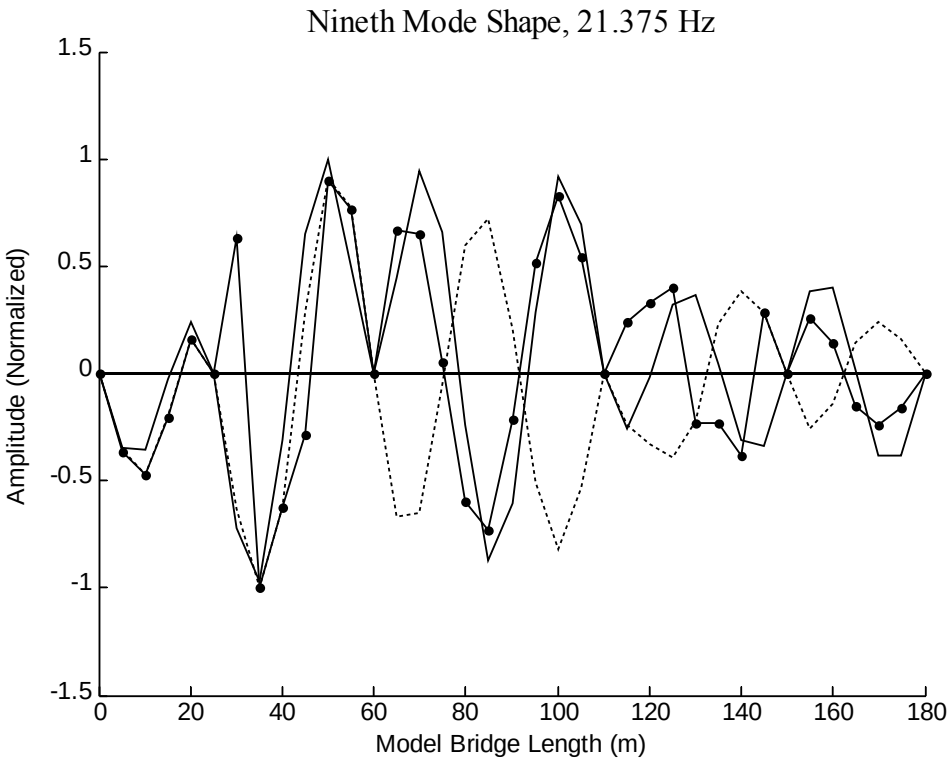

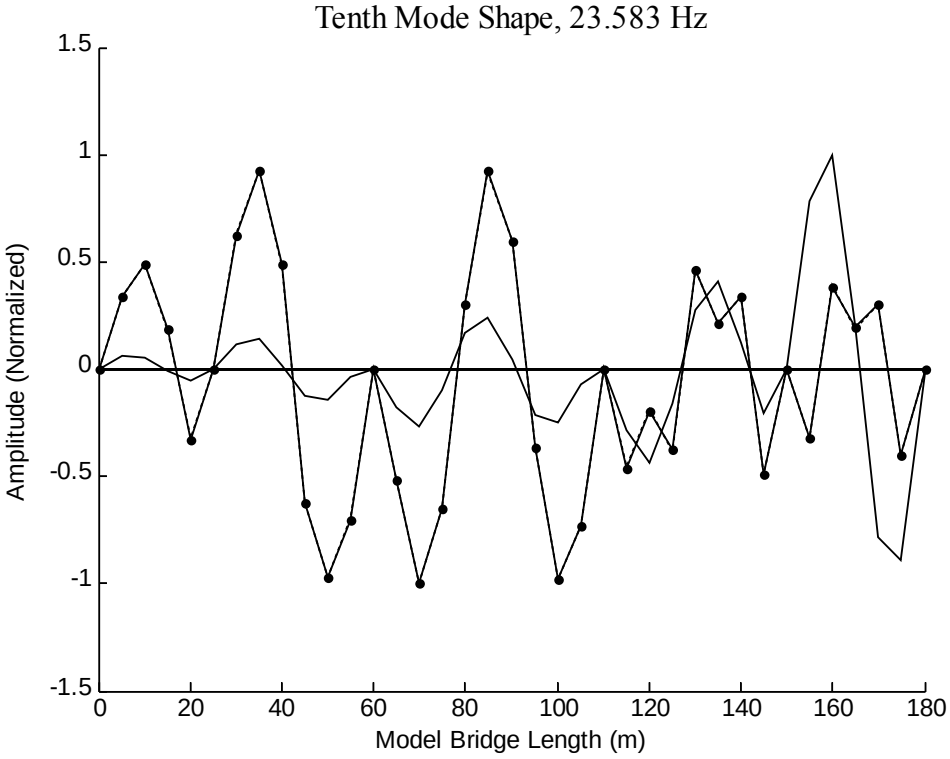

Figure 4.7. (Cont.)

As seen in the each plot of the mode shapes, the mode shapes identified by the grouped response measurements have a good consistency with the actual mode shapes and with the mode shapes identified by the ungrouped response measurements of the 1st simulation.

The results of the three modal parameters (modal frequencies, modal damping ratios and mode shapes) discussed in this section reveal that grouped response measurements can be employed in NExT-ERA after they are transformed into the response measurements equivalent to each other in time in order to estimate modal parameters of large civil structures such as bridges.

4.5. Summary

In the study presented in this chapter, the target is to be able to estimate modal parameters of large civil structures such as bridges by using grouped response measurements which are obtained with a limited number of sensors. In order to perform this study, a finite element model of a continuous beam bridge was set up within the Matlab programing environment and the proposed methodology was implemented on the numerical bridge model. By using this method, group responses can effectively be used to in place of direct and simultaneous response measurements. Thus, this study revealed the fact that the equivalent response data of structures obtained by a transformation process of the grouped response measurements can reflect the actual response behavior of structures and so the obtained equivalent response data could be employed in NExT-ERA in order to estimate modal parameters of the bridge model. The modal parameters estimated by using the grouped response measurements were in a good agreement with the actual ones of the numerical model and also with the modal parameters estimated by using the ungrouped response measurements. As a consequence, the methodology was found to be applicable for measurements of the bridge structures. Using the methodology proposed in this chapter, modal parameters of structures on which no pre-installed measurement sensors exist can be obtained with a low cost work.

CHAPTER 5

CONCLUSIONS

5.1. Summary and Remarkable Findings

In this thesis, two research studies have been presented to obtain modal parameters of civil structures for the assessment of their current structural conditions. Two structures are investigated in this study and their assessments are based on the modal parameters of the structures, which are obtained by a combination of the Natural Excitation Technique (NExT) and the Eigensystem Realization Algorithm (ERA). To this end, an algorithm of the NExT-ERA method is programmed within the Matlab environment.

In the first study, a three-story steel model building located in the Structural Mechanics Laboratory of the Civil Engineering Department of Izmir Institute of Technology (IYTE) is used in the implementation. The NExT-ERA method has been numerically implemented on a mathematical model of this structure which is modeled by Matlab. The structure is modeled with 10 different structural conditions in addition to the unchanged state. The structural changes are simulated by means of changes in story masses, instead of changes in the stiffness matrix. Changing story masses instead of the stiffness matrix does not affect the detection mechanism because the coded algorithm concerns with the frequencies, mode shapes, and the corresponding damping characteristics. In addition, the implementation of the change in mass scenarios will allow an accurate verification of the simulations by using real test data in the near future. As a result of this study, modal parameters of the mathematical model have been obtained by using NExT-ERA and mass changes in each structural condition have been identified by a least squares approach.

According to the numerical and experimental phases of the first study, some remarkable findings are inferred as;

- In the numerical phase, identified modal frequencies and mode shapes of the mathematical model of the three-story model building by using NExT-ERA are found to be consistent with the modal parameters which are obtained by the eigenvalue analysis of the model.
- Identification results of modal damping ratios of the model by using NExT-ERA are found to be inconsistent with those of the eigenvalue analysis, even though some of the results are acceptable. When the literature of the method is reviewed, it is noticed that researchers have also encountered such inconsistent identification results of modal damping ratios by using NExT-ERA and it is accepted that modal damping identification is always crude. Therefore, these inconsistent identification results of modal damping ratios could be expected in case of system identification by NExT-ERA.
- According to the numerical phase, the identification results reveal that the coded software based on the NExT-ERA algorithm fulfills the objectives on output-only system identification.
- In the numerical phase, changes in story masses of the three-story model building which are considered as the changes in structural states are detected with acceptable consistency with the foreknown additional masses on story levels.
- The identification results for the changes in story masses of the model demonstrate that the coded program of the least squares approach is capable of identifying the presence and severity of the change in mass of the structure. However, this specific least squares approach was developed for shear frame structures. Therefore, damage identification of more complex structures cannot be performed using the same least squares algorithm.
- In the experimental phase, identified modal frequencies and mode shapes of the physical structure by using NExT-ERA are found to be consistent with the modal parameters which are obtained by the eigenvalue analysis of the mathematical model. However, only the unchanged state of the physical structure was able to be investigated in the experimental phase. The reason for this was that some problems were encountered during data acquisition processes for the other

structural conditions, possibly due to an unexpected failure in the data acquisition system or the sensors.

- As in the numerical phase, identification results of modal damping ratios of the physical structure by using NExT-ERA are found to be inconsistent with those of the eigenvalue analysis of the mathematical model. In fact, the reason for the inaccurate identification results of modal damping ratios obtained by the NExT-ERA method could be attributed to the ambient vibration nature of the structure. During the ambient excitations, the structure responses with very low amplitudes and therefore damping mechanism of the structure could not be activated. Instead of ambient excitation, the structure should be excited by larger forces. In this case, the structure will have responses with higher amplitudes and successful identification of the modal damping ratios could be possible.
- This experimental study also allows us to modify the NExT-ERA algorithm for real-life applications. Since it is impossible to acquire noiseless acceleration data in real life, it is obliged to deal with the noisy measurement data during the identification process of the structure. Moreover, a Gaussian white noise is added to each response measurement of the numerical model of the three-story building to simulate real measurements. It is a known fact that noise-to-signal ratio of response measurements directly affects the identification process (Caicedo, 2011). Depending on the level of this ratio, the size of the Hankel matrix should be changed for a successful identification. Since some portion of the cross-correlation functions are employed while constructing the Hankel matrix, a larger size of the Hankel matrix should be used in order to include more information of free vibration data into the identification process. In addition to this, while calculating the power spectral density functions, the number of FFT points in a window frame should be changed to include more data in the averaging process. Requirement of such changes restrains the algorithm from being fully autonomous and makes the algorithm dependent on human interference. Besides, longer records of measurements are required in case of noisy data to be able to use a larger size Hankel matrix and to have more averages.
- It should be also noted as a conclusion that the NExT-ERA method is able to identify the modal parameters of current state of the structures and therefore it can be used for the assessment of current structural state only. The certain way to

investigate structural changes is that current investigations of structural state should be compared with the previous ones to have a significant information of presence of any damage. As an example, in the numerical study of the three-story model building, an obtained result of any damage state is meaningless unless it is compared with the results of the undamaged state. In case the previous structural state is unknown, a model updating approach can be performed to be able to have information on the current structural state. In this case, a computer model of the physical structure is constructed and the constructed model is updated by using the modal parameters obtained from the system identification process. The properties of the physical structure are compared with those of the updated model and differences between the properties give a sense of possible damage in the structure.

In the second study, a methodology is proposed to acquire measurements of large structures by using a few sensors, only. These sensors are used in a segmental way to measure the whole structure. Then the grouped response measurements that are obtained at different time frames are transformed into the equivalent response data as if being acquired at a single time interval. The proposed methodology is implemented on a finite element model of a continuous beam bridge. The equivalent response data of the model are employed in NExT-ERA and modal parameters of the model are extracted.

According to the second study, some findings are inferred as;

- The equivalent response data obtained from grouped response measurements are found to be in high consistency with the response measurements which are acquired at a single time interval.
- According to the identification results, the first 10 modal frequencies which are evaluated by using the proposed methodology are in good agreement with the modal frequencies obtained by eigenvalue analysis. According to the identification results the obtained mode shapes are consistent with the results that are obtained by using a single data set measurement, but only the first 6 mode shapes are found to be consistent with the mode shapes evaluated by the eigenvalue analysis of the mathematical model.
- As discussed for the inconsistent identification of modal damping ratios of the three-story model building, the modal damping ratios of this bridge beam model

cannot be identified either. The damping results are inconsistent with the results of the eigenvalue analysis.

Results of this third study lead to the conclusion that acquired responses of structures by using a limited amount of sensors can be employed in NExT-ERA by using the proposed methodology. By means of this method, modal parameter identification of structures which do not have pre-installed measurement sensors can be performed with a low-cost in-situ work.

5.2. Recommendations for Future Work

The main problem encountered in the studies conducted within the scope of this thesis was the measurement noise in the acceleration response signals. Measurement noise in the response data may arise due to external mechanical and electrical sources. Environmental radio waves and electromagnetic fields generated by other devices around data acquisition systems may result in increased noise levels. Long cables during data acquisition also act as antenna and could easily pick-up electromagnetic signals from the environment. In addition, electronic noise from the circuitry of the acceleration sensor itself which is converting the motion into a voltage signal is inevitably included into the response data. The high level of noise-to-signal ratio of the measured data adversely affects the identification process. Therefore, noise reduction techniques could be implemented on the data acquisition systems. It is hard to remove electronic noise from the signal of the sensors. However, external mechanical and electrical sources could be avoided to enter the signal, for instance, by using proper shielding for cables and by removing possible sources of electromagnetic fields. Usage of short cables may also decrease the possibility of electromagnetic signal noise.

Since the acquired acceleration signals always have higher noise-to-signal ratio when compared with the displacement and velocity response data, alternative ways to obtain displacement or velocity response of the structures under ambient excitations could be investigated. Besides, it could be studied on noise reduction methodologies of acceleration data to have more reliable identification results and noise reduction methods would be included in the NExT-ERA algorithm. For instance, analog or digital implementation of high-order low pass filters or usage of Kalman filtering may be the

possible solutions for noise reduction. If noise in response data could be reduced to negligible levels then the NExT-ERA algorithm would become fully autonomous without any requirement of human interference.

In the first study, detection of structural changes of the three-story model building was performed by using a least squares approach. However, this approach is developed to be used for shear frame structures only, but the approach could be modified for identification of structural changes of more complex structures.

The methodology proposed in Chapter 4 were applied on the numerical model of a continuous beam bridge only. Experimental verification of the methodology should be performed to investigate the applicability of the proposed methodology on physical structures. Experimental study would reveal the capability of the methodology in case of using noisy grouped measurement data. The numerical study could be also performed with noise addition to the grouped response measurements. Moreover, the proposed methodology could be implemented on different types of structures for a comprehensive validation.

REFERENCES

Basten, T. G. H., and Schiphorst, F. B. A. (2012). "Structural health monitoring with a wireless vibration sensor network." *Proceedings of the International Conference on Noise and Vibration Engineering, ISMA 2012, 17-19 September 2012, Leuven, Belgium*, 3273–3283.

Bendat, J. S., and Piersol, A. G. (2010). *Random Data: Analysis and Measurement Procedures*. Wiley, Hoboken, New Jersey.

Beyen, K., Kutanis, M., Tanöz, H. Ö., and Başkan, D. (2011). "Yapı Sağlığı İzleme ve Yapı Tanı Çalışmaları için Akıllı Aktarma Protokollu Kablosuz Sensör Ağı." *Seventh National Conference on Earthquake Engineering, 30 May-3 June 2011, Istanbul, Turkey*.

Caicedo, J. M. (2001). "Two Structural Health Monitoring Strategies Based On Global Acceleration Responses: Development, Implementation, And Verification." *Master of Science Thesis*, Washington University, St. Louis, Missouri.

Caicedo, J. M. (2003). "Structural Health Monitoring Of Flexible Civil Structures." *Doctor of Science Thesis*, Washington University, St. Louis, Missouri.

Caicedo, J. M. (2011). "Practical Guidelines For The Natural Excitation Technique (NExT) And The Eigensystem Realization Algorithm (ERA) For Modal Identification Using Ambient Vibration." *Experimental Techniques*, 35(4), 52–58.

Chang, F.-K. (1999). *Structural Health Monitoring, Proc. of the 2nd International. Workshop on Structural Health Monitoring,* Stanford University, September 8–10, 1999, Technomic Publishing Co., Lancaster, PA.

Chopra, A. K. (2012). *Dynamics of Structures*. Prentince Hall Inc., Upper Saddle River, NJ.

Dyke, S. J., Bernal, D., Beck, J., and Ventura, C. (2004). "Experimental Phase II of the Structural Health Monitoring Benchmark Problem." *16th Engineering Mechanical Conference.*

Farrar, C. R., and Worden, K. (2012). *Structural Health Monitoring: A Machine Learning Perspective*. John Wiley & Sons Inc., United Kingdom.

James, G. I., Carne, T., and Lauffer, J. (1993). "The Natural Excitation Technique (NExT) for modal parameter extraction from operating wind turbines." *Sandia National Laboratories, Albuquerque, NM and Livermore, CA, SAND92-1666.*

Johnson, E. A., Lam, H. F., Katafygiotis, L. S., and Beck, J. (2000). "A benchmark problem for structural health monitoring and damage de tection. " *Proceedings of the 14th ASCE Engineering Mechanics Conference* (EM2000) (CD-ROM), J. L. Tassoulas, ed., ASCE, Reston, Va.

Johnson, E. A., Lam, H. F., Katafygiotis, L. S., and Beck, J. L. (2004). "Phase I IASC-ASCE Structural Health Monitoring Benchmark Problem Using Simulated Data." *Journal Of Engineering Mechanics*, 130(1), 3–15.

Juang, J.-N., and Pappa, R. S. (1985). "An Eigensystem Realization Algorithm for Modal Parameter Identification and Model Reduction." *Journal Of Guidance, Control, And Dynamics*, 8(5), 620–627.

Juang, J.-N., and Pappa, R. S. (1986). "Effects of Noise on Modal Parameters Identified by the Eigensystem Realization Algorithm,." *Journal of Guidance, Control, and Dynamics*, Vol. 9(No. 3), 294–303.

Mahmood, S. M. F., Haritos, N., Gad, E., and Zhang, L. (2014). "A multi-reference-based mode selection approach for the implementation of NExT–ERA in modal-based damage detection." *Structural Control & Health Monitoring*, 21(8), 1137.

Manolakis, D. G., and Proakis, J. G. (2007). *Digital Signal Processing, 4/e*. Pearson, New Delhi, India.

Moaveni, B. (2007). "System and Damage Identification of Civil Structures." *Doctor of Philosophy in Structural Engineering*, University of California, San Diego.

Nagy-Grögy, T. (2012). "Structural Health Monitoring (SHM)." <http://www.ct.upt.ro/users/TamasNagyGyorgy/Tehnici_Experimentale/3_SHM__Nagy-Gyorgy_T_2012_12_03.pdf>.

Nayeri, R. D., Tasbihgoo, F., Wahbeh, M., Caffrey, J. P., Masri, S. F., Conte, J. P., and Elgamal, A. (2009). "Study of Time-Domain Techniques for Modal Parameter Identification of a Long Suspension Bridge with Dense Sensor Arrays." *Journal Of Engineering Mechanics*, 135(7), 669–683.

Turan, G., and Aydın, E. (2011). "Değişken Sönümleme Katsayılı Amortisörlerin Deprem Simülasyonu ile Üç Katlı Bir Yapıya Olan Etkisinin Değerlendirilmesi". *Report of the project with a project number of 107M353, supported by TÜBİTAK Mühendislik Araştırma Grubu*. İzmir.

Wei Fan and Pizhong Qiao. (2011). "Vibration-based Damage Identification Methods: A Review and Comparative Study." *Structural Health Monitoring*, 10(1), 83.

Yıldırım, U. (2014). "System Identification Towards Diagnosis To Prognosis." *Doctor of Science Thesis*, University of Pavia, Pavia, Italy.

APPENDIX A

TECHNICAL SPECIFICATIONS OF ACCELERATION SENSORS THAT ARE USED IN THIS STUDY

1.	**Trademark – Model**	**: PCB – 356B18 (Triaxial)**
	Sensitivity	: 1000 mV/g
	Measurement Range	: +- 5g
	Frequency Range (+- 5%)	: 0.5 to 3000 Hz
	Frequency Range (+- 10%)	: 0.3 to 5000 Hz
	Resonant Frequency	: ≥ 20 kHz
	Spectral Noise (1 Hz)	: 11.4 μg/ $\sqrt{Hz}$
	Spectral Noise (10 Hz)	: 4.0 μg/ $\sqrt{Hz}$
	Spectral Noise (100 Hz)	: 1.2 μg/ $\sqrt{Hz}$
2.	**Trademark – Model**	**: PCB – 356A16 (Triaxial)**
	Sensitivity	: 100 mV/g
	Measurement Range	: +- 50g
	Frequency Range (+- 5%)	: 0.5 to 5000 Hz
	Frequency Range (+- 10%)	: 0.3 to 6000 Hz
	Resonant Frequency	: ≥ 25 kHz
3.	**Trademark – Model**	**: PCB – 393B04 (Uniaxial)**
	Sensitivity	: 1000 mV/g
	Measurement Range	: +- 2.5g
	Frequency Range (+- 5%)	: 0.025 to 800 Hz
	Frequency Range (+- 10%)	: 0.01 to 1200 Hz
	Resonant Frequency	: ≥ 3.5 kHz